AIRCRAFT RADIO DIRECTION FINDING AND HOMING SYSTEM IN THE 40-100 MC RANGE

N6-ori-71 Task 37
TECHNICAL REPORT NO. 1

RADIO DIRECTION FINDING SECTION
ELECTRICAL ENGINEERING RESEARCH LABORATORY
ENGINEERING EXPERIMENT STATION
UNIVERSITY OF ILLINOIS
URBANA, ILLINOIS

Copy No. 8

AIRCRAFT RADIO DIRECTION FINDING AND HOMING SYSTEMS IN THE 40-100 MC RANGE

N6 ori 071 Task 37

Technical Report No. 1

Date:

May 1953

NOTICE:

This document contains information affecting the national defense of the United States within the meaning of the Espionage Laws, Title 18, USC, Sections 793 and 794. The transmission or the revelation of its contents in any manner to an unauthorized person is prohibited by law.

Prepared by:

D. Royal
Research Associate

N. Yaru
Research Associate

Approved by:

E.C. Jordan
Professor

RADIO DIRECTION FINDING SECTION
ELECTRICAL ENGINEERING RESEARCH LABORATORY
ENGINEERING EXPERIMENT STATION
UNIVERSITY OF ILLINOIS
URBANA ILLINOIS

ABSTRACT

This report summarizes work done on the problems of homing and radio direction-finding for Navy type AF and P4M aircraft in the frequency range 40-100 mc The work of Part I (homing systems) is essentially completed Some interim answers are given for the problems of Part II (aircraft RDF systems) but work on these problems is continuing

Part I - Homing Systems

Quite successful homing system antennas have been developed for Navy type AF and P4M aircraft The antennas used are electrically-small units which may be faired-in or flush-mounted They may be tuned over the 40-100 mc band by a remotely-driven tuning condenser operated by the receiver tuning dial Alternatively, they may be operated fixed-tuned to cover approximately a 20 mc band anywhere within the 40-100 mc range With some sacrifice of sensicivity they may be operated fixed-tuned to cover the ertire 40-100 mc band By utilizing the "edge-effect", remarkably high sensitivities are obtained despite the small size of the antenna elements The sensitivity is high enough to permit homing on the side-lobes of radar antennas located at distances well beyond the line of sight Antenna locations have been found on the leading edge of the wing or forward part of the fuselage which yield very satisfactory patterns over the entire range of frequencies With a small amount of additional pattern measurement work these results can be extended to other types of aircraft

Part II - RDF Systems

Two different aircraft RDF systems have been investigated experimentally, using model techniques Both of these systems utilize a set of four of the same antenna units used for homing Because of the fundamental difficulty of maintaining patterns suitable for RDF over the frequency band 40-100 mc there are regions of bearing indeterminacy To date the systems and antenna locations investigated indicate the possibility of obtaining complete azimuthal RDF coverage except for a 60° sector off the tail There will be regions of azimuth where the bearing may be quite inaccurate, but correct sector identification will always be given The bearings will be relatively accurate in three critical regions, viz., in a 40° sector about the nose, and a 40° sector off each wing tip

The accuracy increases as the direction of arrival of the signal approaches the line of aircraft heading or the perpendicular to this line Work on the RDF problem is continuing

TABLE OF CONTENTS

INTRODUCTION

The difficulties of homing and radio direction-finding from aircraft in the VHF band are many and severe. In addition to all the problems associated with ground-based RDF, airborne systems suffer serious limitations because of their location on an aircraft. Aerodynamic considerations require that the antennas be flush-mounted or faired-in, and of reasonably small physical dimensions. In the frequency range of interest these factors necessitate electrically-small antennas, which ordinarily means low sensitivity. Even more serious is the effect of the aircraft structure on the radiation patterns. In the frequency range 40-100 mc. a wavelength is of the same order of magnitude as the dimensions of various portions of the aircraft structure, so that the radiation patterns are determined primarily by the shape of the aircraft. Despite these complications it has proven possible to develop, for this frequency range, a completely satisfactory homing system and a partially satisfactory RDF system.*

*Much of the work reported in this technical report has been described in the status reports ADF-1 through ADF-5 issued under this contract. Because these status reports had only a very limited circulation, all of the important results have been summarized in this technical report. However references are made occasionally to the status reports for more detailed information.

PART I

HOMING SYSTEMS (40-100 mc)

The antenna requirements for an aircraft homing system in the frequency range 40-100 mc may be summarized as follows

a) The antenna should produce a suitable radiation pattern over the frequency range of interest Ideally this pattern would be a cardioid but a pattern which covers slightly more than a quadrant is satisfactory as long as the pattern has the right amount of "lean" away from the nose of the aircraft

b) The sensitivity should be as high as possible In any event the sensitivity should be high enough for the aircraft to detect a radar before the radar can see the aircraft

c) The antenna should be capable of being faired-in or flush mounted for use on high speed aircraft Because a wavelength is of the order of 5 meters in this frequency range reasonable physical dimensions require an electrically-small antenna element

d) The polarization should be *horizontal* Assuming level flight, the longer dimensions of the aircraft are horizontal At these frequencies where the vertical dimensions are small in wavelengths the only currents of appreciable magnitude that are excited are horizontal This means that reflection from the aircraft at these frequencies is much less for vertical polarization than for horizontal polarization so that the radar must use horizontal polarization in order to see the aircraft.

1. Partial-Sleeve Antenna

An antenna which can be made to satisfy all of the above requirements is the partial sleeve antenna* which is described briefly below This antenna was originally designed as an electrically-small tunable transmitting antenna of reasonably high efficiency The description below is based upon the assumption that the antenna will be remotely tuned to cover the band However it is quite feasible to operate it fixed-tuned over about a 20 mc spot frequency band anywhere within the 40-100 mc range Also with a sacrifice of sensitivity it can be operated untuned over the whole frequency range

A sketch of the partial sleeve antenna is shown in Fig 1 In practice the antenna could be suppressed resulting in a completely flush design However because of its shape which conforms to the aircraft surface and small size (approximately 20" × 20" × 2") it can also be mounted externally on the leading edge of the wing A brief description of its operation follows

For any antenna that is small in terms of wavelength it is necessary to match from a standard cable impedance of 50 ohms to a very low antenna resistance or conductance One method of accomplishing the impedance transformation is shown in the figure The feed point, in-

*The partial-sleeve antenna was developed in the Antenna Laboratory at the University of Illinois under Air Force Contract W33-038-ac-20778 A complete analysis of its operation can be found in progress reports I.R. 1, 2 3 and 4 issued under that contract. Formal permission to use this antenna on the present problem has been given.

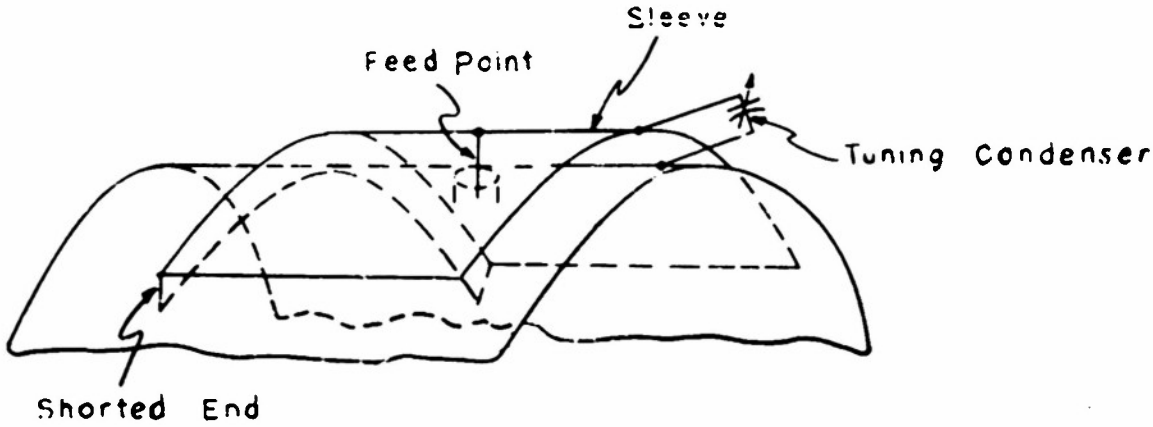

FIGURE 1

stead of being at the open end of the antenna, is tapped down the shorted line to present the proper impedance. The capacitor across the open end tunes out the inductive susceptance.

The equivalent circuit of the antenna is indicated in Fig. 1a.

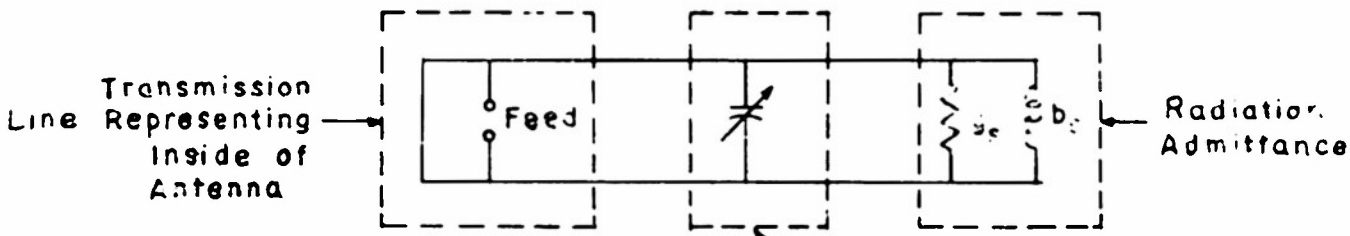

FIGURE 1a

As far as its radiation characteristics are concerned the antenna may be thought of as a U-shaped slot folded around the wing. The electric field distribution along the transverse slot will be essentially uniform, while the distribution along the axial slots will be sinusoidal, starting from zero at the shorted end.

The antenna dimensions shown in Fig. 1b are small in terms of wavelengths, with $S = \frac{\lambda}{100}$, $W = \frac{\lambda}{10}$, $L = \frac{\lambda}{10}$ at midband frequency.

A modification in the physical design so that the antenna takes the form of a folded radiator should be effective in reducing any undesired cross-polarization pickup. The vertical and horizontal patterns of the antenna are not the same, so that if the antenna were equally sensitive to both polarizations an error in bearing would result.

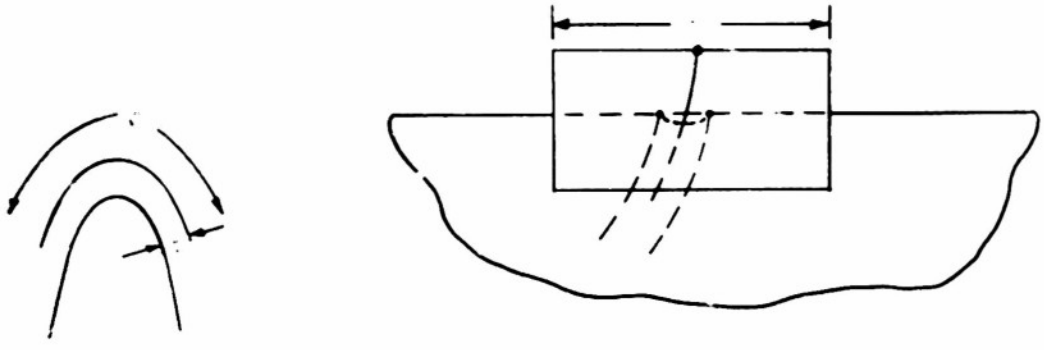

FIGURE 1b

Figure 1c indicates the form of the folded, wing-edge radiator

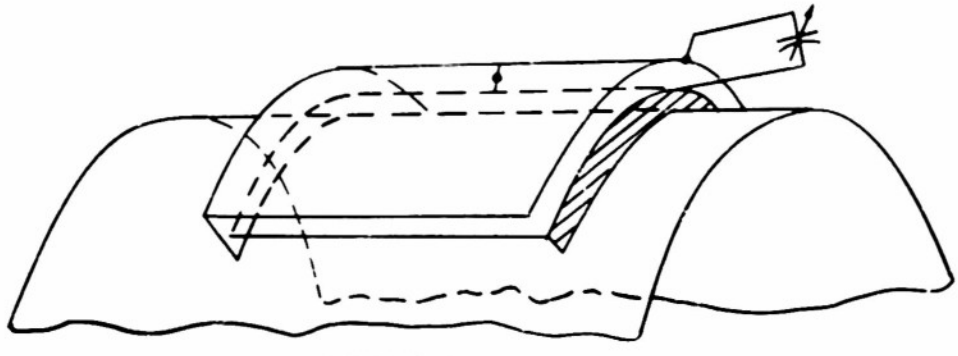

FIGURE 1c

2. Antenna Impedance Data

An approximate analysis of the impedance characteristics of this antenna is carried out in Appendix V. When the tap point is properly positioned, it is expected that the input impedance will vary from about 20 ohms at 100 mc up to 120 ohms at 40 mc. Figure 2 is a plot of the untuned antenna impedance as measured on a 1/10th scale AF type aircraft. The measurements indicate the order of magnitude of antenna input impedance which can be expected and present data useful for designing a prototype impedance matching network. The A.I.L. tuning head offers a 50 ohm input impedance and a servo output capable of driving a tuning condenser. The antenna impedance is inductive over the band so that tuning the condenser to anti-resonance of the circuit and tapping down the strip transmission line (Fig. 1) to an appropriate point yields a useful matching network.

The tapped down impedances at 40 mc 63 3 mc and 100 mc have been calculated and are listed below. The tap point was chosen to minimize the S.W.R.

Frequency	Anti-resonance Impedance	Tap Point Resistance
40 mc	1450Ω	46Ω
63.3 mc	1560Ω	84Ω
100 mc	555Ω	30Ω

Figure 3 indicates the tuning capacity necessary for the anti-resonant condition versus the frequency.

The possibility of using a *folded* wing-edge antenna to decrease vertical polarization sensitivity was mentioned. A plot of this antenna impedance is shown in Fig. 4. Folding the antenna doubles the length of the strip transmission line which accounts for the impedance passing through anti-resonance as indicated in the figure.

These impedance studies made of the partial-sleeve antenna on the Grumman Guardian model indicate that it should be feasible to arrange a condenser with suitably shaped plates servo driven from the A.I.L. tuning head, to tune the antenna over the band and thus provide a good match to the 50Ω input of the receiver.

3. Sensitivity Data

When an antenna is used for reception the important criterion of performance is system sensitivity or signal-to-noise ratio developed at receiver input, rather than antenna impedance characteristics. If the system sensitivity is more than adequate (over the frequency band of interest) impedance characteristics may be quite immaterial.

When tuned, the efficiency and sensitivity of the partial-sleeve antenna are remarkably high for an antenna that is electrically small. One of the reasons for this desirable result is that when mounted on a curved surface, such as the leading edge of the wing, the antenna takes advantage of what can be called "edge effect". Edge effect describes the tendency for current to concentrate along an edge rather than spread over a flat surface. As a consequence the open end of the antenna interrupts relatively large currents induced by the received field intensities, and relatively large voltages are developed across the open end (or across the tuning condenser, if tuned). Theory and experiment have shown that a three-to-seven-fold increase of radiation resistance or radiation conductance due to this edge effect can be expected for an antenna of the size used here, depending upon the sharpness of curvature of the surface on which it is mounted.

In order to estimate the sensitivity of this antenna in the frequency range of interest, laboratory measurements were made with the antenna mounted on the rounded corner of a V shaped ground screen (to simulate the edge of the wing). The results of these measurements are

shown in Fig 5 for the antenna tuned to a midband frequency of 70 mc The curves show voltage developed across a 50 ohm load when immersed in an electric field equal to the free space field intensity that would be radiated by a 100 kw radar (with an assumed antenna gain of 7) at a distance of 100 miles The three curves show the effect of varying the position of the feed point (measured from the shorted end of the antenna). The 50% tap point gives quite satisfactory results if a 5 mc bandwidth is desired (5 mc is the bandwidth of the A.I.L developed RF tuning unit which has been proposed for use on this problem.)

Assuming a receiver with a 6 db noise figure, the noise level at receiver input would be 4 1 microvolts It is seen that the received signal would be 90 to 100 db above noise under the assumed conditions For a low-flying aircraft at an altitude of only 1200 feet and at a distance of 100 miles, the received field intensity can be expected to be about 60 db below the free-space value This still leaves a factor of 30 to 40 db above receiver noise - sufficient to home on the sidelobes of the radar antenna. Hence it is concluded that the antenna when tuned has considerably more than adequate sensitivity Further tests have shown that it is possible to operate the antenna fixed-tuned over about a 20 mc band with some decrease in sensitivity There is reason to believe that the entire 40-100 mc band can be covered with adequate sensitivity using a single fixed-tuned element but as yet this has not been tried experimentally

4. Wing-Edge Partial-Sleeve Antenna Patterns on Navy Type AF Aircraft

In order to find locations that would yield radiation patterns suitable for homing purposes, an extensive series of pattern studies were made using accurate scale models of the aircraft involved The antenna mounting is sketched in Fig 6 Figures 6a through 6m show the field strength patterns obtained with a partial-sleeve antenna mounted on the leading edge of the wing, near the fuselage of a Navy AF type plane The patterns were taken every 100 mc throughout the range 800 mc to 2000 mc on a 1/20th scale model. For the full-size aircraft this corresponds to patterns every 5 mc throughout the range 40-100 mc. The antenna dimensions were $S = \frac{\lambda}{100}$ $W = \frac{\lambda}{10}$ $L = \frac{\lambda}{10}$ at midband frequency

Except for the 800 mc pattern (corresponding to 40 mc full-scale) these patterns are good homing patterns A noteworthy feature is the relatively low response to vertically polarized signals. This feature insures freedom from error which could result from a large pick-up of cross-polarized signal An additional series of patterns* were run to determine the criticalness of the position of the wing-edge antenna with respect to the fuselage. The conclusion drawn was that the open end of the wing-edge-mounted antenna could be located anywhere between 6 cm and 60 cm from the fuselage of the (full-scale) aircraft without adversely affecting the patterns. Beyond this point the patterns deteriorated seriously.

*These patterns, as well as many others not included in this report because of space considerations, are shown in status reports ADF-1 through ADF-5 issued on this project

In order to verify the suitability of these patterns for homing, a model homing system, described in Appendix I, was built. Results obtained on the model system indicated excellent homing pattern sensitivity* and definition** using these patterns. The model system was also used to investigate the effects of propeller modulation which were shown to be negligble.

5. Rudder-mounted Antennas for Vertical Polarization Homing

It has been pointed out that a radar operating in this frequency range must use horizontal polarization in order to obtain a large reflection from the aircraft. However, in case there should be need for homing on vertically-polarized signals, experiments were undertaken to locate a suitable antenna position on the vertical rudder which might be expected to result in appreciable pick-up of vertical polarization. The mounting is sketched in Fig. 7. The patterns are shown in Figs. 7a-7m. The antenna in this case is of the same type as the fixed, flush, wing-edge antenna except that it is mounted flush with the side of the rudder rather than being wrapped around a wing-edge. The radiation conductance is not as great in this configuration as in the wing-edge antenna due to its not being wrapped around a sharp edge. For vertical homing there is no suitably disposed sharp edge available on the aircraft. The antenna dimensions are the same as used in the wing-edge mount, namely $S = \frac{\lambda}{100}$, $W = \frac{\lambda}{10}$, and $L = \frac{\lambda}{10}$ at midband frequency. From 800 mc through 1000 mc (corresponding to 40 mc through 50 mc full-scale) the patterns indicate a high definition and low sensitivity in a homing system. From 1100 mc through 1300 mc the homing system would have a low definition with moderate sensitivity. From 1400 mc through 2000 mc the homing system would show both a rather high sensitivity and definition.

This group of patterns was the most useful of those obtained for vertical polarization homing. They are much less satisfactory than those obtained with the wing-edge antennas. The high sensitivity to horizontally polarized signals would be apt to render the rudder-mounted antennas useless for signals of mixed polarization. However the use of the folded form of partial-sleeve antenna shown earlier (Fig. 1c) should be effective in reducing the response to the undesired polarization. In contrast with these rudder-mounted antennas, the wing-edge mounted antennas show a very low sensitivity to vertically polarized signals. An aircraft having both wing-edge mounted antennas and rudder-mounted antennas could successfully use the wing-edge antennas for most signals, and could switch over to the rudder-mounted antennas only when an extremely low response by the wing-edge antennas indicated that received signals were vertically polarized. This fact would then be verified by a large response from the rudder-mounted antennas.

---

*Homing pattern sensitivity is a comparative measure of the pattern *magnitude* at the crossover point to the maximum pattern magnitude.

**Homing pattern definition is a measure of the pattern *slope* at the crossover point. A large slope at crossover results in a large deflection per degree off-course.

It is concluded that if it is necessary to be able to home on vertically-polarized signals such homing can be achieved However the relatively small reflection from the aircraft for vertical polarization as compared with horizontal polarization seems to insure that only horizontally polarized signals are likely to be of interest in this frequency range.

6. Fuselage-Mounted Partial-Sleeve Antenna on Navy Type P4M Aircraft

An extensive series of antenna patterns were run for a partial-sleeve antenna mounted at various positions along the leading edge of the wing of a P4M aircraft. With the antenna mounted between the fuselage and engine the patterns obtained were fairly satisfactory for homing except for a small range of frequencies near midband where a two-lobed pattern was obtained. With the antenna mounted on the edge of the wing but outboard of the engine, the patterns had too much "lean" away from the forward direction to be entirely satisfactory for homing. Finally, a mounting position on the fuselage (Fig. 8) was found which yielded patterns almost ideal for homing These radiation patterns are shown in Figs. 8a through 8i for the frequency range 1300 mc to 2900 mc. For the 1/30 scale model used in this case, the corresponding full-scale frequencies are 43.3 mc to 96.7 mc. These patterns will produce a homing system which has high signal sensitivity, and excellent homing pattern sensitivity and definition over the entire band of frequencies.

7. Conclusions on Homing Systems

Satisfactory homing antenna systems to cover the 40 - 100 mc frequency range have been developed for Navy type AF and P4M aircraft (Because of similarity of aircraft types these results will also apply to Navy type AD and P2V aircraft). The antenna patterns are very good for homing and the antenna sensitivity is excellent. The antennas are electrically-small and may be flush-mounted or mounted externally. They may be tuned over the band by a remotely-operated tuning condenser connected with the associated A.I.L. receiver. Alternatively they may be operated fixed-tuned with good sensitivity over about a 20 mc band or with some decrease of sensitivity they may be operated fixed-tuned over the entire frequency band. These homing antennas may, of course, be used with any of the standard homing systems.

PART I

ILLUSTRATIONS

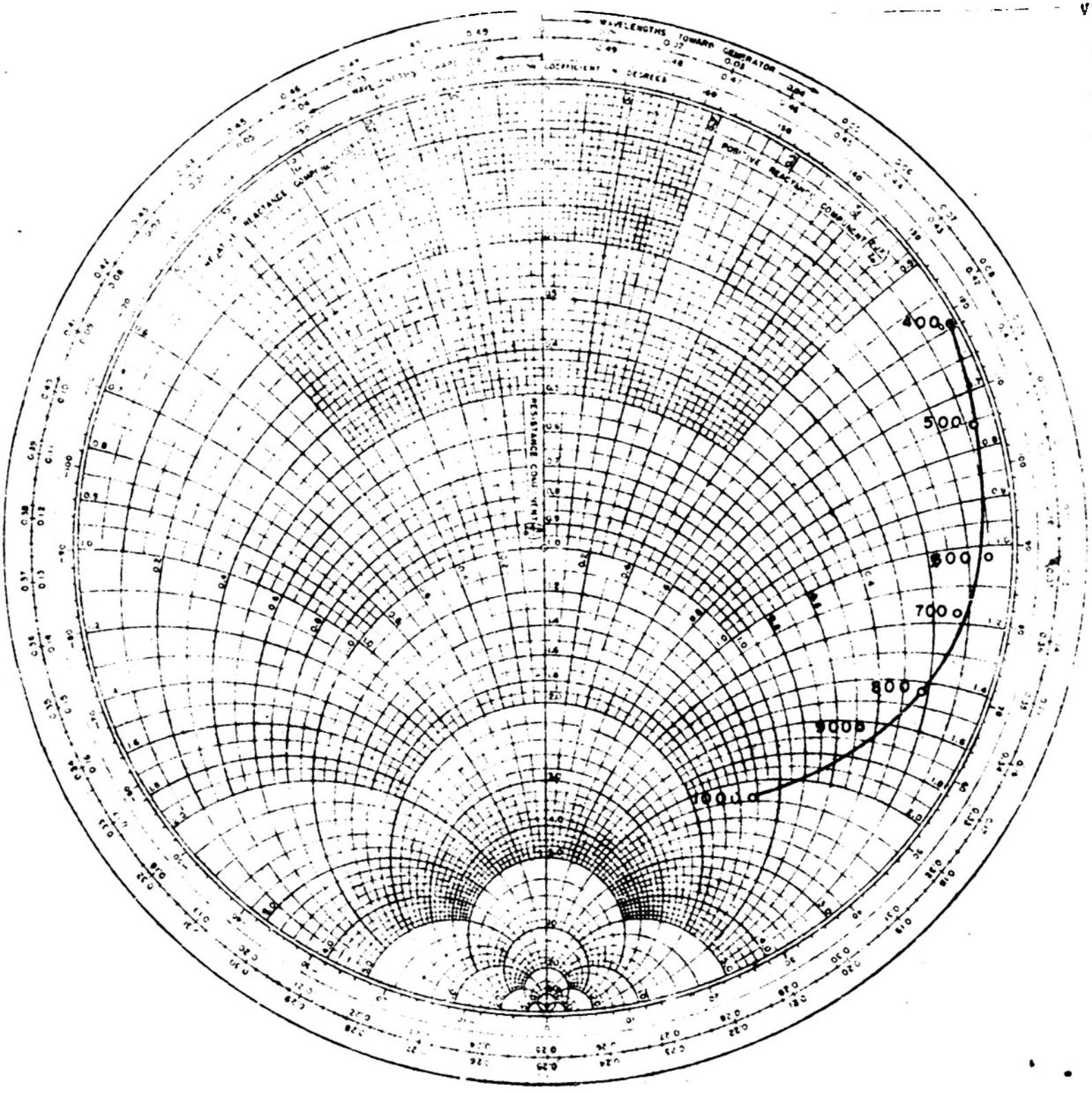
WAVELENGTHS TOWARD GENERATOR
POSITIVE REACTANCE COMPONENTS
RESISTANCE COMPONENTS
400
500
600
700
800
900
1000

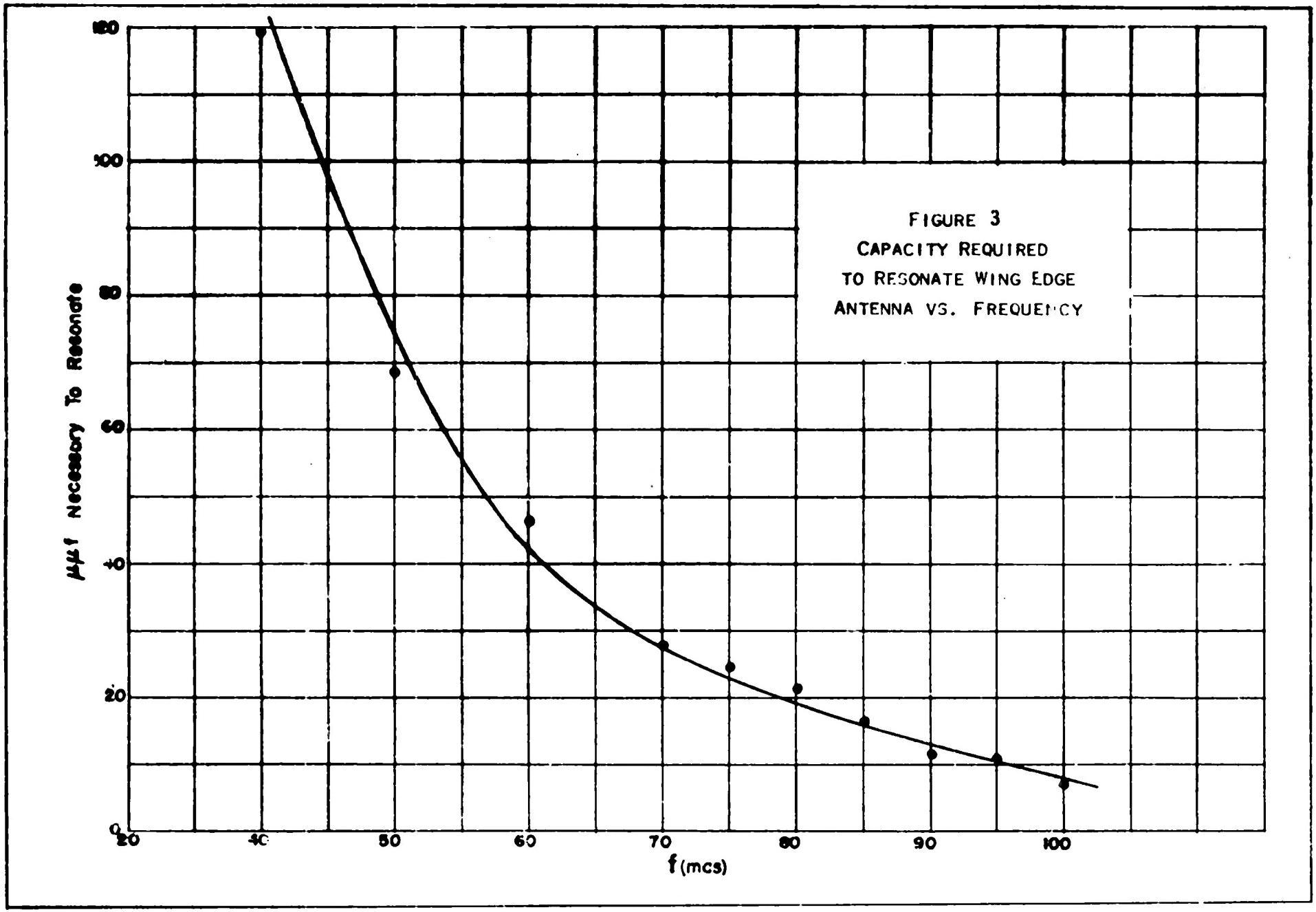

FIGURE 3
CAPACITY REQUIRED
TO RESONATE WING EDGE
ANTENNA VS. FREQUENCY

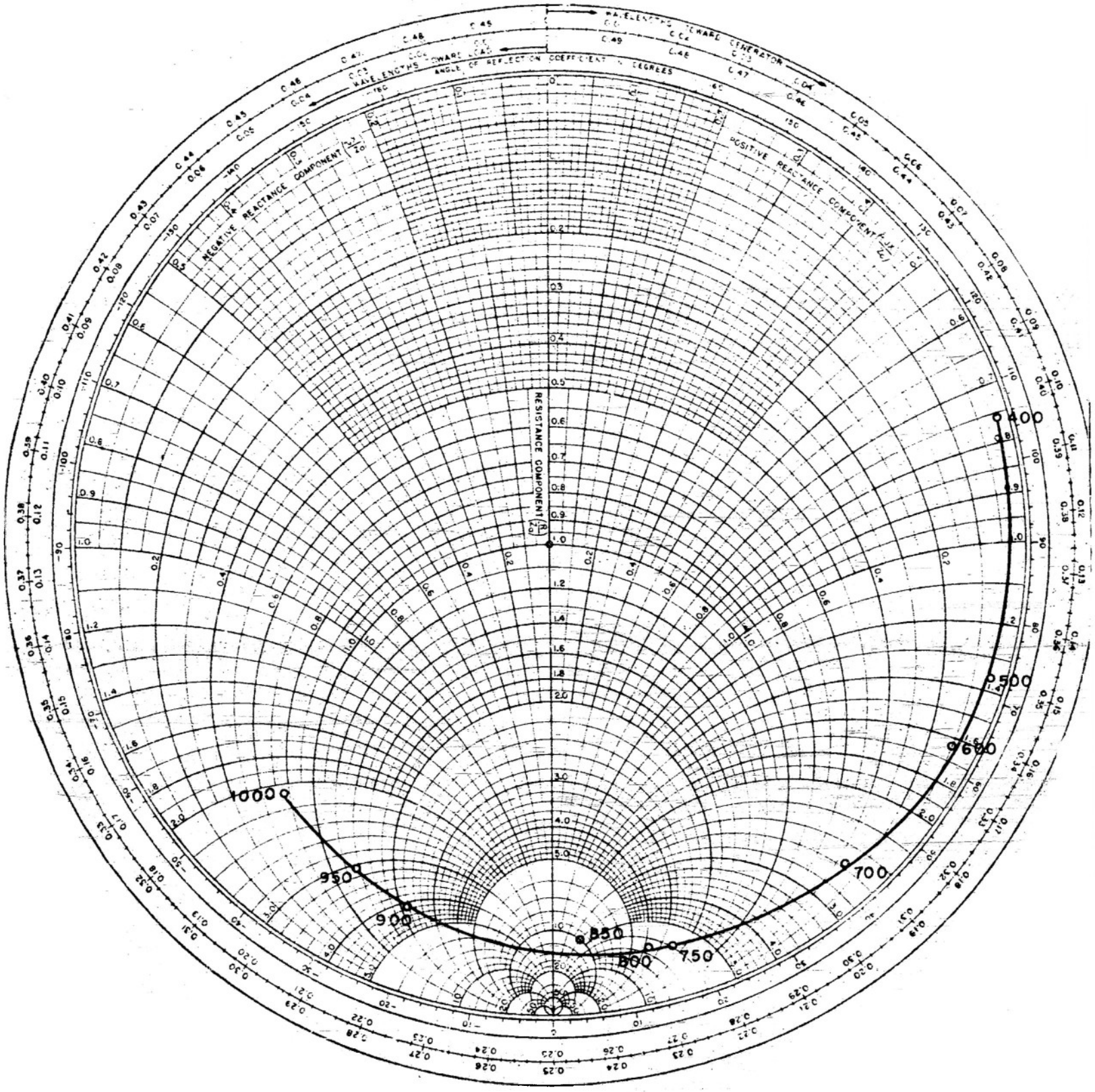

FIGURE 4 - FOLDED WING EDGE ANTENNA MOUNTED ON V-GROUND SCREEN. IMPEDANCE MEASURED WITH HEWLETT-PACKARD SLOTTED LINE

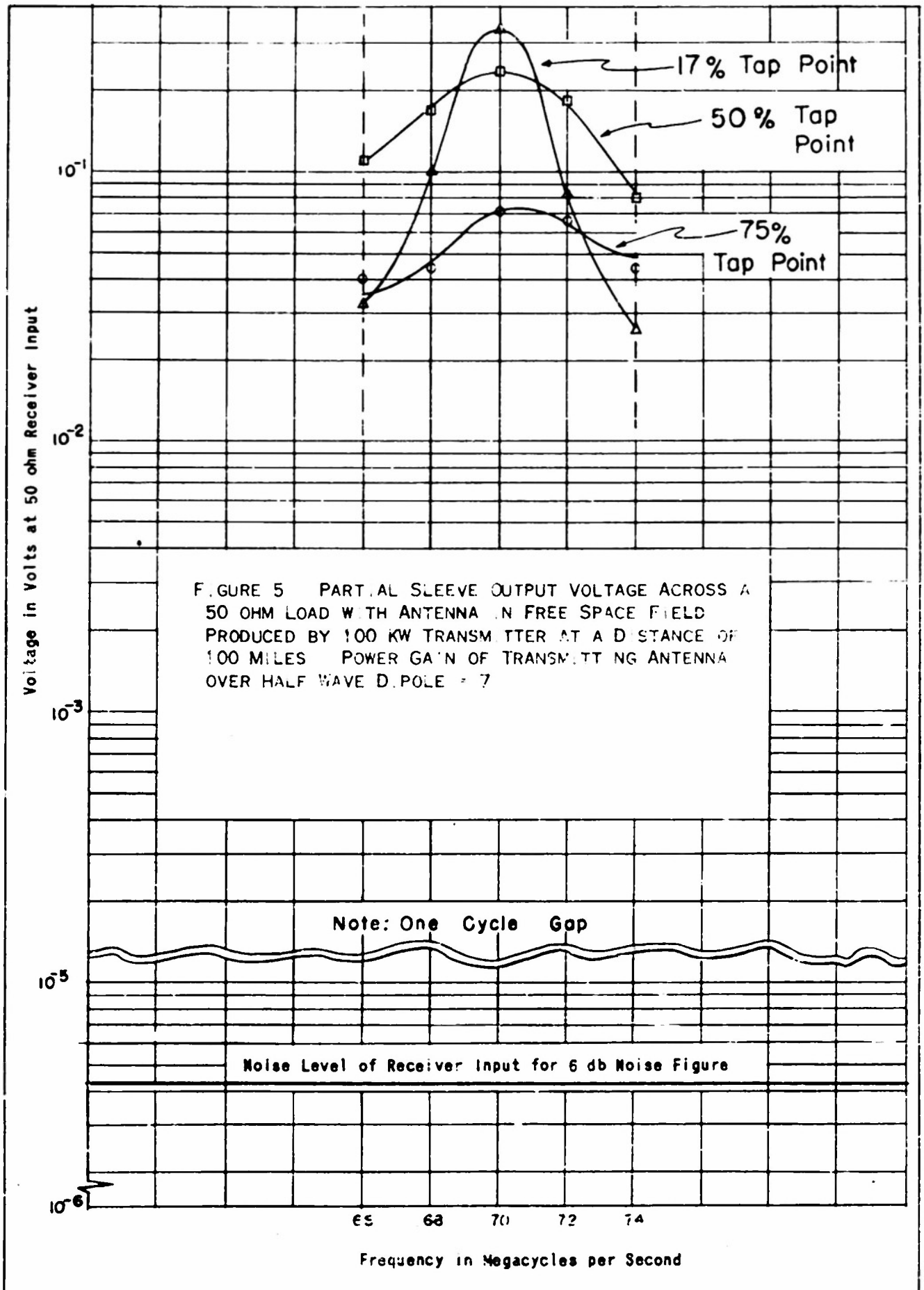

FIGURE 5 PARTIAL SLEEVE OUTPUT VOLTAGE ACROSS A 50 OHM LOAD WITH ANTENNA IN FREE SPACE FIELD PRODUCED BY 100 KW TRANSMITTER AT A DISTANCE OF 100 MILES POWER GAIN OF TRANSMITTING ANTENNA OVER HALF WAVE DIPOLE = 7

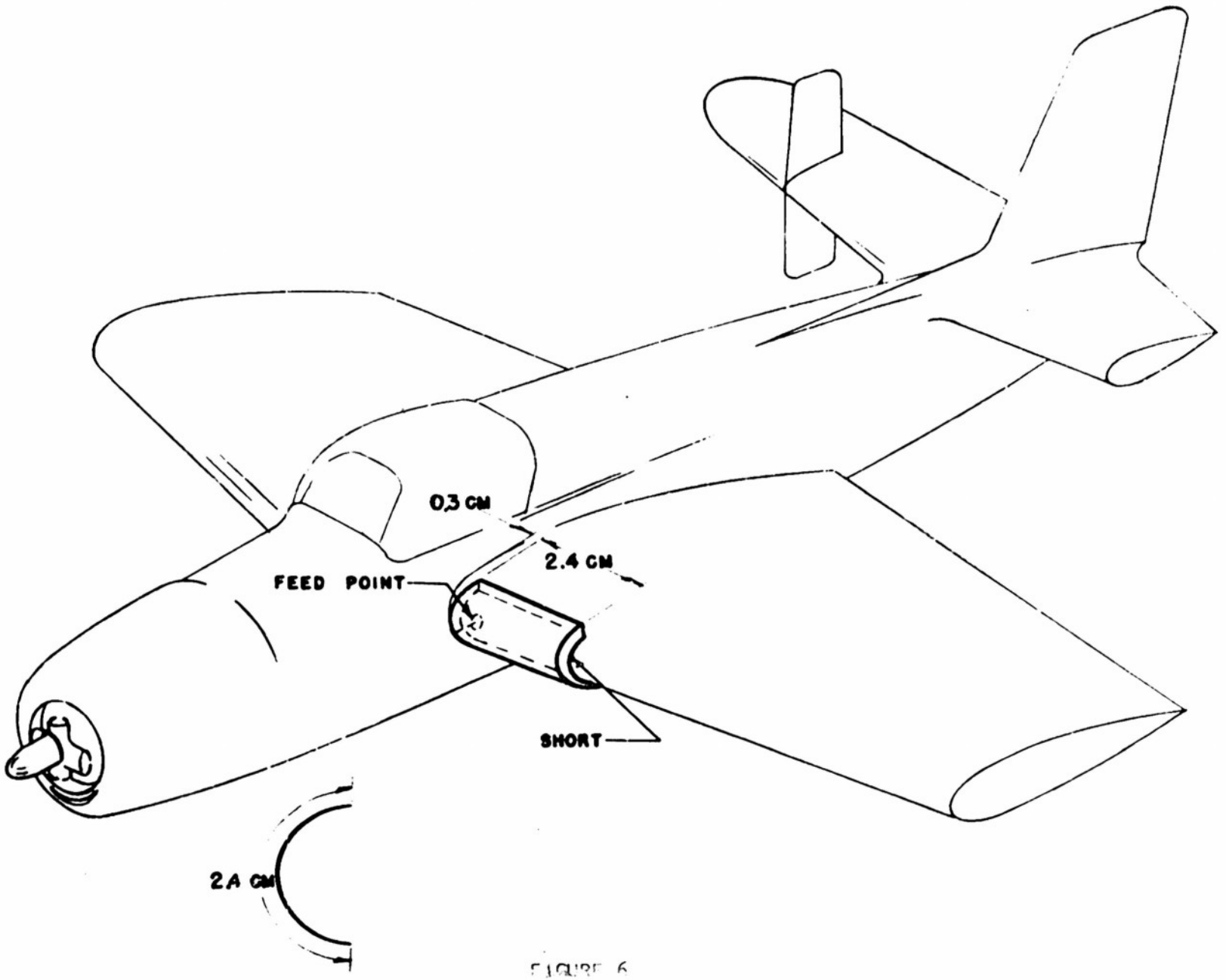

FIGURE 6

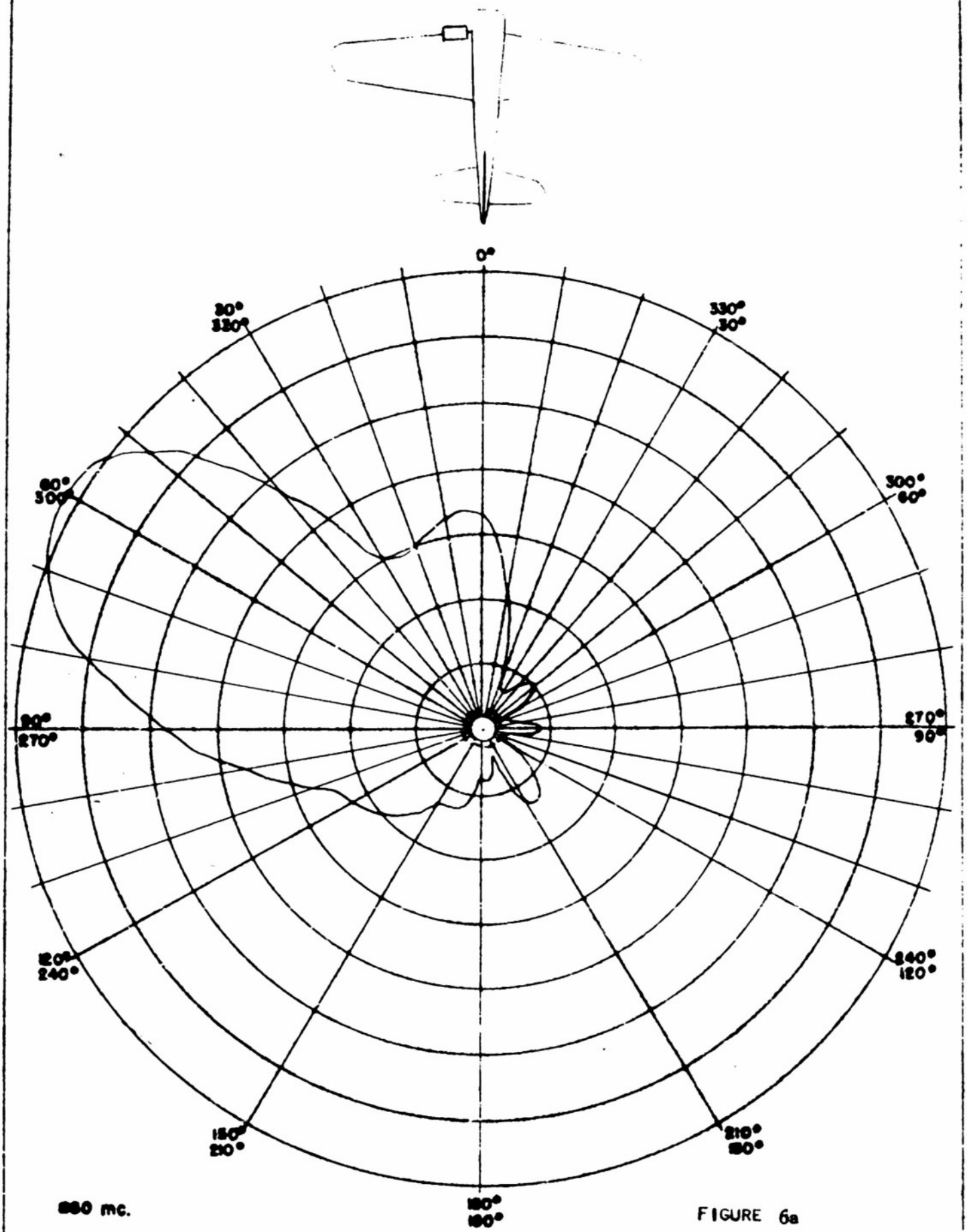
0°
30°
330°
60°
300°
90°
270°
120°
240°
150°
210°
180°
880 mc.
Horizontal Polarization Pattern
Vertical Polarization Pattern

FIGURE 6a

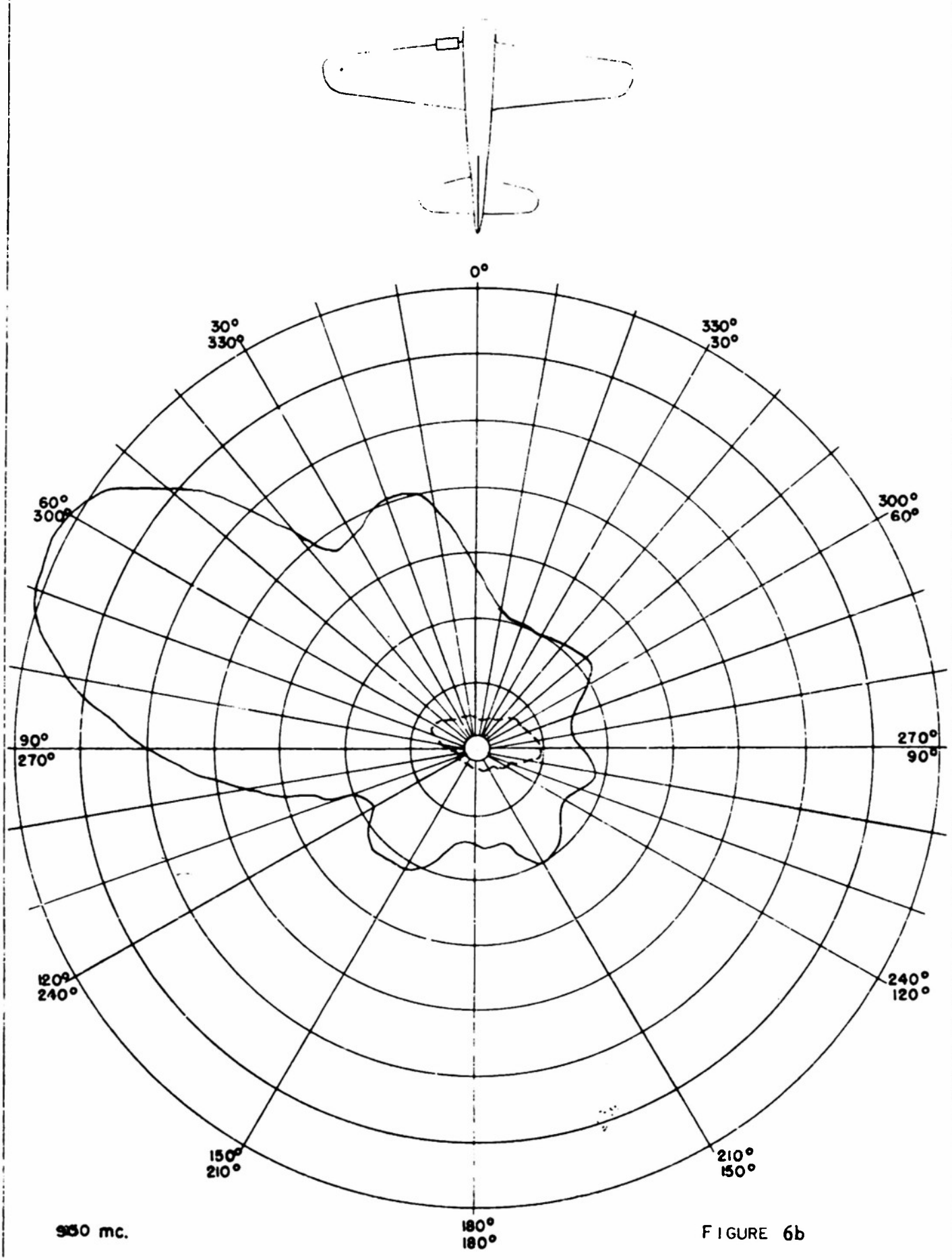
0°
30°
330°
330°
30°
60°
300°
300°
60°
90°
270°
270°
90°
120°
240°
240°
120°
150°
210°
210°
150°
180°
180°
9350 mc.
Horizontal Polarization Pattern
Vertical Polarization Pattern

FIGURE 6b

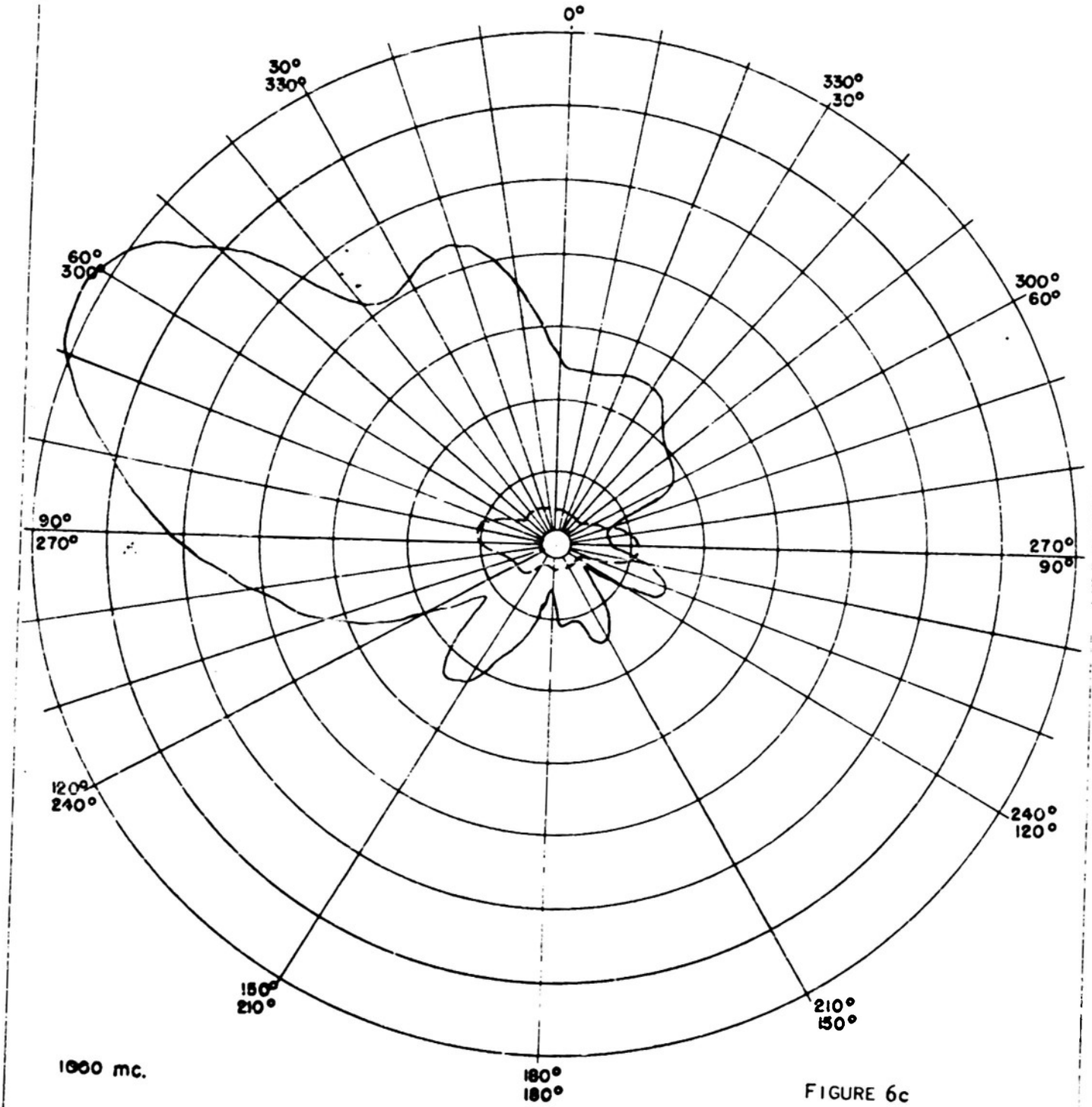

FIGURE 6c

——— Horizontal Polarization Pattern

– – – – – – Vertical Polarization Pattern

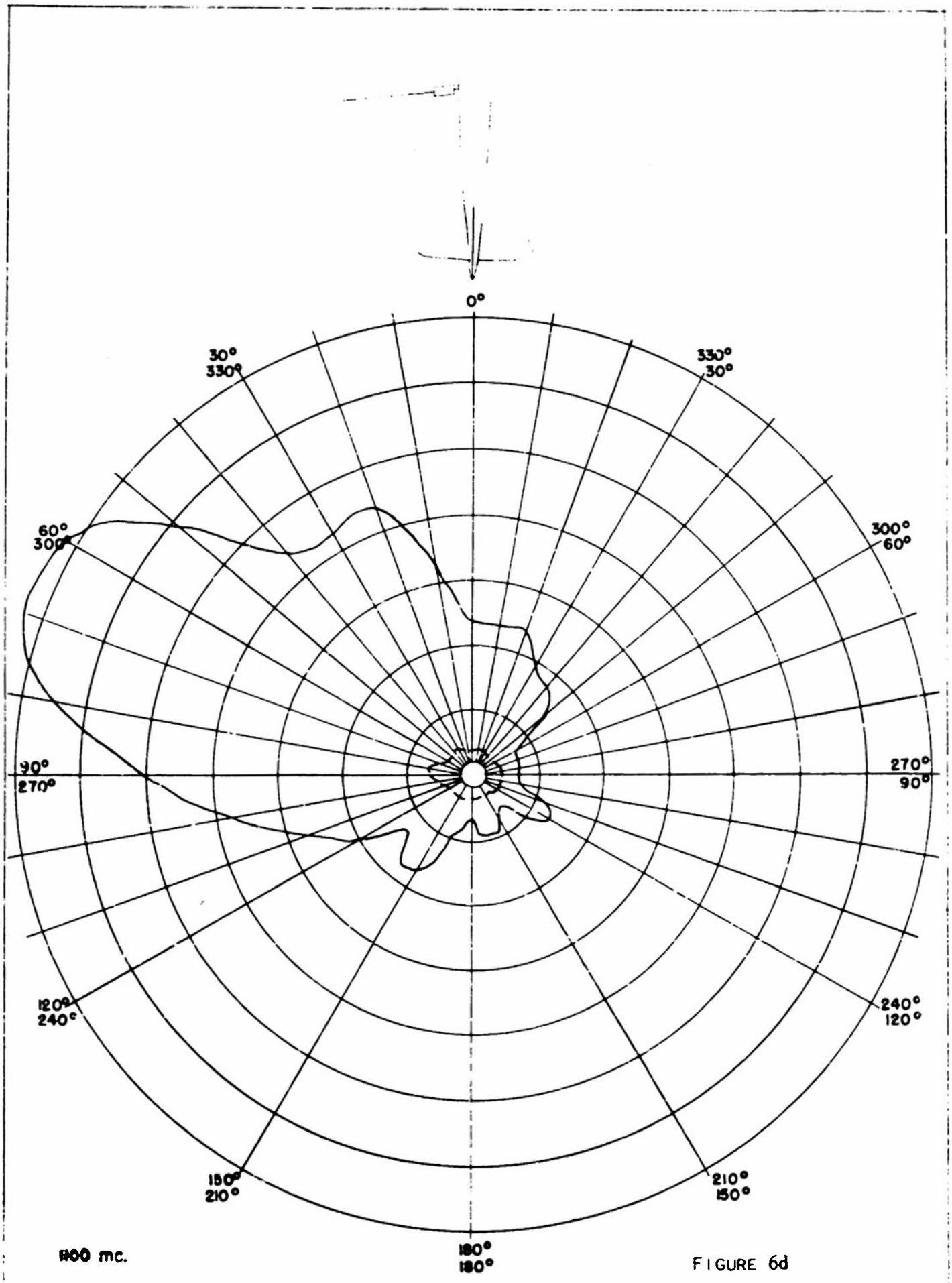

FIGURE 6d

——— Horizontal Polarization Pattern

– – – – – – Vertical Polarization Pattern

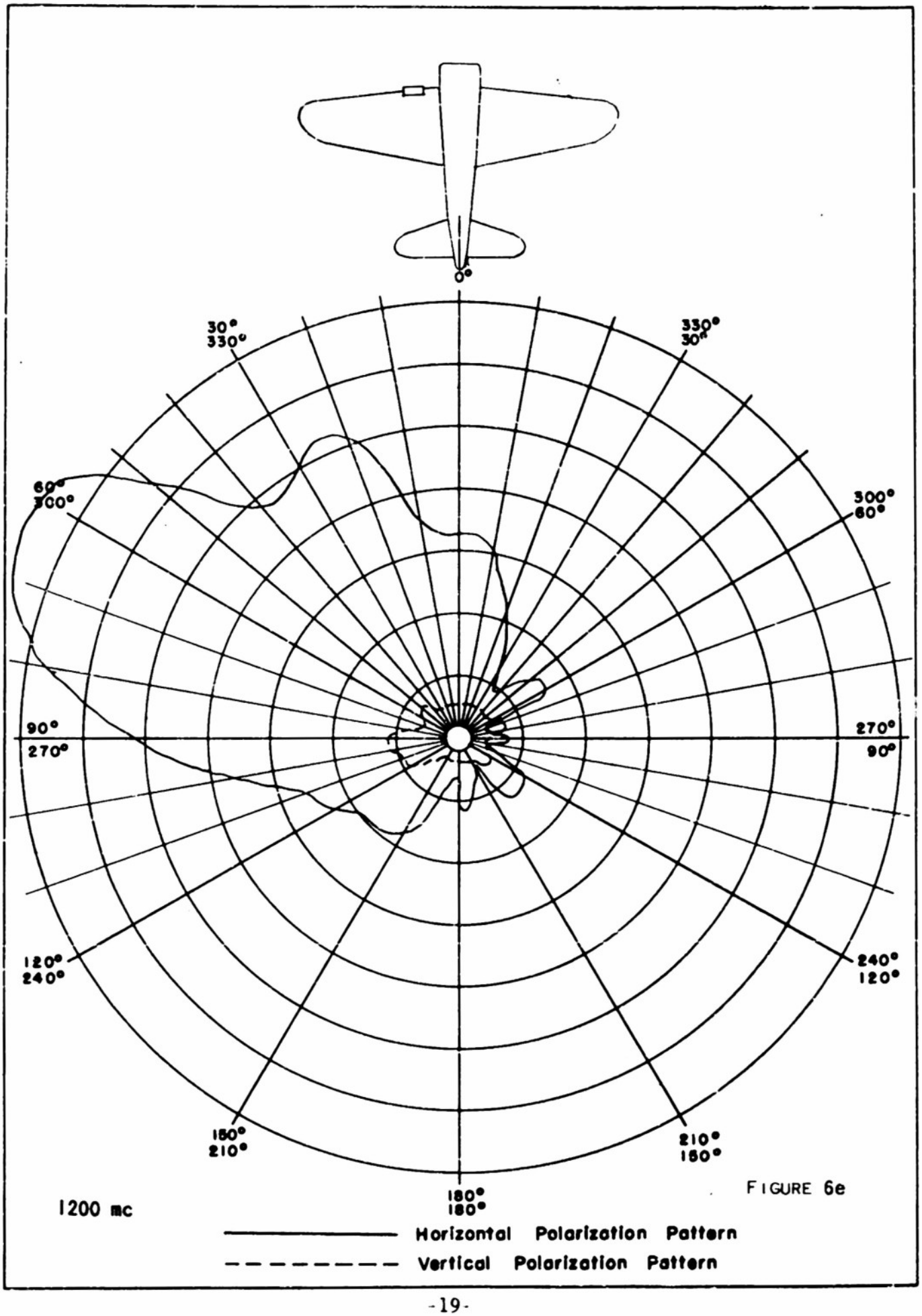
0°
30°
330°
330°
30°
60°
300°
300°
60°
90°
270°
270°
90°
120°
240°
240°
120°
150°
210°
210°
150°
180°
180°
1200 mc
Horizontal Polarization Pattern
Vertical Polarization Pattern

FIGURE 6e

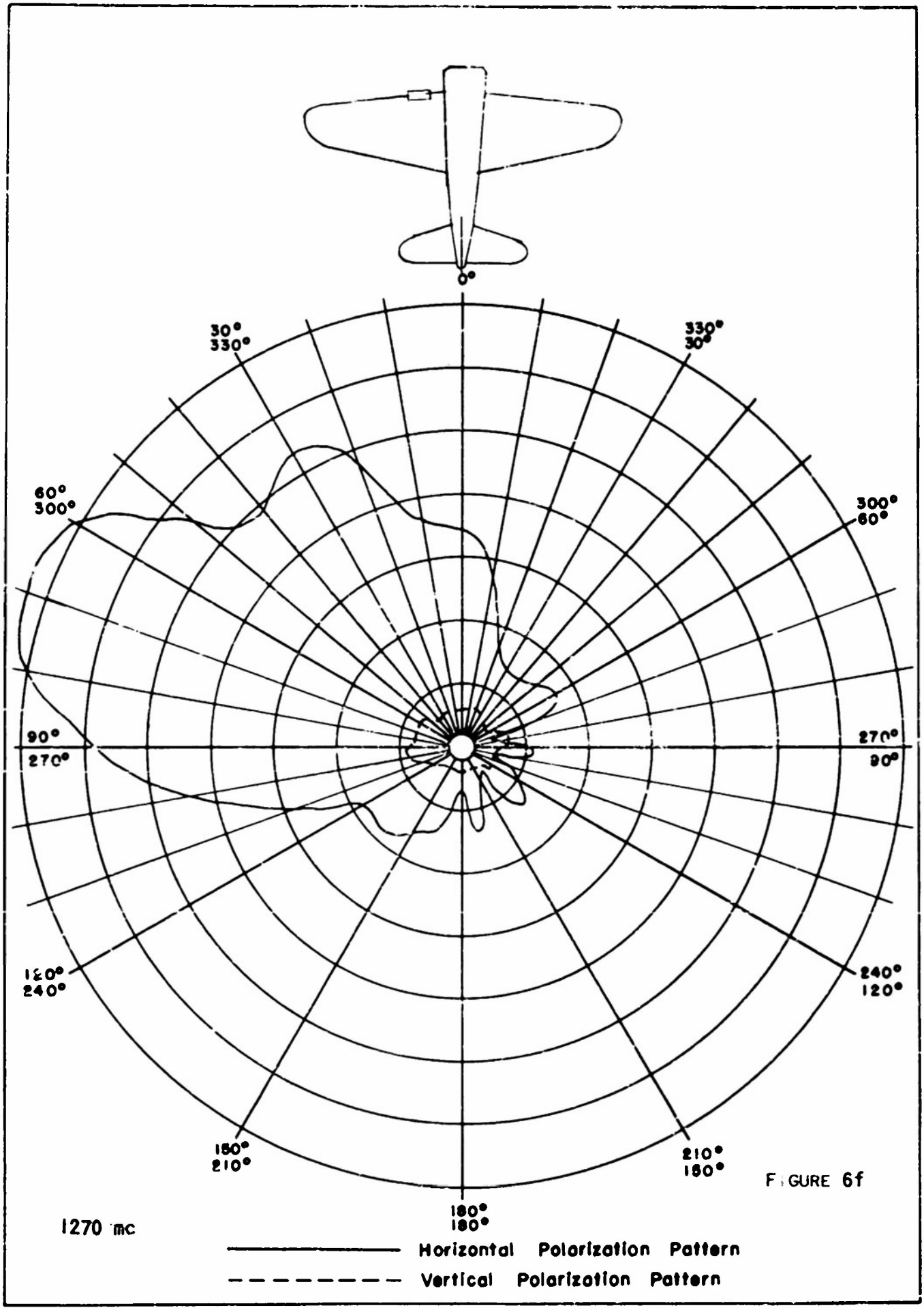
0°
30°
330°
330°
30°
60°
300°
300°
60°
90°
270°
270°
90°
120°
240°
240°
120°
150°
210°
210°
150°
180°
180°
1270 mc
Horizontal Polarization Pattern
Vertical Polarization Pattern

FIGURE 6f

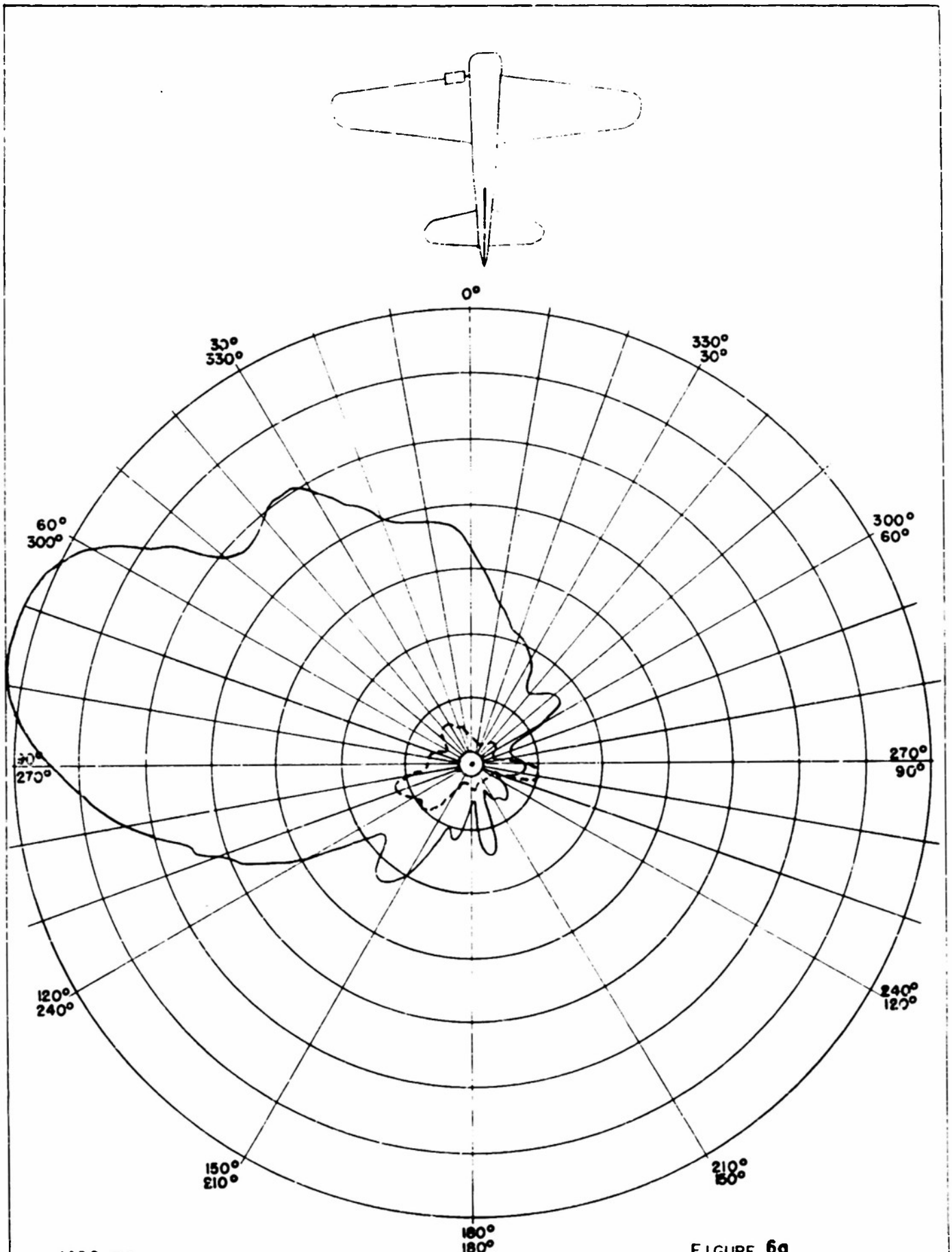
0°
30°
330°
60°
300°
90°
270°
120°
240°
150°
210°
180°
1400 mc
Horizontal Polarization
Vertical Polarization

FIGURE 6g

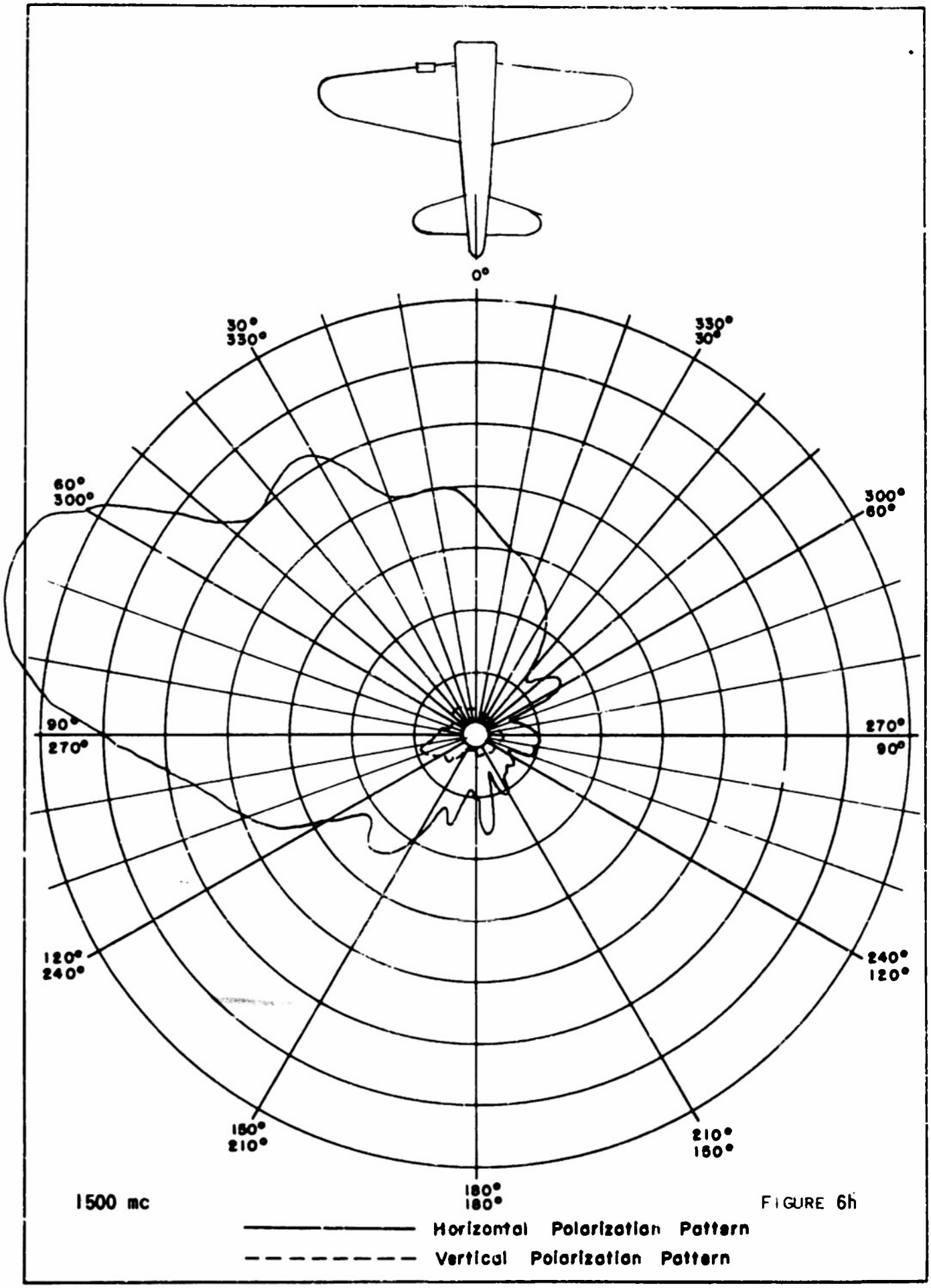
0°
30°
330°
330°
30°
60°
300°
300°
60°
90°
270°
270°
90°
120°
240°
240°
120°
150°
210°
210°
150°
180°
180°
1500 mc
Horizontal Polarization Pattern
Vertical Polarization Pattern

FIGURE 6h

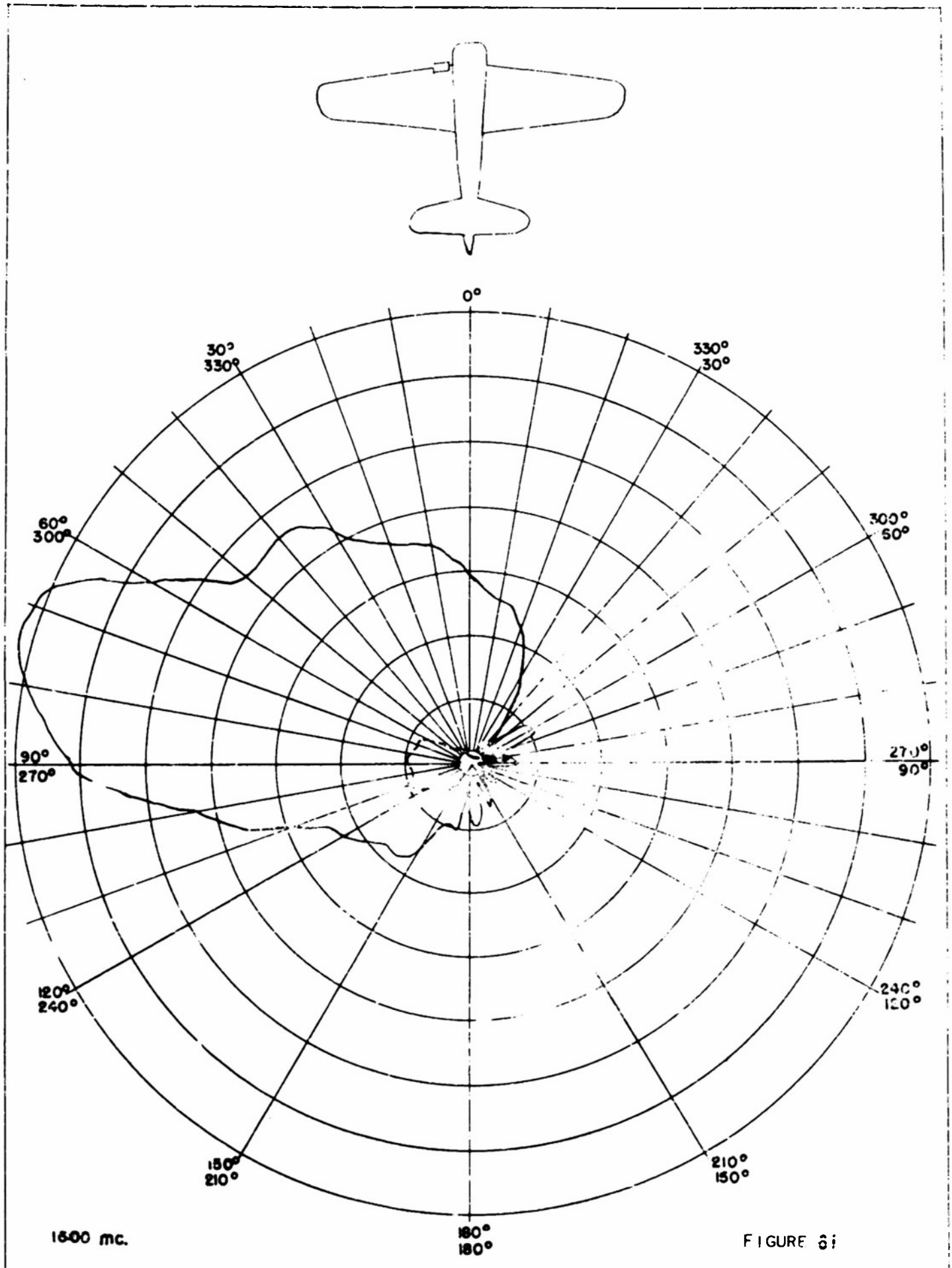
0°
30°
330°
330°
30°
60°
300°
300°
60°
90°
270°
270°
90°
120°
240°
240°
120°
150°
210°
210°
150°
180°
180°
1600 mc.
Horizontal Polarization Pattern
Vertical Polarization Pattern

FIGURE 8

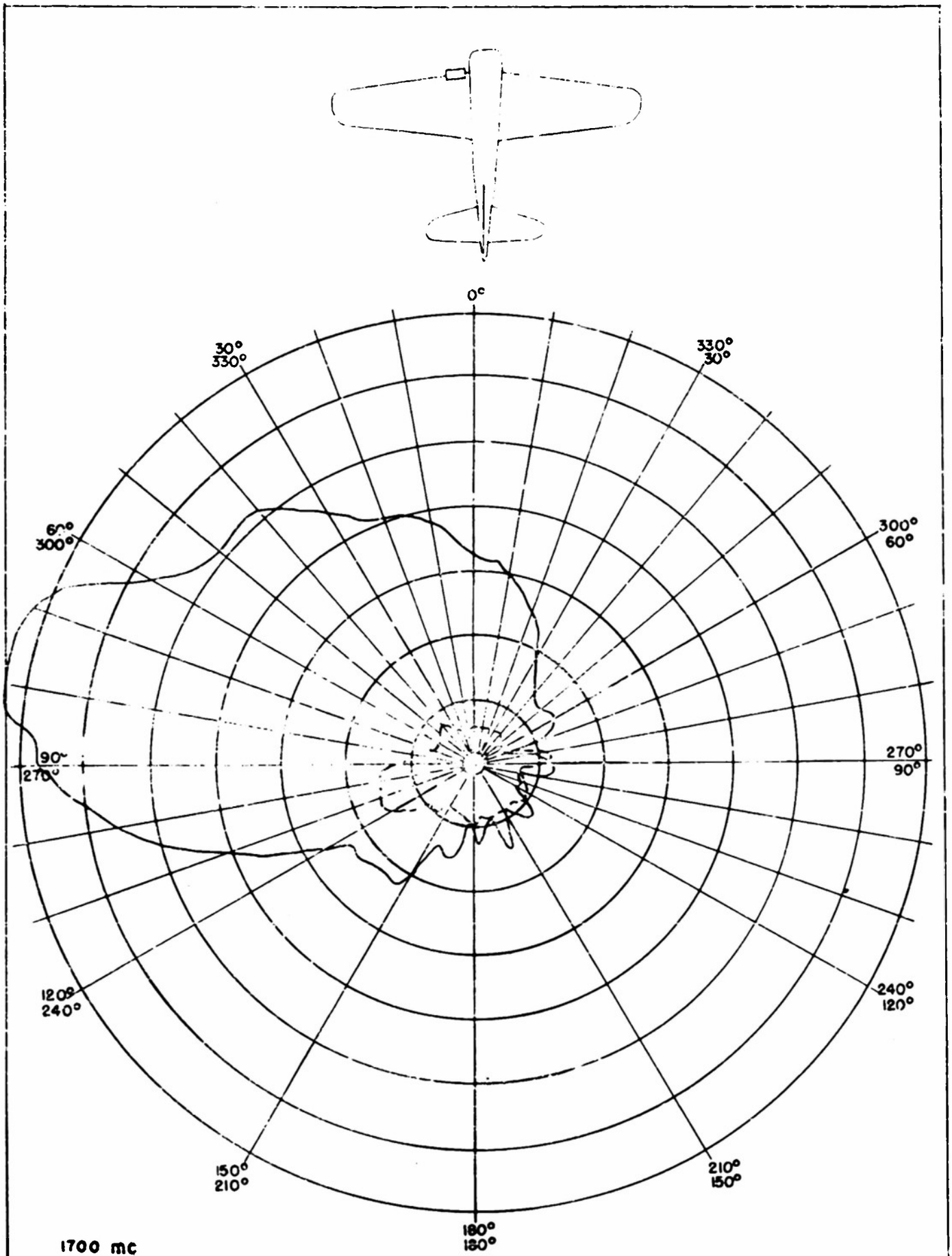
0°
30°
330°
330°
30°
60°
300°
300°
60°
90°
270°
270°
90°
120°
240°
240°
120°
150°
210°
210°
150°
180°
180°
1700 mc
Horizontal Polarization Pattern
Vertical Polarization Pattern

FIGURE 6j

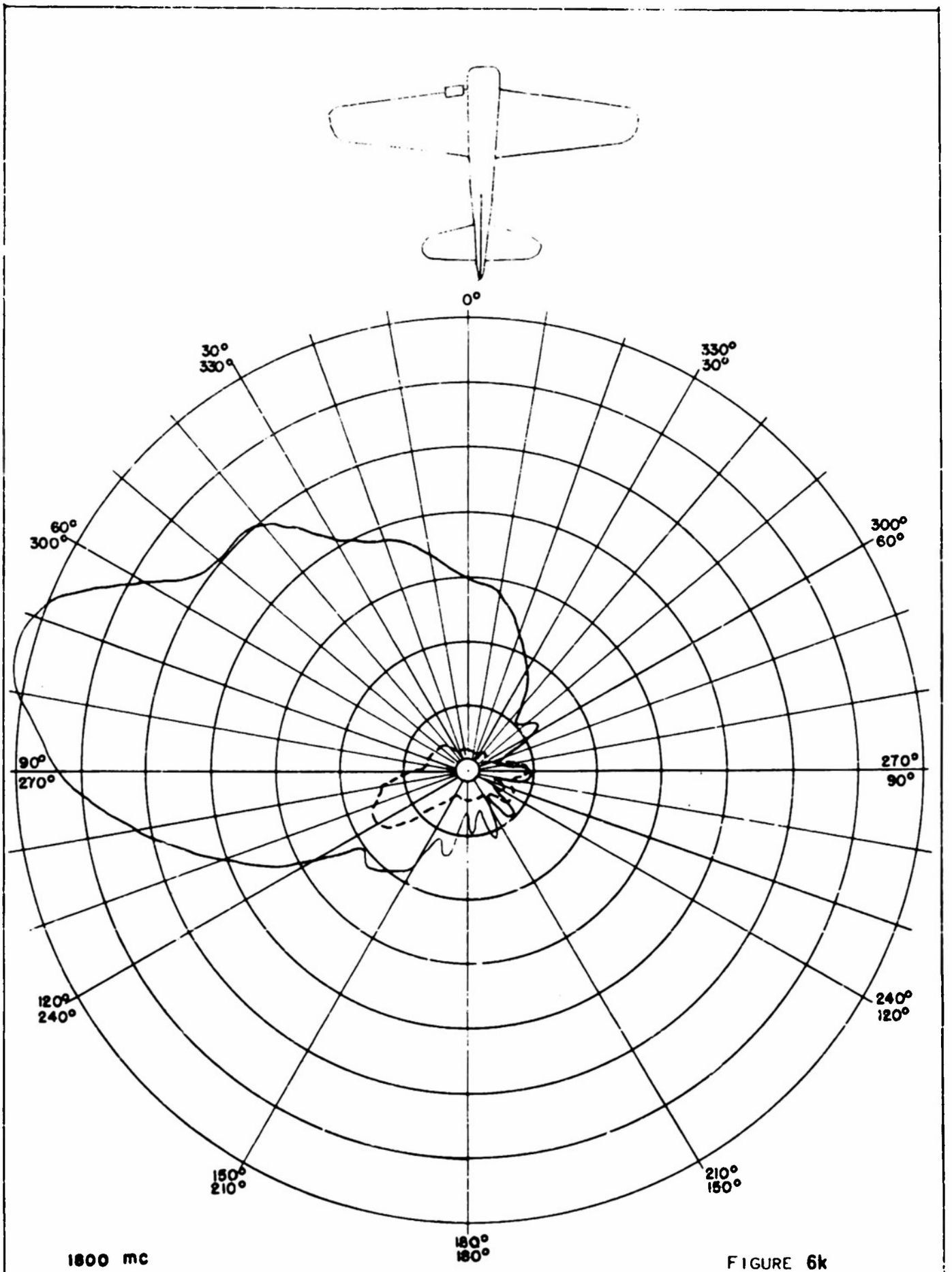

1800 mc

FIGURE 6k

——————— Horizontal Polarization Pattern

- - - - - - - - - - Vertical Polarization Pattern

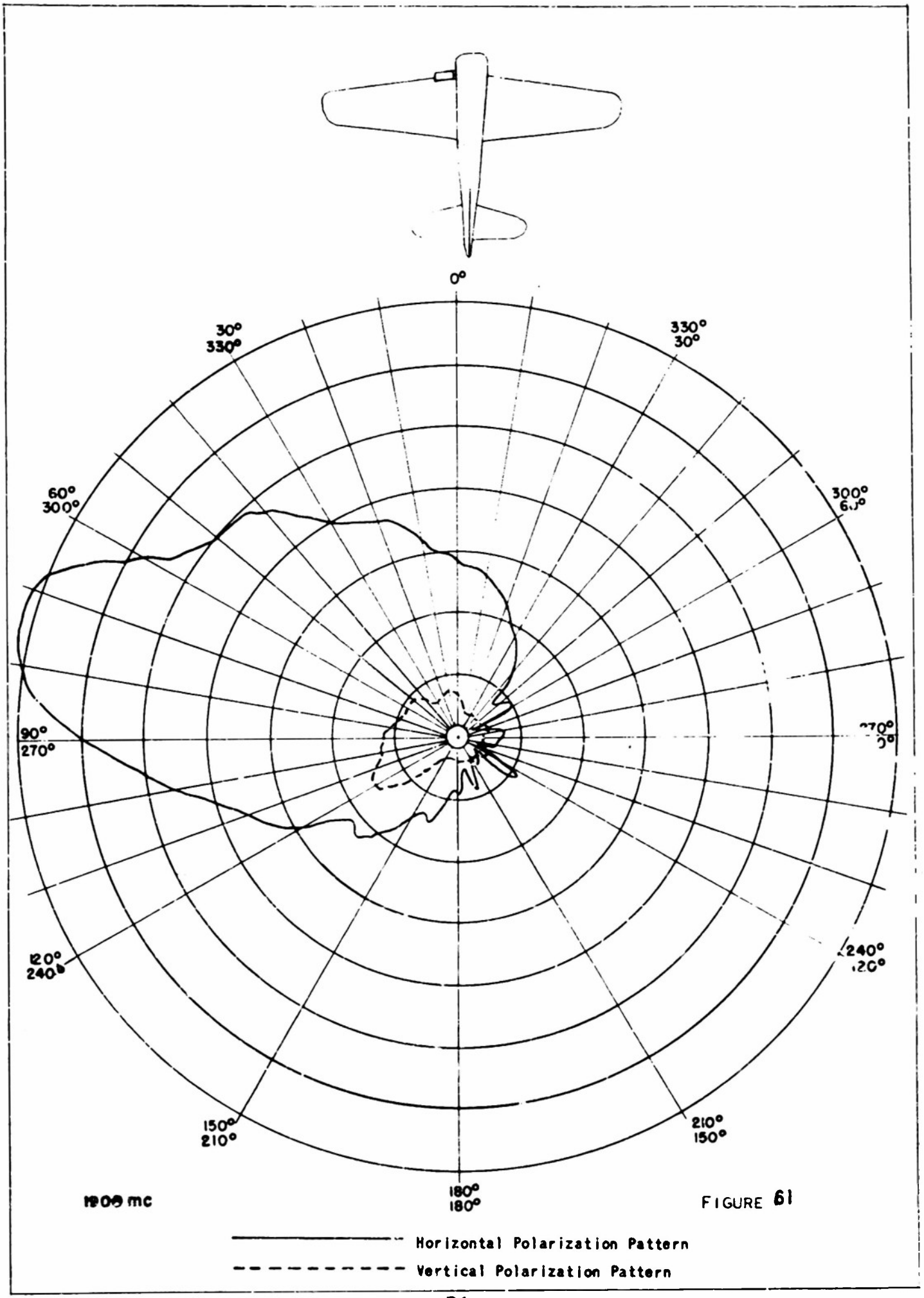
0°
30°
330°
330°
30°
60°
300°
300°
90°
270°
120°
240°
240°
120°
150°
210°
210°
150°
180°
180°
Horizontal Polarization Pattern
Vertical Polarization Pattern

FIGURE 61

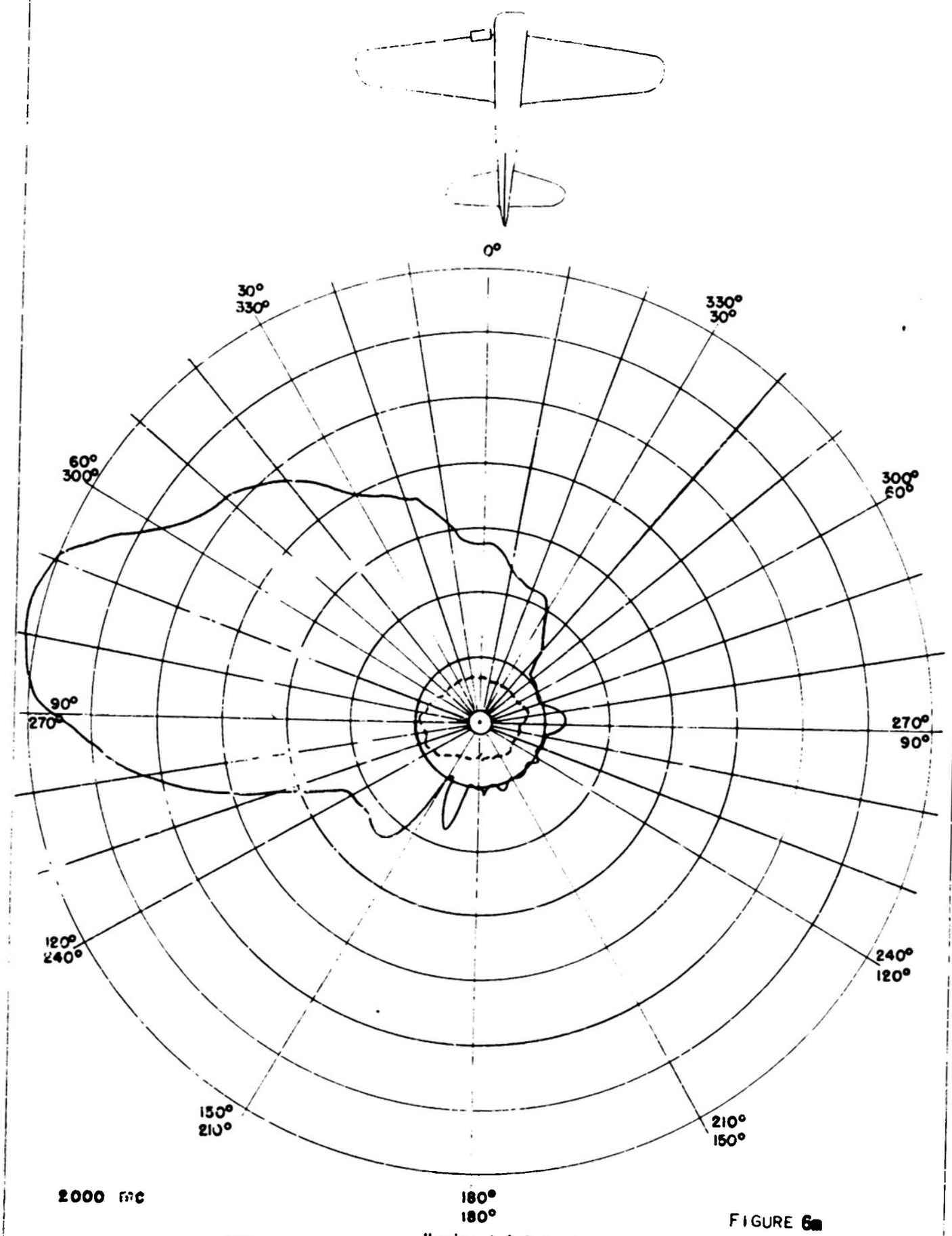

2000 mc

FIGURE 6a

Horizontal Polarization Pattern

Vertical Polarization Pattern

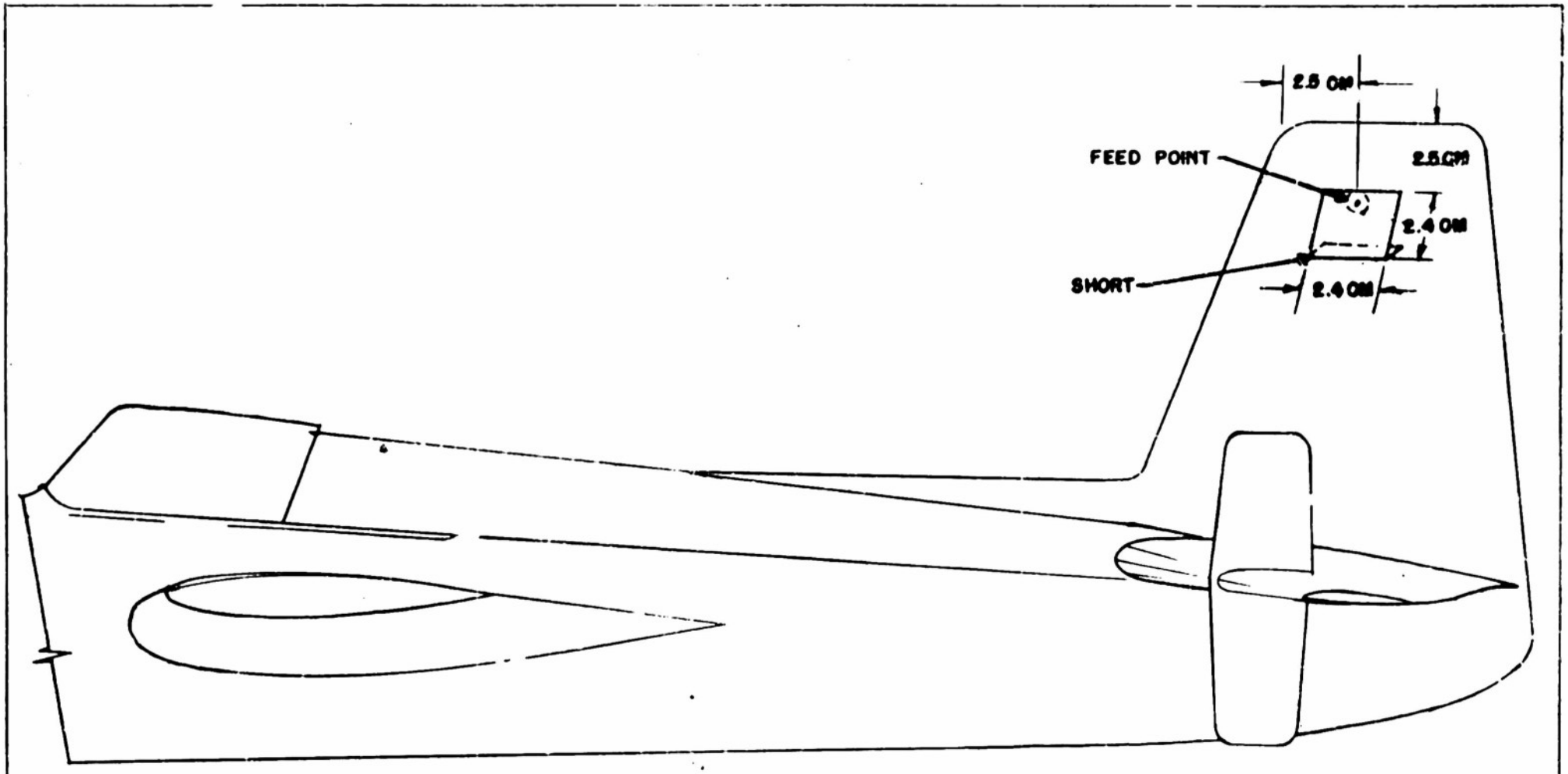

FIGURE 7

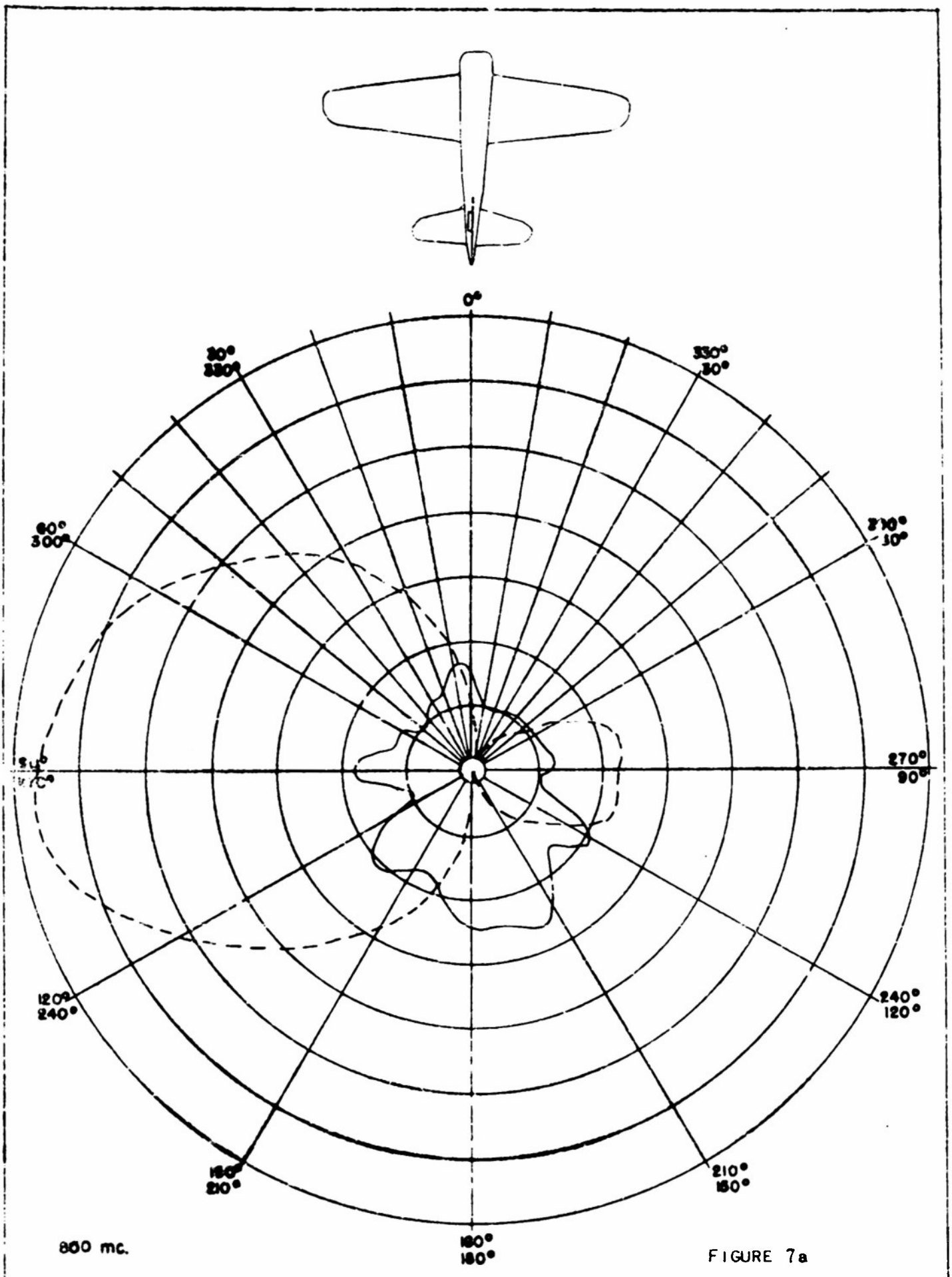
0°
30°
330°
60°
300°
270°
90°
120°
240°
150°
210°
180°
180°
800 mc.
Horizontal Polarization Pattern
Vertical Polarization Pattern

FIGURE 7a

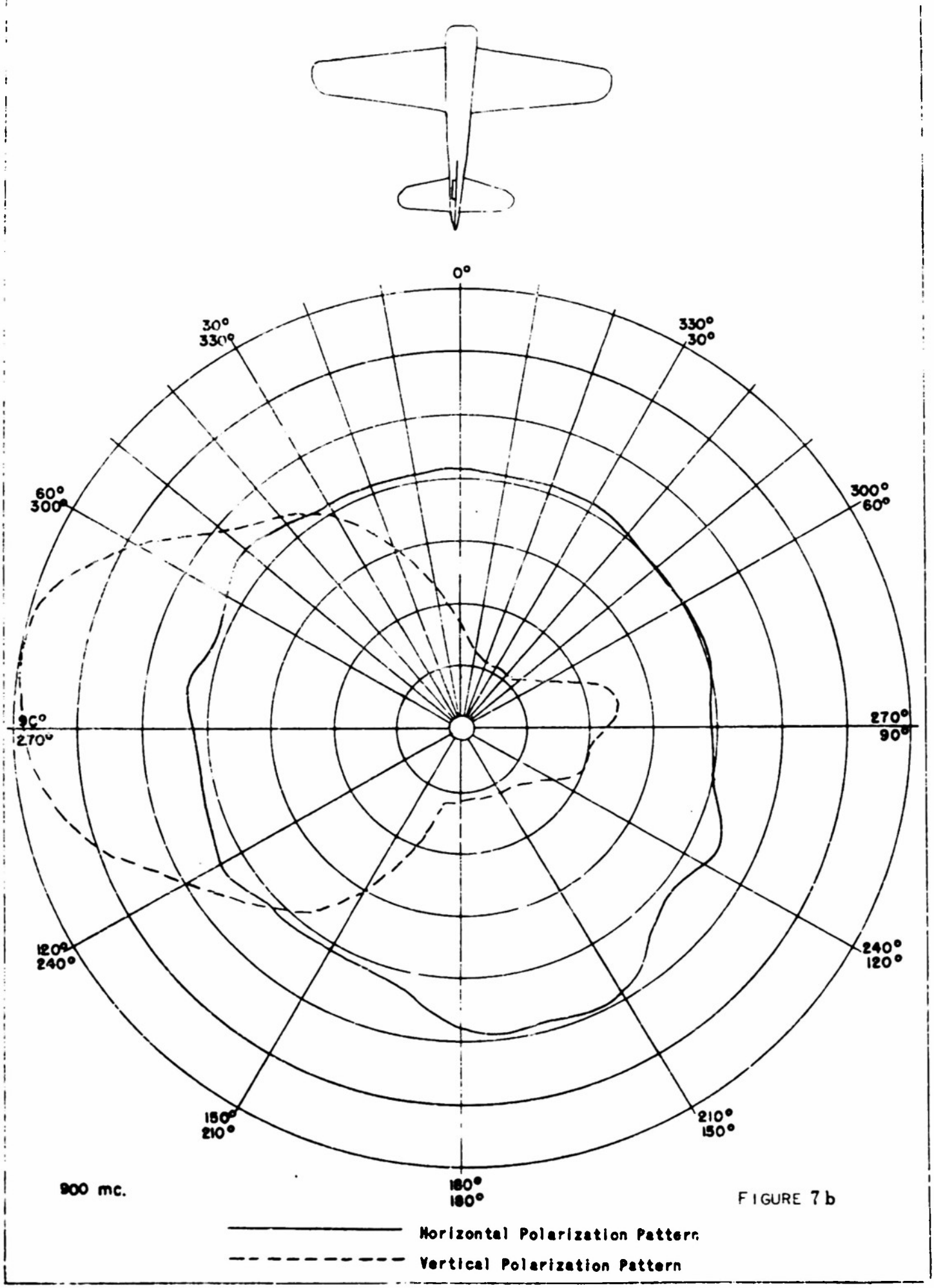
0°
30°
330°
330°
30°
60°
300°
300°
60°
90°
270°
270°
90°
120°
240°
240°
120°
150°
210°
210°
150°
180°
180°
900 mc.
Horizontal Polarization Pattern
Vertical Polarization Pattern

FIGURE 7b

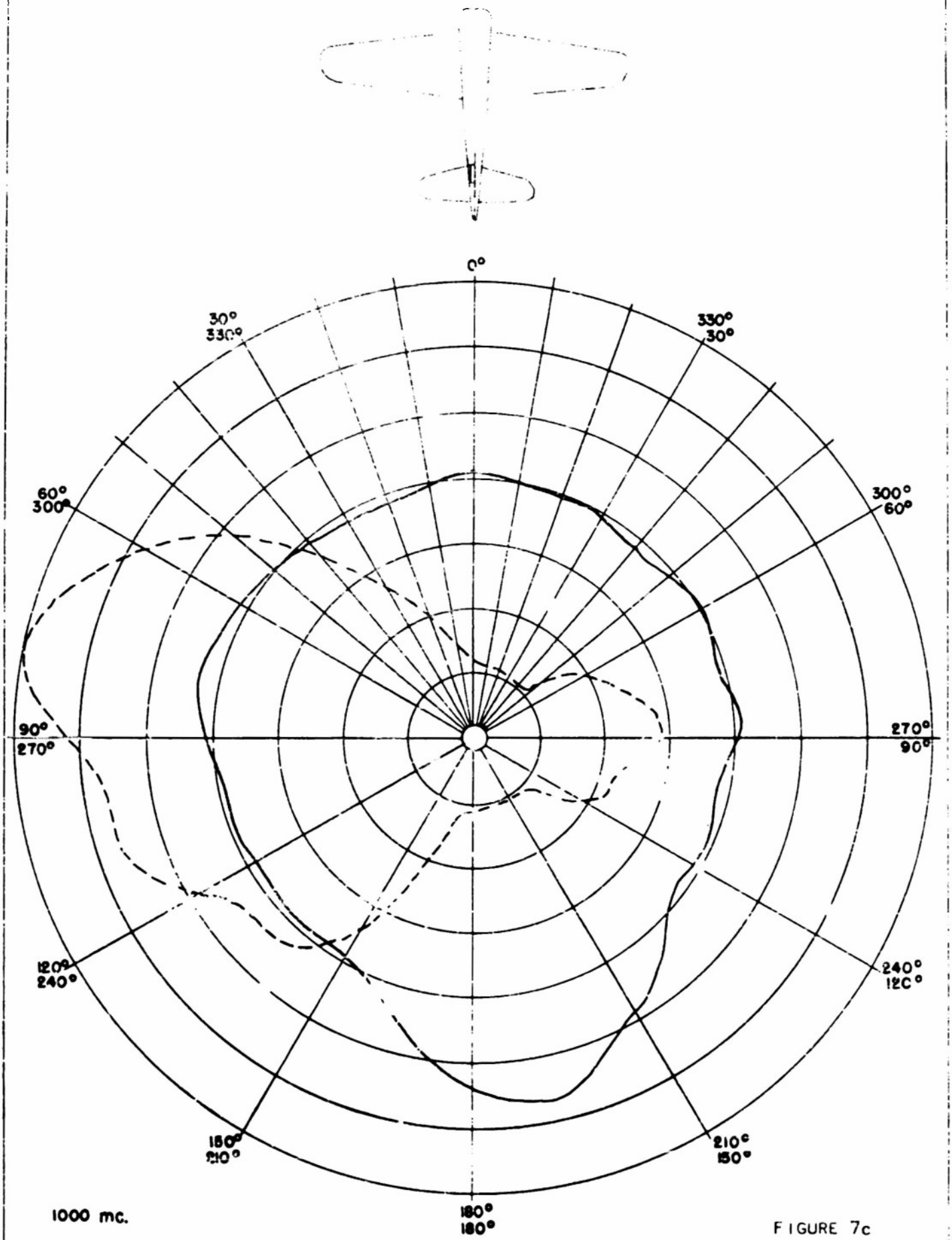
0°
30°
330°
330°
30°
60°
300°
300°
60°
90°
270°
270°
90°
120°
240°
240°
120°
150°
210°
210°
150°
180°
180°
1000 mc.
Horizontal Polarization Pattern
Vertical Polarization Pattern

FIGURE 7c

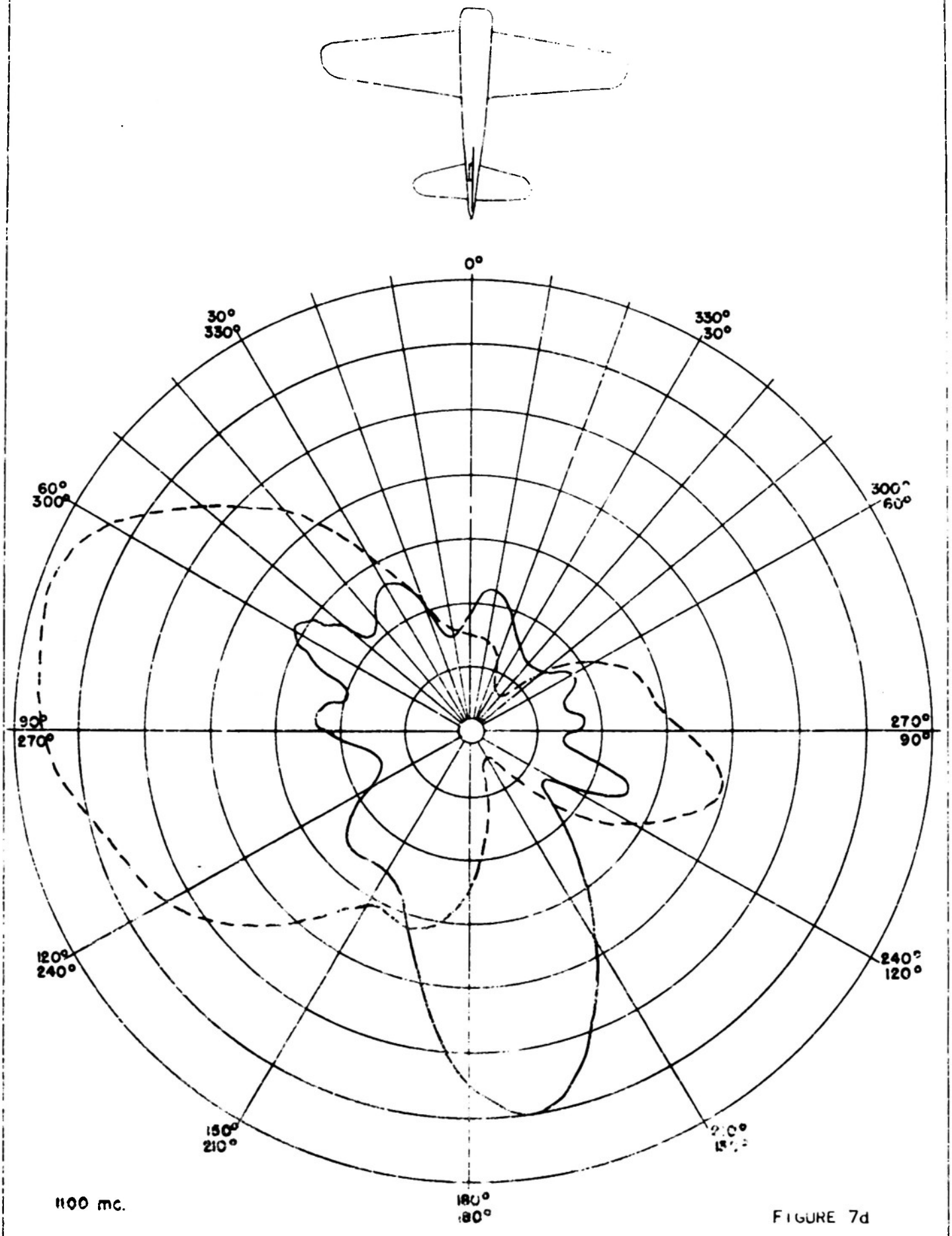

1100 mc.

FIGURE 7d

Horizontal Polarization Pattern

Vertical Polarization Pattern

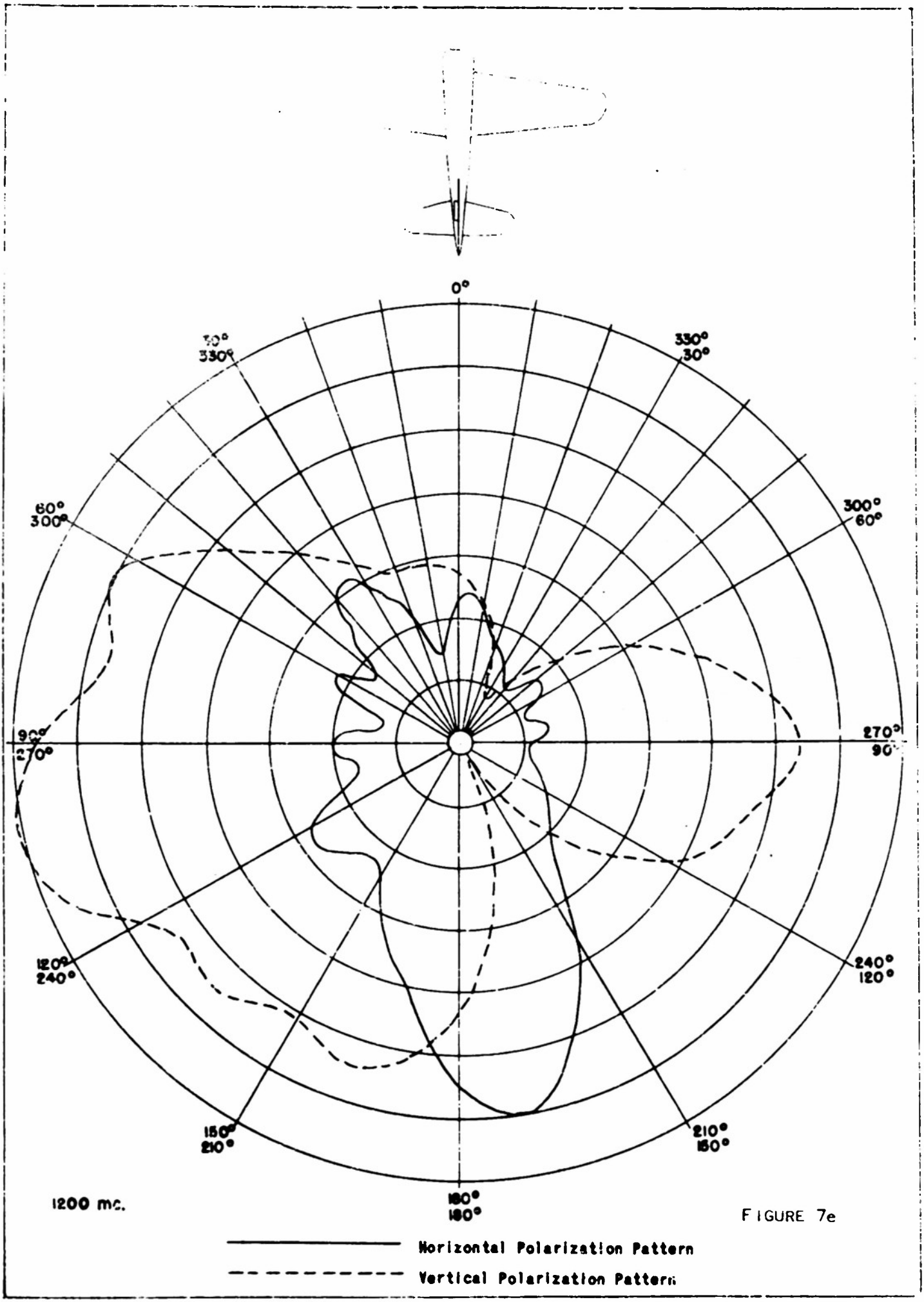
0°
30°
330°
330°
30°
60°
300°
300°
60°
90°
270°
270°
90°
120°
240°
240°
120°
150°
210°
210°
150°
180°
180°
1200 mc.
Horizontal Polarization Pattern
Vertical Polarization Pattern

FIGURE 7e

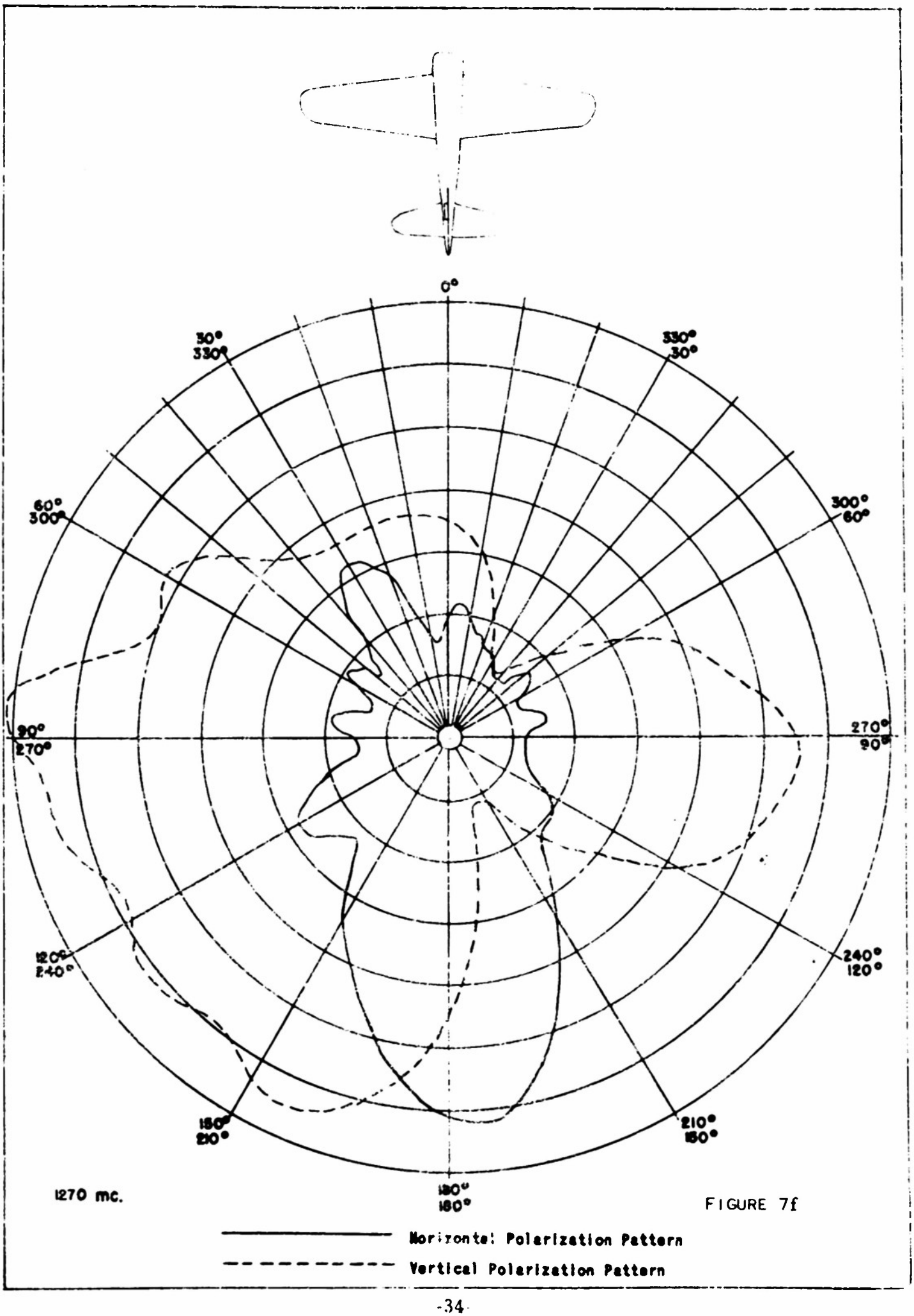
0°
30°
330°
330°
30°
60°
300°
300°
60°
90°
270°
270°
90°
120°
240°
240°
120°
150°
210°
210°
150°
180°
180°
1270 mc.
Horizontal Polarization Pattern
Vertical Polarization Pattern

FIGURE 7f

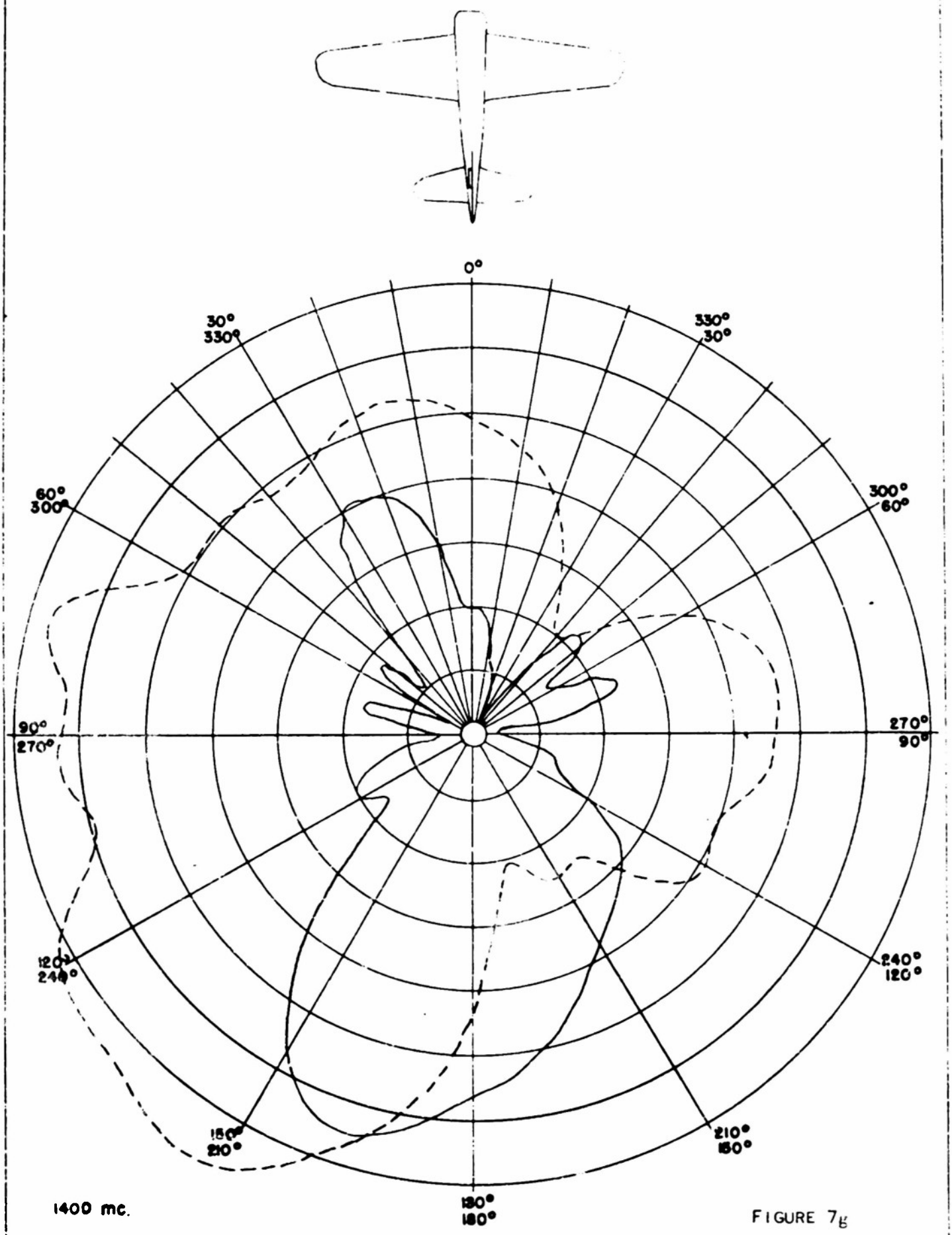

1400 mc.

FIGURE 7g

Horizontal Polarization Pattern

Vertical Polarization Pattern

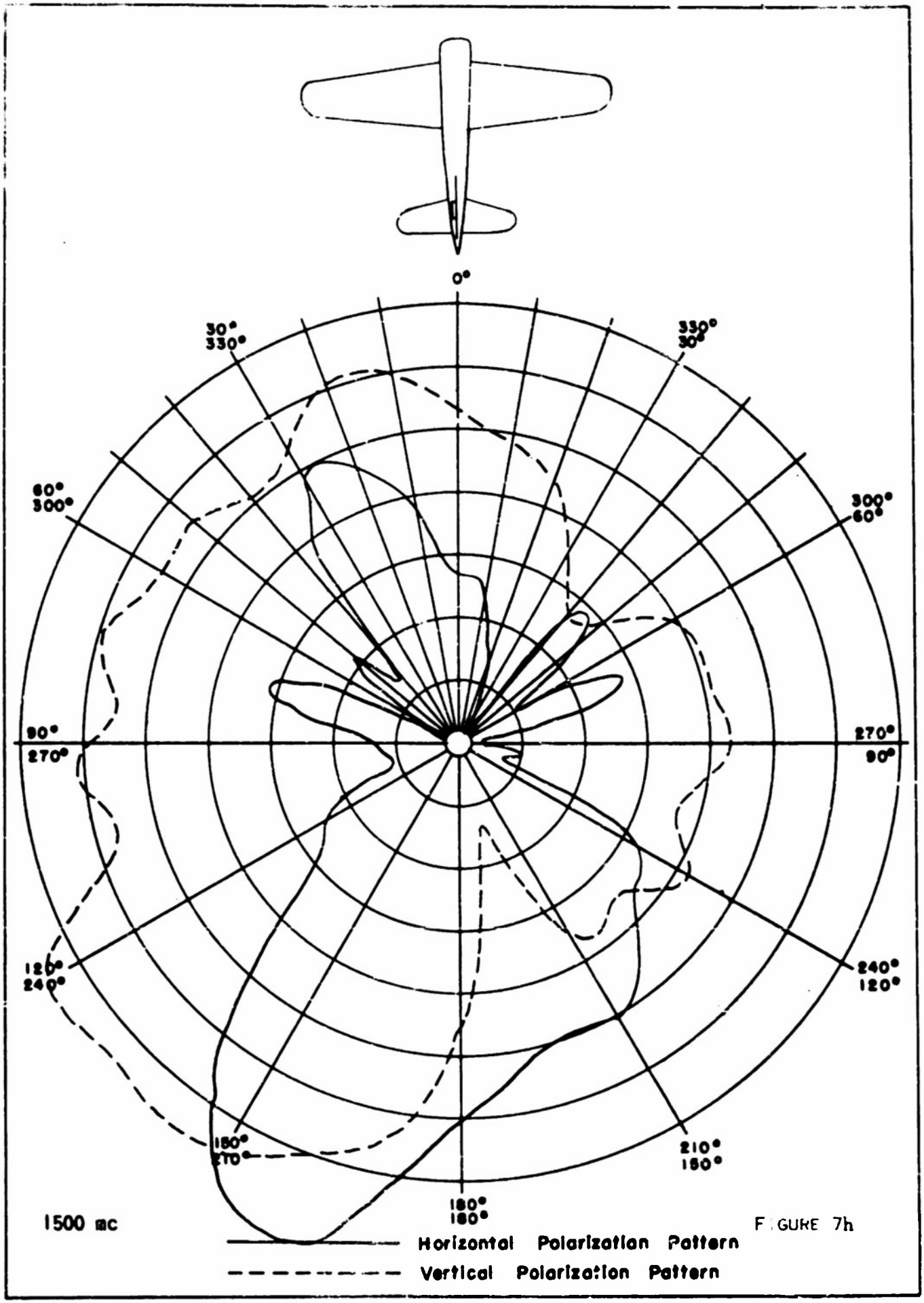
0°
30°
330°
330°
30°
60°
300°
300°
60°
90°
270°
270°
90°
120°
240°
240°
120°
150°
210°
210°
150°
180°
180°
1500 mc
Horizontal Polarization Pattern
Vertical Polarization Pattern

FIGURE 7h

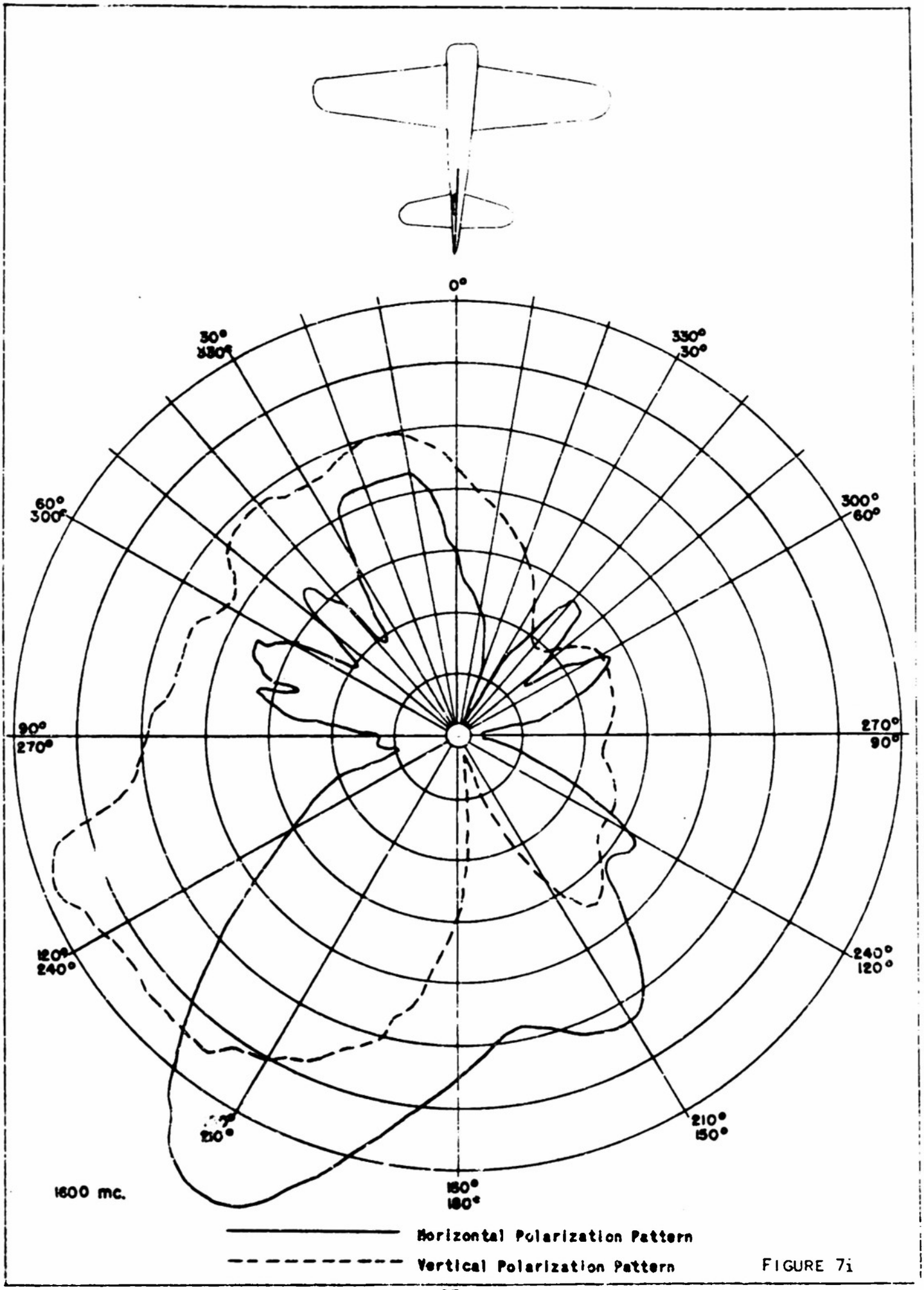
0°
30°
330°
60°
300°
90°
270°
120°
240°
150°
210°
180°
1600 mc.
Horizontal Polarization Pattern
Vertical Polarization Pattern

FIGURE 7i

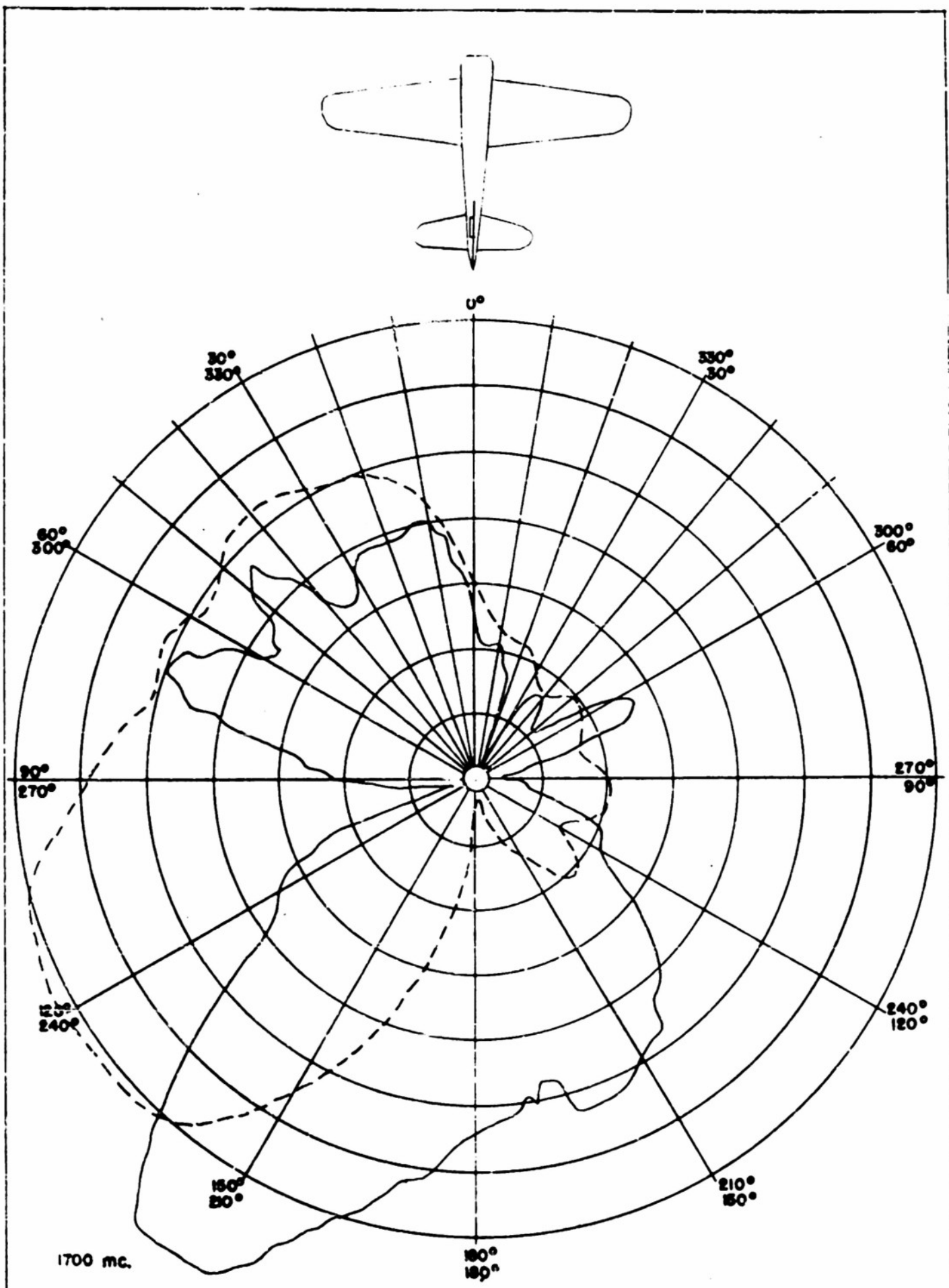
0°
30°
330°
330°
30°
60°
300°
300°
60°
90°
270°
270°
90°
120°
240°
240°
120°
150°
210°
210°
150°
180°
180°
1700 mc.
Horizontal Polarization Pattern
Vertical Polarization Pattern

FIGURE 7J

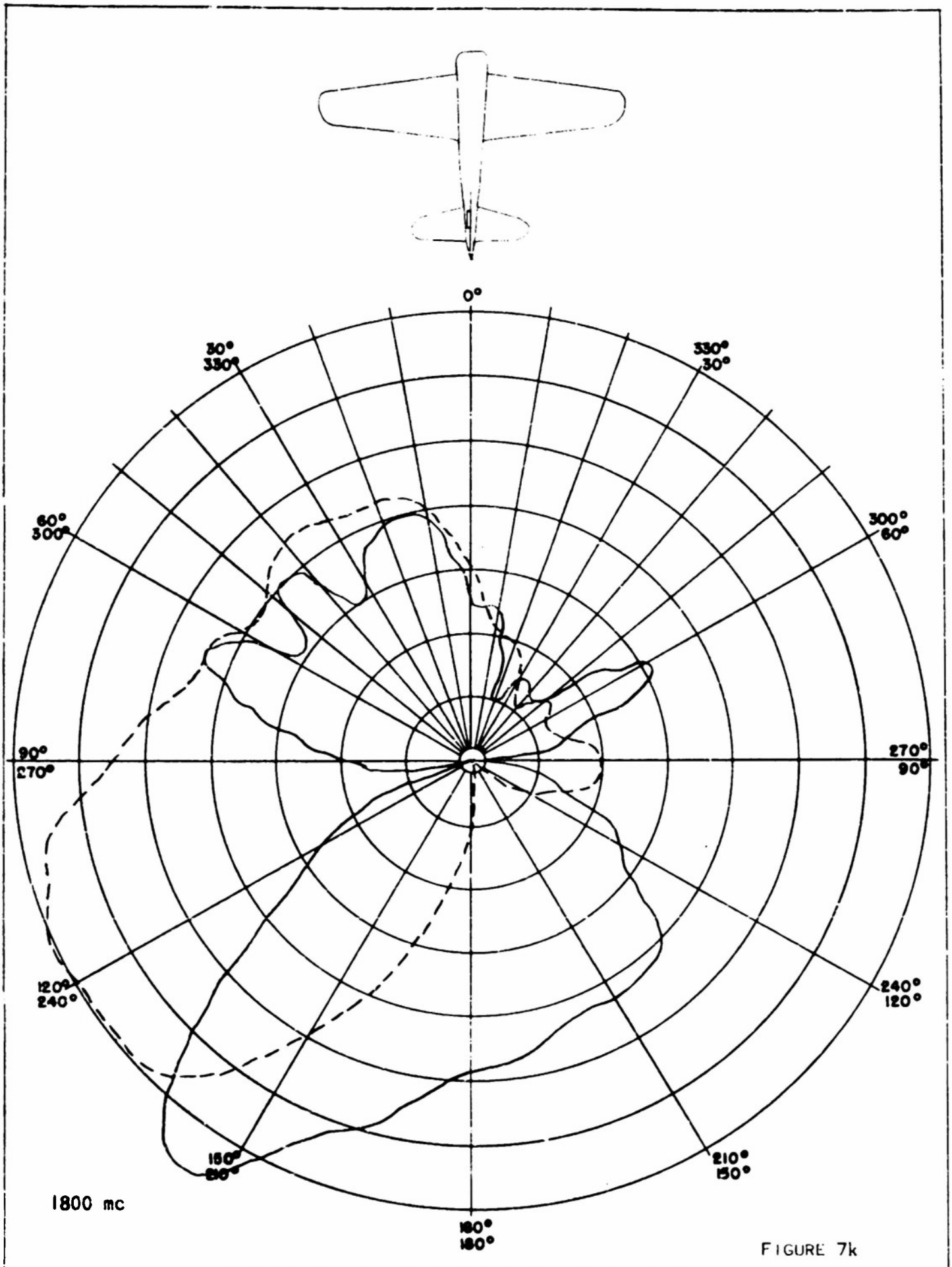
0°
30°
330°
60°
300°
90°
270°
120°
240°
150°
210°
180°
1800 mc
Horizontal Polarization Pattern
Vertical Polarization Pattern

FIGURE 7k

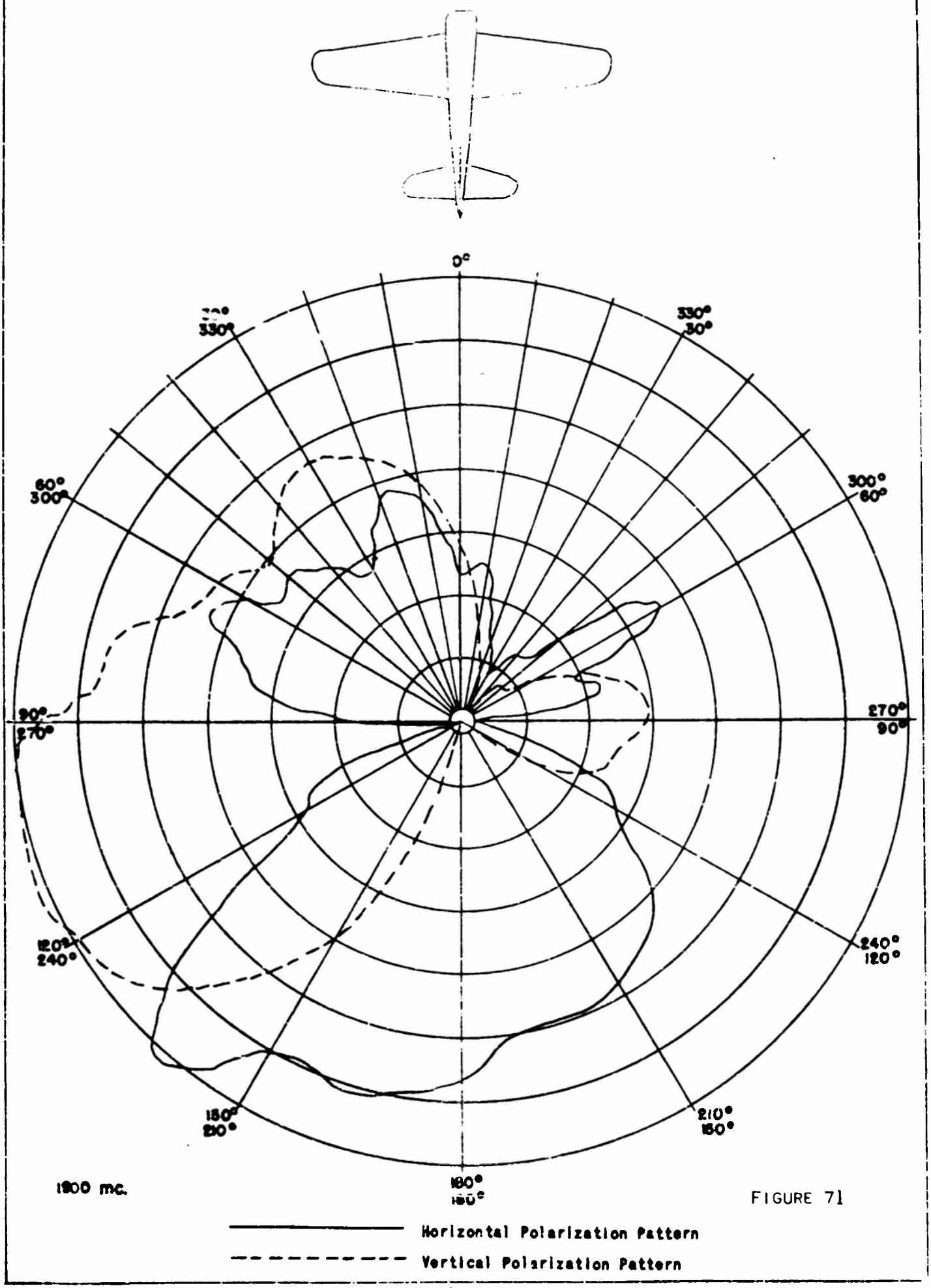
0°
330°
30°
300°
60°
270°
90°
240°
120°
210°
150°
180°
1800 mc.
Horizontal Polarization Pattern
Vertical Polarization Pattern

FIGURE 71

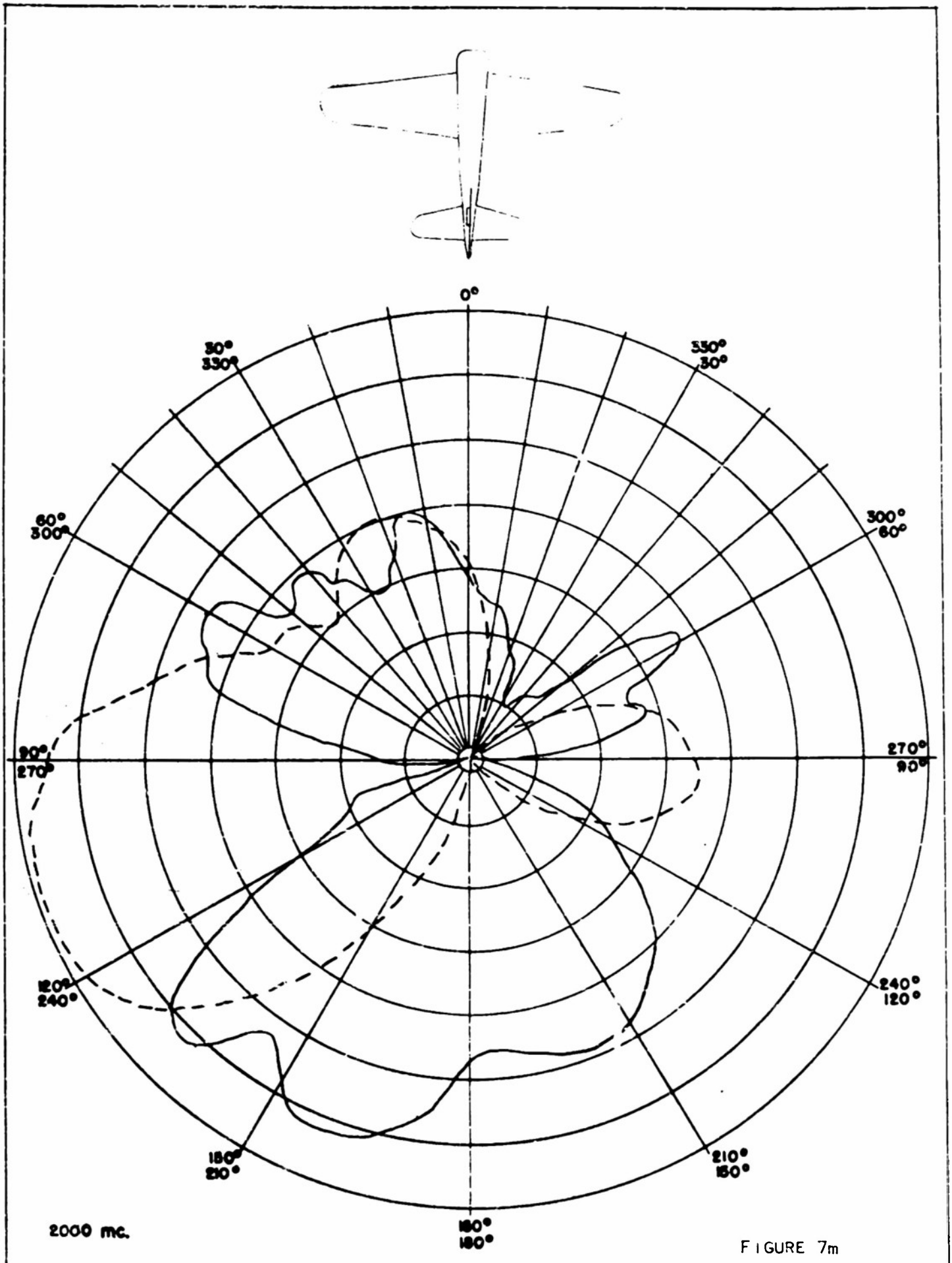

FIGURE 7m

Horizontal Polarization Pattern

Vertical Polarization Pattern

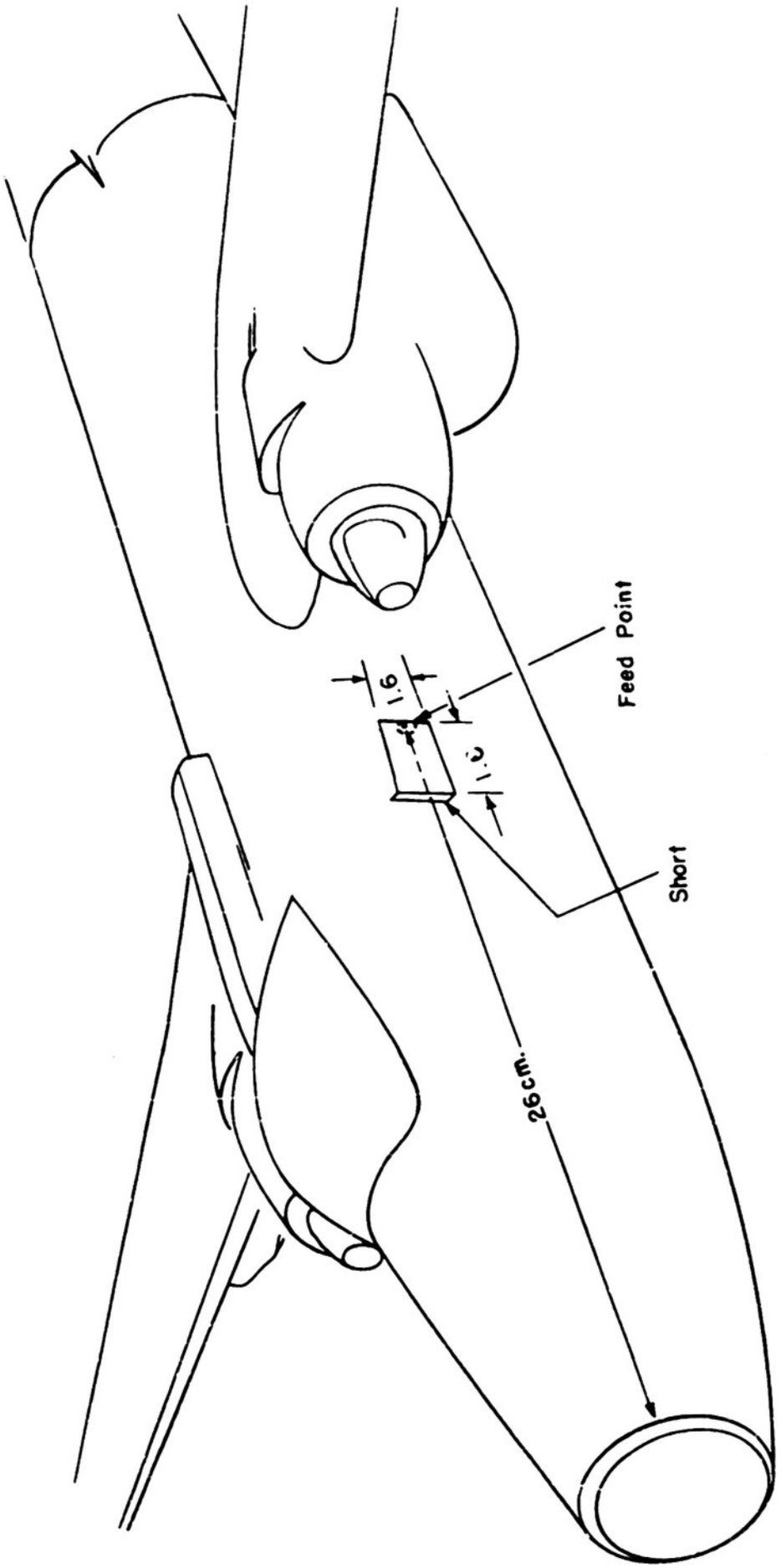

FIGURE 8

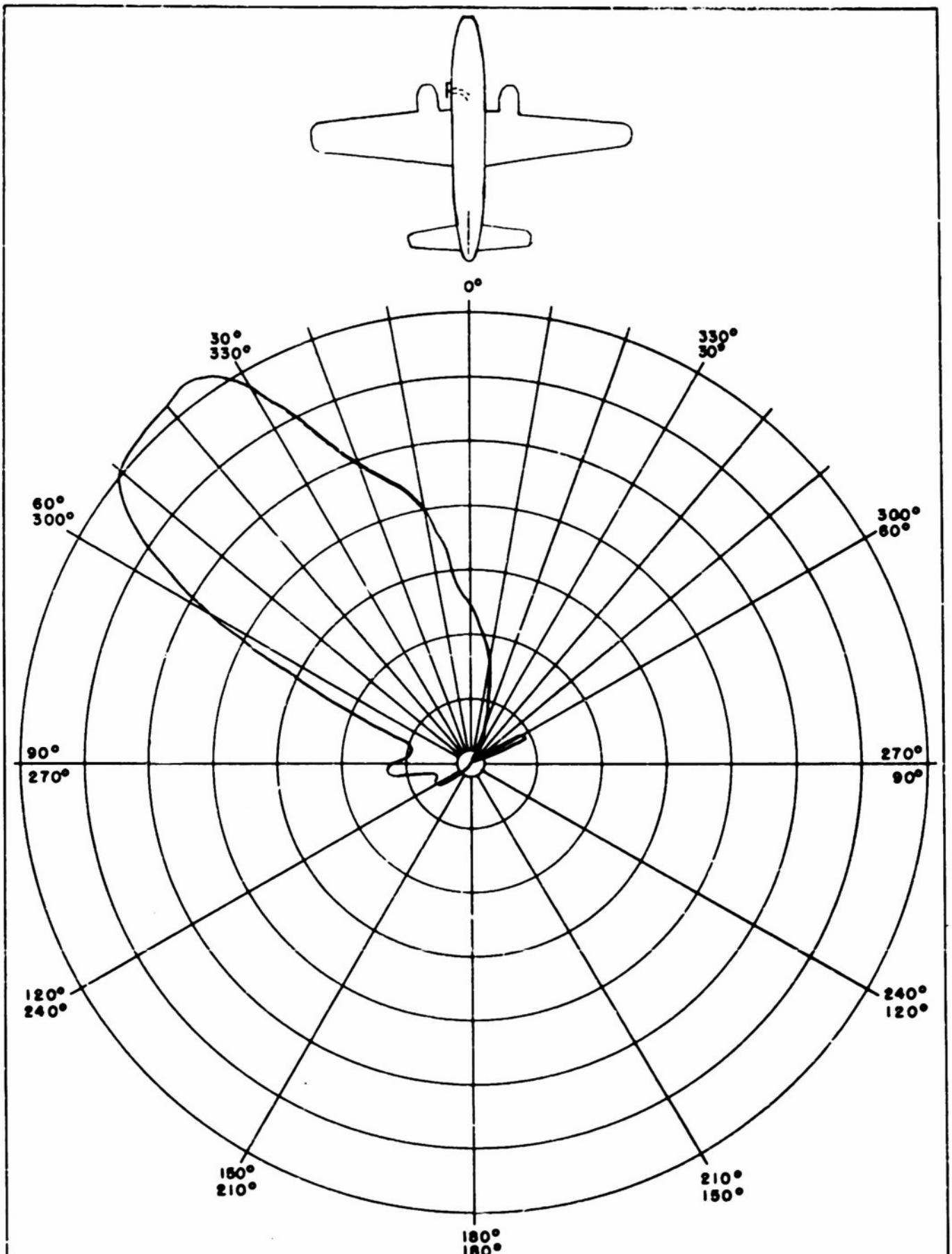

1300 mc

F.GURE 8a

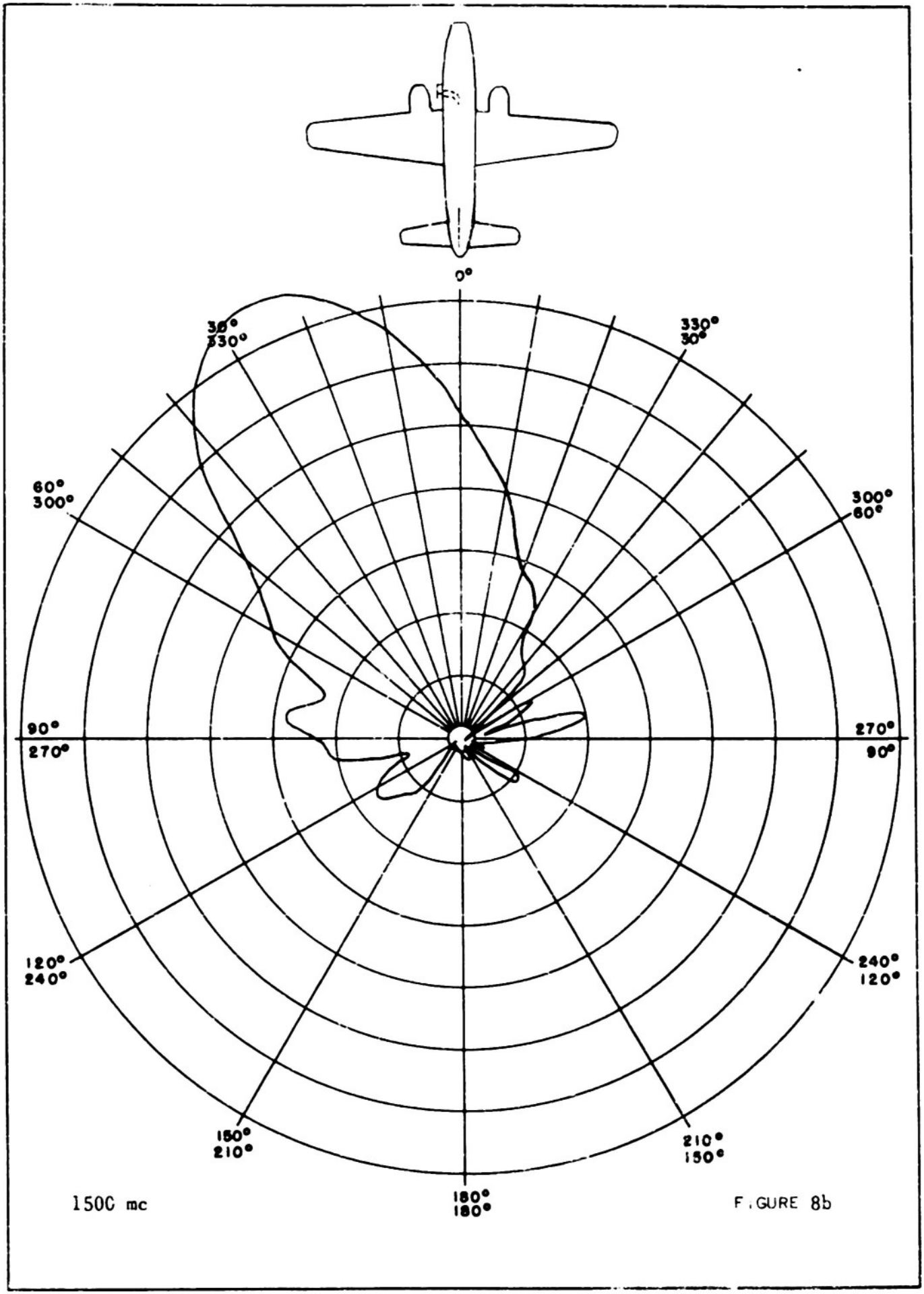

1500 mc

FIGURE 8b

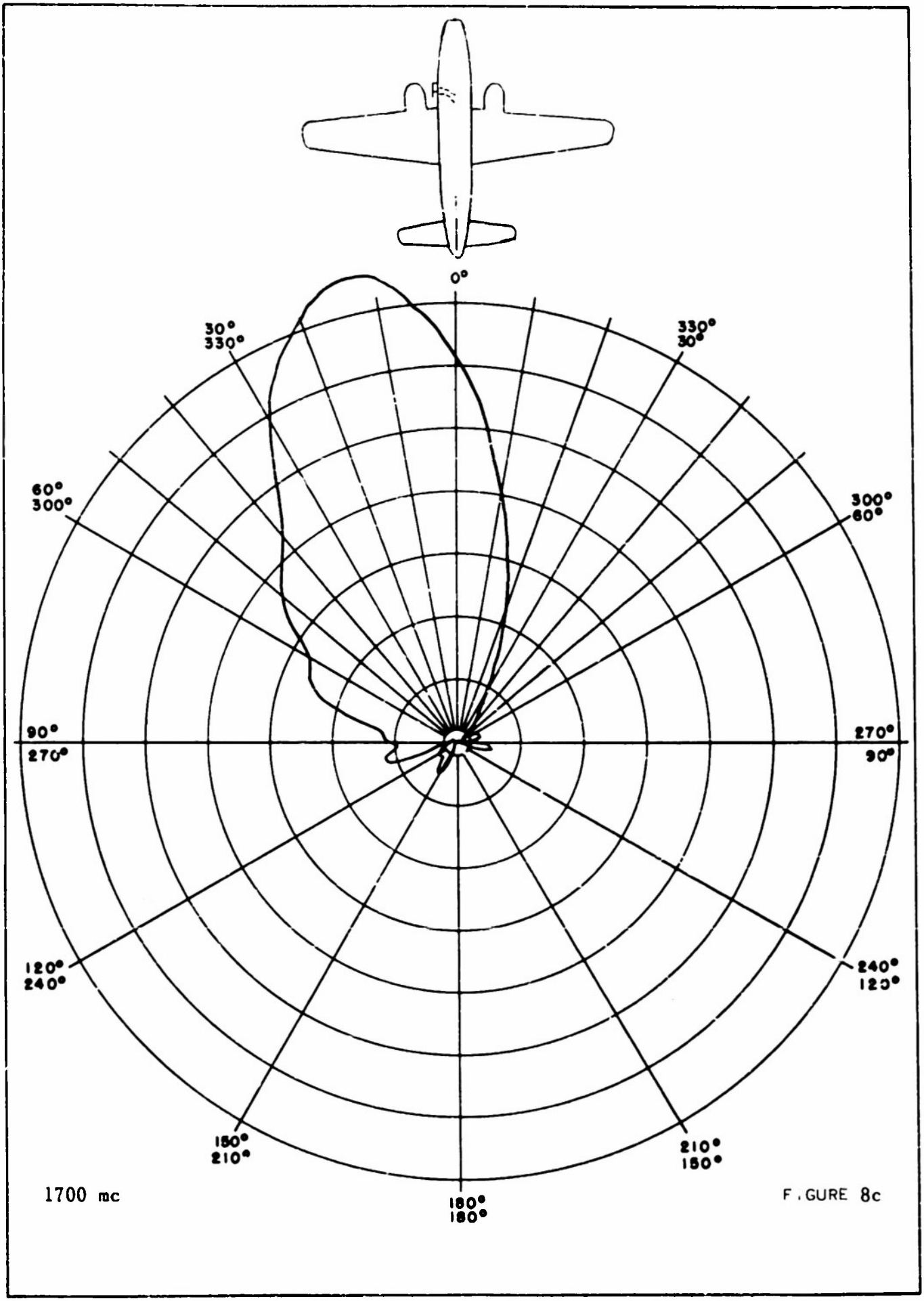

1700 mc

FIGURE 8c

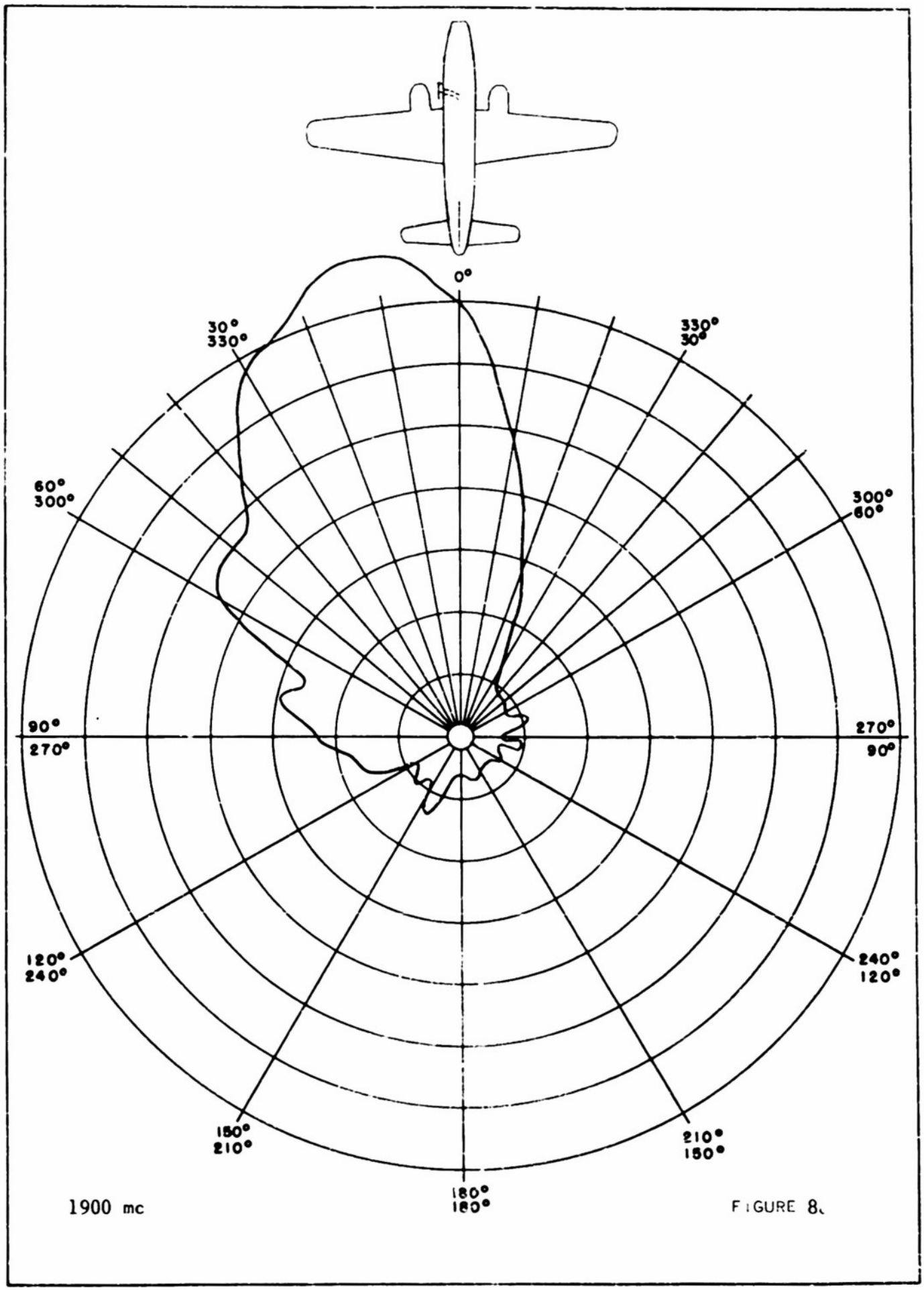

1900 mc

FIGURE 8.

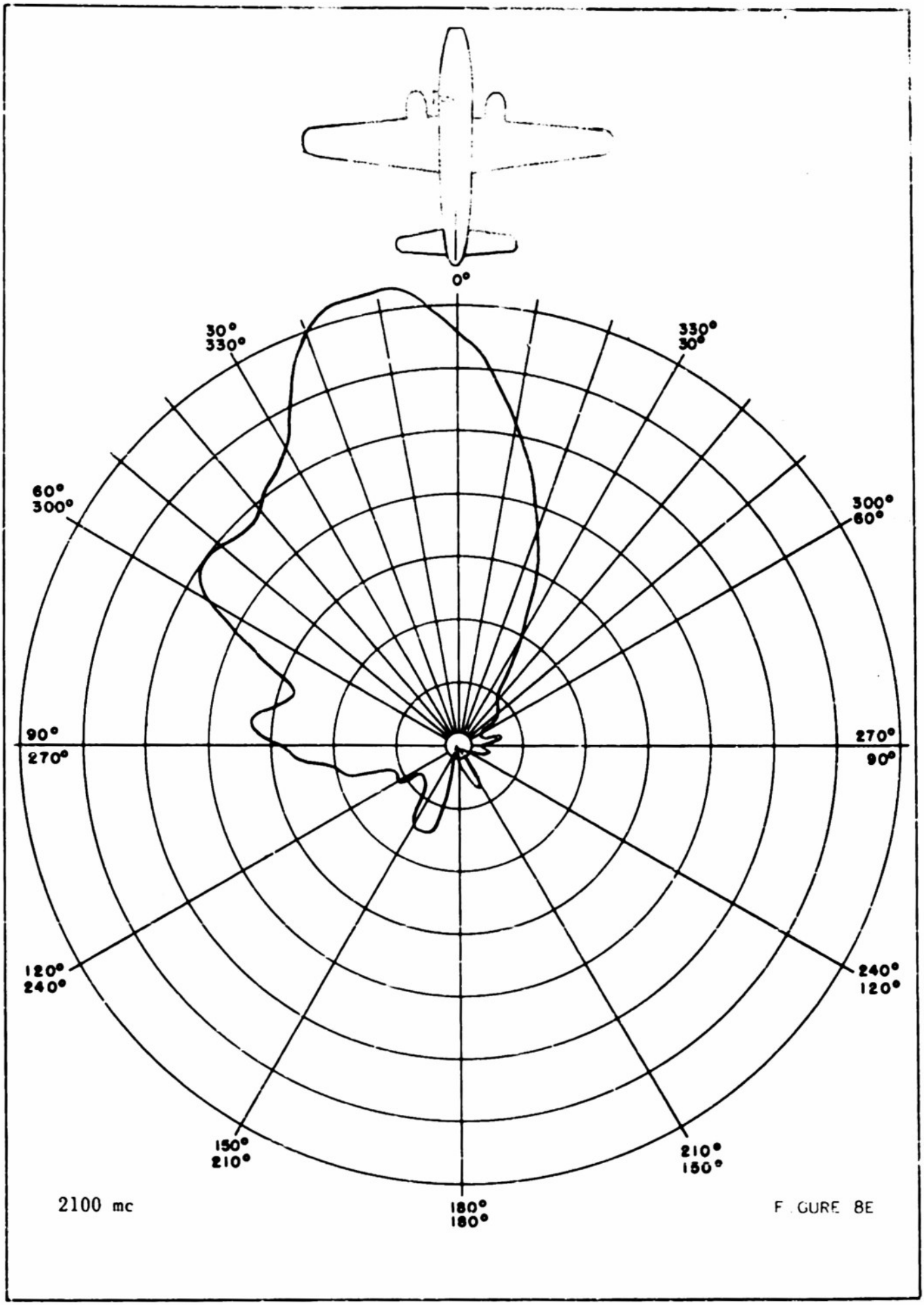
0°
30°
330°
330°
30°
60°
300°
300°
60°
90°
270°
270°
90°
120°
240°
240°
120°
150°
210°
210°
150°
180°
180°
2100 mc

FIGURE 8E

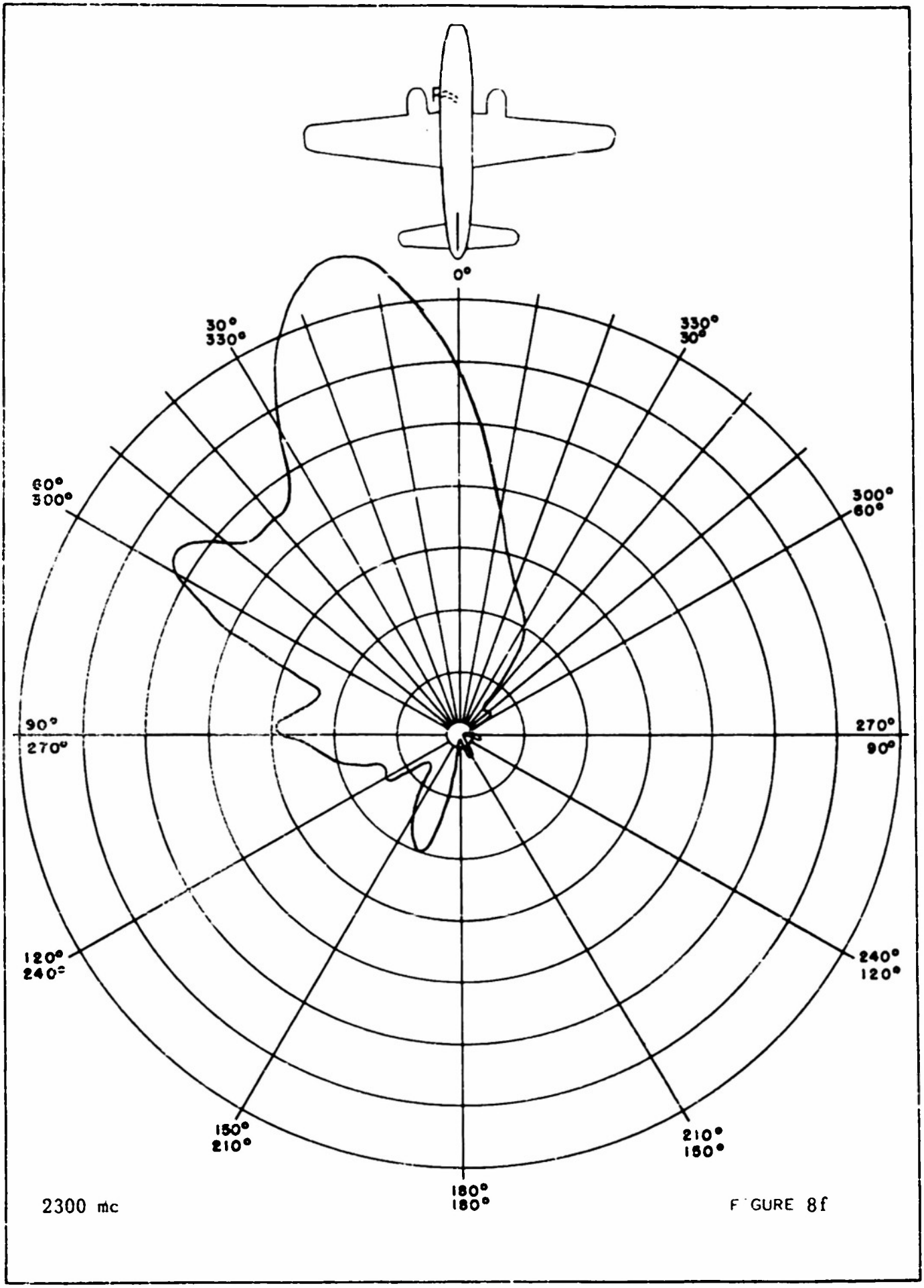

2300 mc

FIGURE 8f

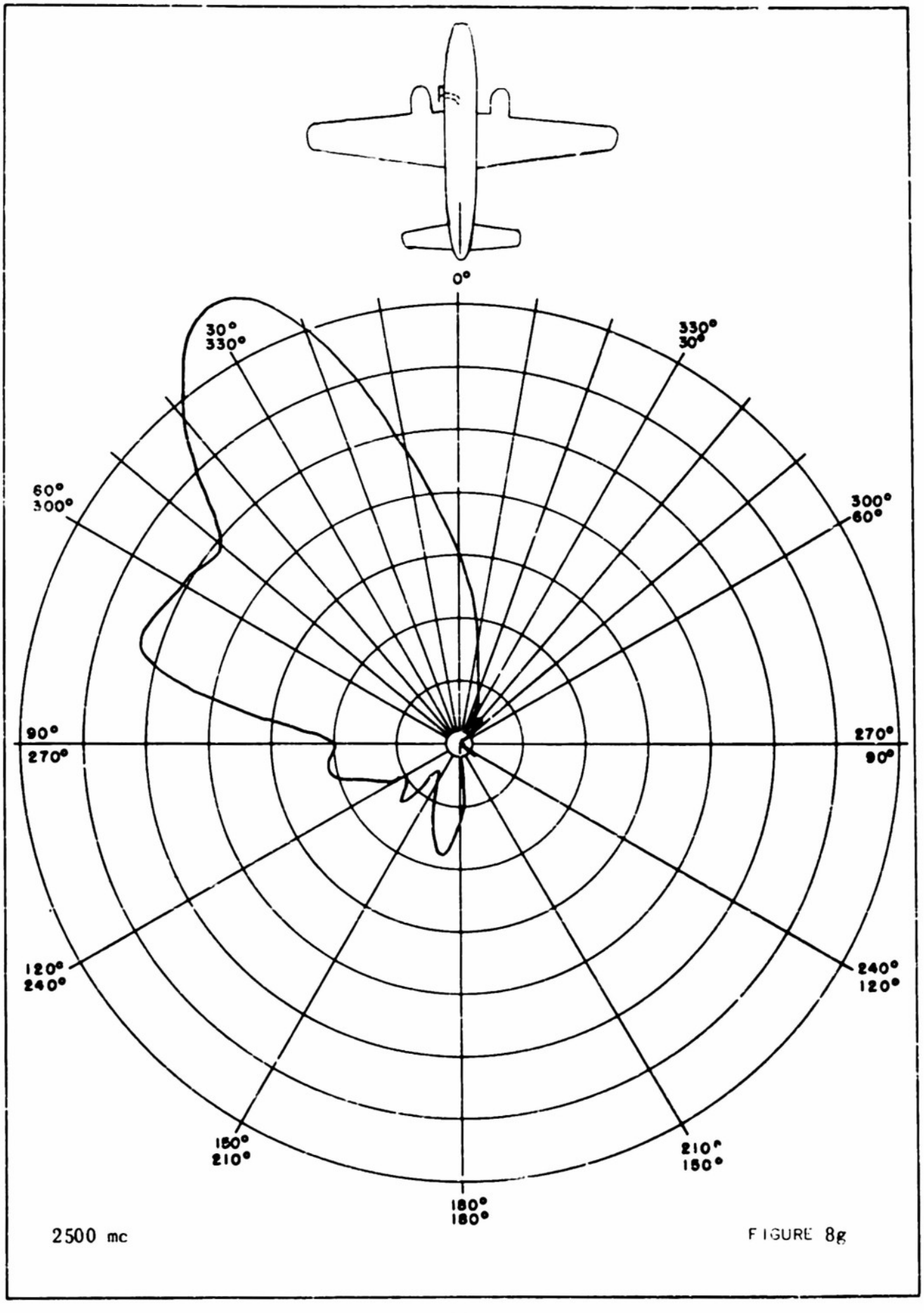

2500 mc

FIGURE 8g

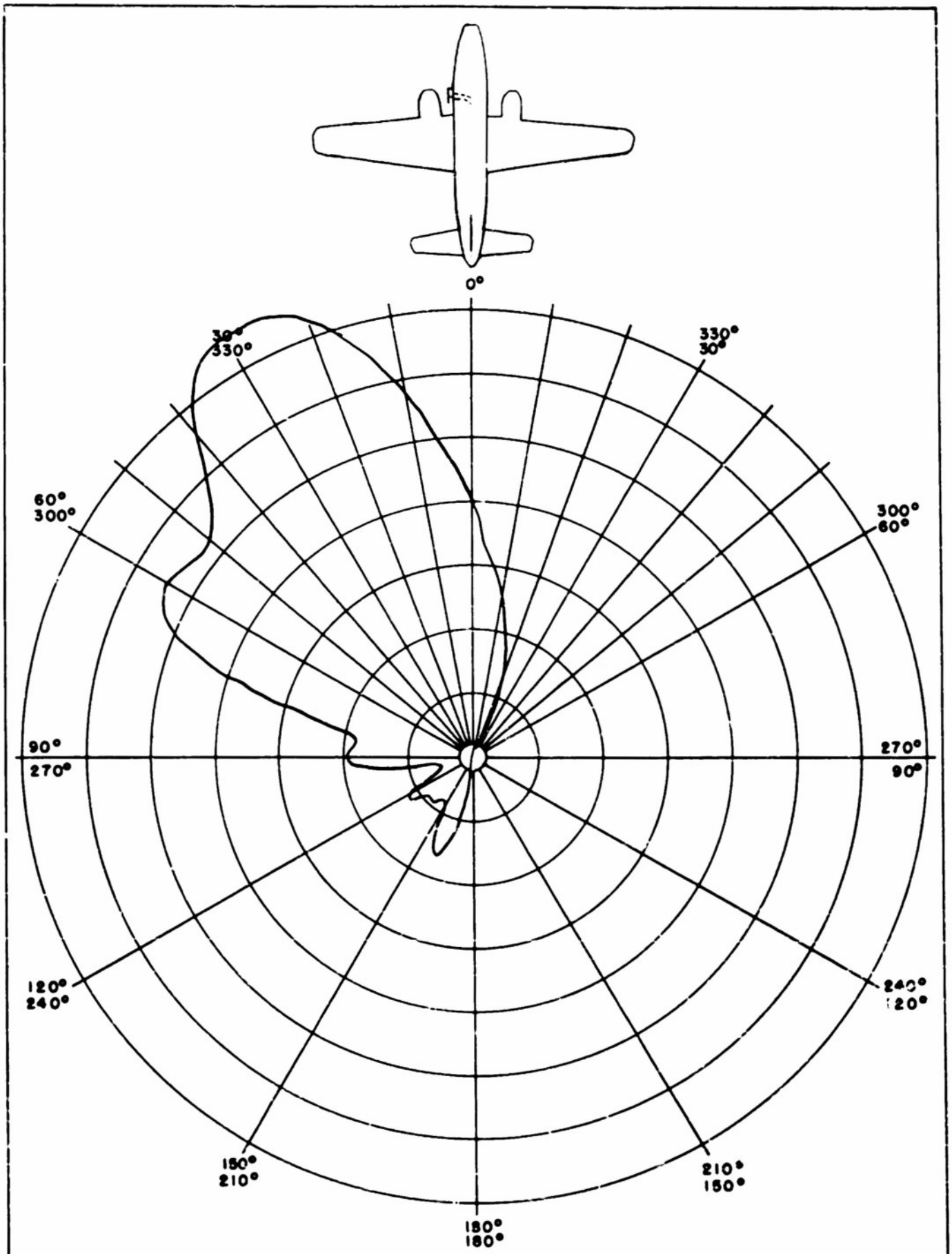

2700 mc

FIGURE 8h

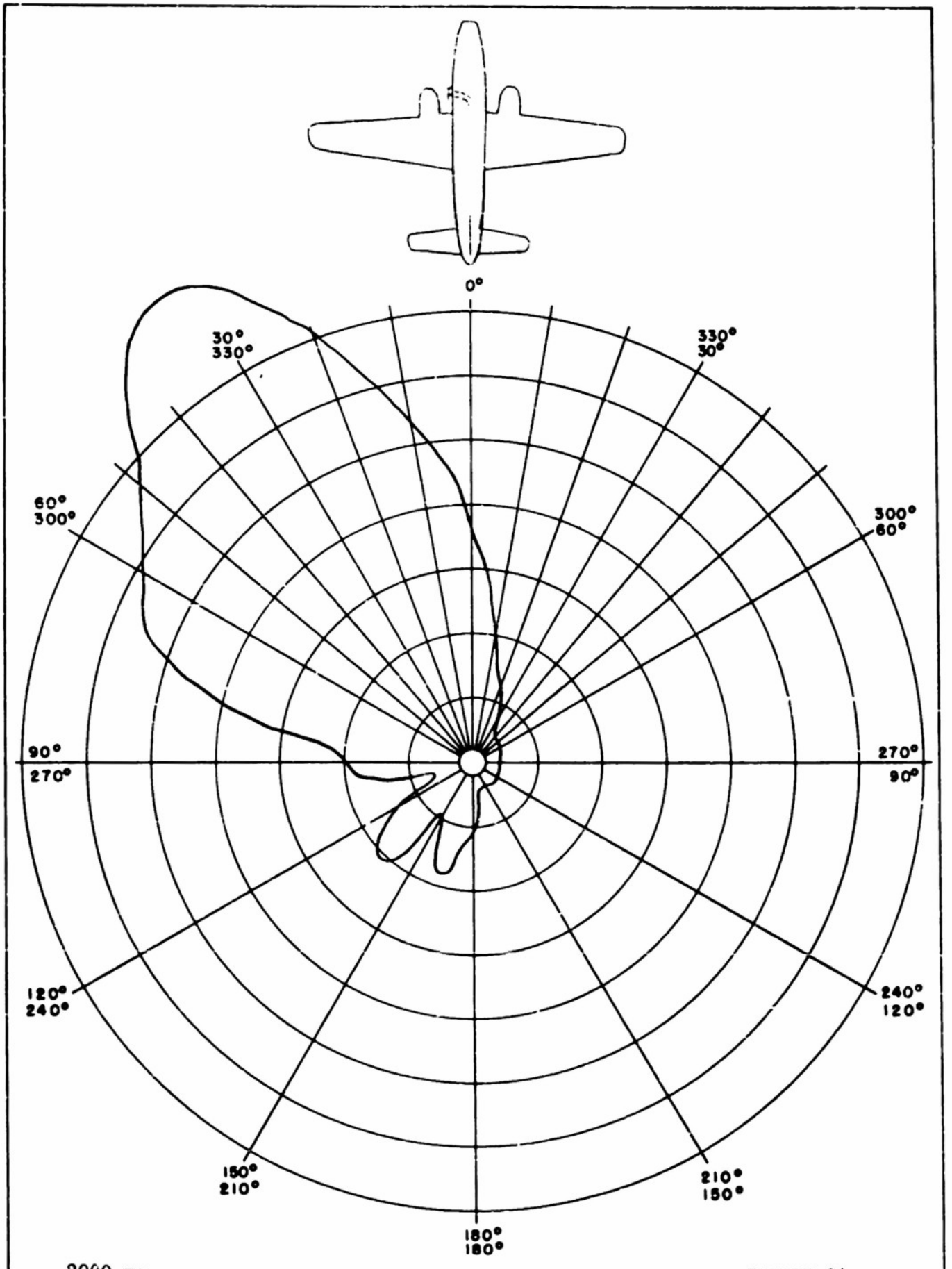

2900 mc

FIGURE 8i

PART II
AIRCRAFT RDF SYSTEMS (40 100 MC)

A survey of possible types of aircraft radio direction finding systems suitable for this frequency range was summarized briefly in Status Report ADF 1 It was concluded that the most promising attack on this difficult problem was to attempt to devise a sector-type system which could utilize the same antennas developed for the homing problem Consequently a determined effort has been and is being made along this line with the results reported below The direction finding antenna problem is, of course, more difficult than the homing antenna problem because the pattern requirements are much more severe

1. Partial-Sleeve Antenna Patterns

The patterns shown in Figs 6a through 6m represent the most useful of a great number of antenna arrangements tried on the Grumman Guardian Usefulness of a given pattern in a DF system naturally depends somewhat upon the type of system under consideration During the pattern studies made on this aircraft all known types of DF systems were kept in mind with a view of proposing for use whatever system would best utilize the patterns that could be obtained In the frequency range 40-100 mc on aircraft of the size of interest in this contract this method of attack is the most feasible because it is extremely difficult to obtain an arbitrary desired pattern Thus there must be a certain amount of mutual adjustment between the DF system proposed and antenna arrangement used None of the patterns obtained could be used with any of the better known DF systems Two systems which can use patterns of the type obtained on the Grumman are proposed in this report With these systems in mind the antenna locations on the aircraft were exhaustively studied The antenna placements and patterns shown herein are the result The merits and disadvantages of the patterns are discussed under the two system proposals

2. Phase-Shift Direction-Finding System

The phase shift scheme of bearing indication as originally proposed in Report ADF-3 for use in homing is adaptable for use in direction finding over certain sectors of the azimuth in particular, the head-on and off the wing tip regions Bearings taken off the wing tips to obtain DF fixes on transmitters would seem to be an important application of DF on naval aircraft in the 40-100 mc range The patterns obtained using the partial-sleeve antenna located on the leading edge of the wing next to the fuselage for the Grumman Guardian are shown in Figs. 6a through 6m The patterns for the same antenna mounted on the horizontal tail structure are shown in Figs 9a through 9n It is proposed that the four antennas yielding these patterns and their mirror images be used in the phase-shift DF system

The tail antennas are mounted on the horizontal stabilizer elevators. Connections to them can be made through flexible coaxial cable. If it is found that this mounting position is detrimental to the aerodynamics of the aircraft an alternative mounting position along the fuselage 2.6 meters behind the fuselage wing juncture is possible. Patterns for this antenna location are shown in Figs. 10a through 10c. Some loss in radiation conductance compared to that for the tail location occurs. This may not be serious as the antenna sensitivity is shown to be high.

Figure 11 is a block diagram of this phase-shift system. It makes use of the pair of the four available antennas which cover the bearing range of interest. The antenna outputs are fed into A. I. L. developed tuning heads which are modified to the extent that all the local oscillators are disabled save one whose output is supplied to the mixer of all the heads via coaxial cables. The output of one mixer is fed directly into the single channel IF amplifier.

The output of the other mixer is fed through a phase shifter and then to the input of the IF amplifier where it is added to the output of the first mixer. The IF amplifier is provided with an ordinary amplitude detector whose output is amplified and impressed across the vertical deflection plates of an oscilloscope tube. The phase shifter unit provides a phase shift in the IF voltage of the mixer preceding it which is directly proportional to a control voltage from the control unit. A voltage proportional to this control voltage is also applied to the horizontal plates of the indicator tube. There results a one to one correspondence between horizontal position of the scope beam and degrees of phase shift present between the mixer signals at the input and output of the phase shifter. Suppose the control voltage is of sinusoidal wave shape. The beam of the indicator tube will be constantly swept horizontally while its position vertically will depend upon the combined outputs of the antenna pair in use. A cusp-shaped figure will be formed similar to those sketched in Fig. 12 for several positions of the transmitter with respect to a reference line on the aircraft.

Suppose it is desired to DF on a transmitter off the left wing of the aircraft. Then the two antennas on the left side would be in use. The phase shifter and control unit can be so adjusted that when the transmitter is directly off the wing tip a cusp-shaped figure with cusp at center of scope face will be formed. As the plane turns and the position of the transmitter with respect to it changes, the position of the cusp-shaped figure with respect to the center of the oscilloscope face changes proportionally. The bearing of the transmitter can be read off the calibrated scope face.

This DF system requires that patterns covering neighboring sectors of the azimuth have a region in common. This common region is the operating range of the system for the particular antenna pair used. The two apparent limitations on the azimuthal coverage of a given antenna pair result from pattern amplitude change and pattern phase change. Since the cusp-shaped figure of the bearing indication is produced by the antiphase addition of the two antenna voltages, the depth of the

cusp is determined by the relative amplitudes of the two patterns at the particular bearing. The useful range is then no greater than to the first null of either pattern. An inspection of the patterns shows that, with the two antennas having forward coverage, a range of about 50° to either side of head on is available at all frequencies save at 800 mc, corresponding to 40 mc in the full-size aircraft, which pattern has a range of about 20° off head on. The A.I.L. tuning head having a lower limit of 50 mc makes this limitation less serious.

For the two antennas having side coverage (one at the fuselage-wing juncture and one at the tail-fuselage juncture) the patterns show a range of usefulness of about 20 degrees to either side of a line perpendicular to the head on position line of the plane. A method of obtaining bearing fixes on a transmitter is to fly two courses perpendicular to each other and so located that the transmitter is somewhere off the plane's wing tip. If this is done at a distance of about 100 miles from the transmitter the range of 40° of bearing indication gives a base length of around 70 miles between bearing fixes on each course. This, for a 300 mph aircraft, involves a flying time of some 20 minutes between bearing readings. The base lengths of 70 miles would seem to be ample to obtain a reasonably accurate "cocked hat" within which the transmitter is located. On the basis of this reasoning the angular coverage provided by this phase-shift system should be adequate.

No error in bearing indication is caused by the pattern amplitude change. When the patterns are of equal amplitude, a perfect null (full depth cusp) is formed. When the pattern amplitudes are in a ratio of 5 to 1 a 20% depth cusp is formed. If a minimum usable depth of cusp is selected, then the azimuthal coverage can be read off the patterns. On this basis the foregoing coverages were estimated.

The phase-shift system was tested on the 1/20 scale Grumman model. The plane was equipped with wing and tail partial-sleeve antennas and mounted on the pattern range turntable. The RF outputs of the two antennas in use were added together with a calibrated telescoping line length in one antenna cable. The antennas were excited with the pattern range antenna. The antenna sum voltage was detected and measured. Curves of sum voltage vs. phase shift in one antenna line are shown in Fig. 13 for the wing antennas, and Fig. 14 for a wing and a tail antenna on the same side of the aircraft. Each curve corresponds to the indicated azimuthal direction of arrival of the signal. The proposed cathode ray indication would look just like these curves. The data were taken at the high end of the frequency band (2000 mc). The chart below shows a comparison between the experimentally determined shift in the bearing indication and the shift that would be expected based on an assumption of omnidirectional antennas in free space separated by the same distance as the antennas on the aircraft.

	Bearing Indication	
Signal Arrival Direction Degrees From Head On	*Two Isolated Omn.-Directional Antennas*	*Two Wing-Edge Antennas*
0°	0°	0°
5°	14.6°	17°
11.5°	33.5°	45°
15.5°	45.6°	65°

Signal Arrival Direction Degrees From a Perpendicular to Head On	Bearing indication	
	Two Isolated Omni-Directional Antennas	One Wing-Edge and One Tail Antenna
0°	0°	0°
6°	109°	115°
12°	216°	235°
17°	318°	355°

These data represent an experimental check on the workability of the phase-shift system. The accuracy of the equipment was investigated. A pair of vertical sleeve monopoles was mounted on the pattern range turntable. Their outputs were added with the telescoping line in one lead. A plot of line length addition versus angular rotation of the antenna pair is shown in Fig. 15. Its shape agrees very well with the theoretical sinusoidal. On this basis the results obtained on the aircraft antennas are considered reliable.

The wing-edge antenna pair yield bearing indications as shown in Fig. 13. The curves are for bearings towards one side of head on. A similar displacement occurs in the opposite direction for signals coming from the other side of head on. It is seen that for signals occurring in the forward 30° of azimuth the bearing indications are quite definite. As the azimuthal bearing deviation from head on increases ($> \pm 15°$) the bearing indications become less definite. The limiting value was not ascertained.

The combination of a wing and a tail antenna gave the results shown in Fig. 14. The total range of phase shift which can be employed, corresponding to the full horizontal traverse of the bearing indication is 360°. The displacement in electrical degrees between the two antennas at 2000 mc is 1100. The bearing null occurs for a line phase shift of $1100° \sin \Phi$ where Φ is the angular direction from a perpendicular to head on. Suppose the bearing indicator is arranged so that when the beam is at the center of the tube there is 0° phase shift in the one line and when it is at an edge of the tube there is ± 180° phase shift in the line. Then Fig. 14 indicates that the total azimuthal coverage is about 17°. A signal coming in from about 19° off the wing tip would give the same null position as one coming in directly off the wing tip except the null depth would be considerably less. Thus the azimuthal range could be increased beyond the 17° value provided the null depth information were taken into consideration. As in the case of the two wing-edge antennas the actual limit of angular coverage of the antenna pair is the neighborhood wherein the bearing null becomes poorly defined. On this basis a total coverage of 40° off the wing tip seems feasible at this frequency. The 2000 mc information obtained above corresponds to 100 mc in the actual aircraft and is considered as the worst case, at least insofar as the wing and tail antenna pair is concerned. At lower frequencies there is a corresponding closer electrical spacing of the antennas.

Patterns for a fuselage mount location of the antenna are shown. It is considered that this location is an excellent substitute for the tail mount location. The electrical spacing between the wing-edge antenna and one at this position is about 780°. The patterns are fully as good as the tail mount patterns. A lowered radiation conductance and a somewhat higher sensitivity to vertical polarization are the disadvantages.

While accurate bearing information is obtained only over restricted ranges of azimuth with this system, the antenna patterns do provide coverage over the entire azimuth except for some 60° of range centered on the tail. To be able to receive a transmitter located in some arbitrary direction while flying, provision could be made to have all antennas switched in to the IF amplifier whose detector could supply an audio amplifier for detection of a transmission. The scope indicator would not be in use. Upon detection of the transmission the antennas could be switched out one at a time. The quadrant in which the transmitter is located would be given by the antenna producing the maximum signal. The proper antenna pair and scope indicator would then be used to DF accurately on the transmitter. Using this method of operation the aircraft would have available first an instantaneous and practically omnidirectional receiving system to detect a transmission; secondly it would have an effective quadrant type bearing indicator; and finally it would have an accurate DF system for taking fixes on the transmitter when the latter is located within approximately 40° sectors off the nose or either wing tip.

3. Amplitude Comparison Direction-Finding System

A study of the patterns presented in Figs. 6a through 6m, 9a through 9n, and in particular Figs. 16a, 16b, and 16c indicates pattern coverage for the 360° azimuth. Figures 16a, 16b, and 16c corresponding to frequencies of 800, 1260, and 2000 mc/sec respectively, show the four antenna patterns superimposed and make evident their relative sector coverages and their similarity. The three frequencies correspond to the end and midband scale frequencies of the specified range of 40 - 100 mc.

Because of this coverage and pattern similarity the feasibility of using an amplitude comparison system providing instantaneous DF over the azimuth was investigated. This system is shown in Fig. 17 which presents a block diagram of the direction-finder's components and shows the orientation of the four flush-mounted antennas used in the system. A "bread-board" model of the system was built up to investigate experimentally the results that might be achieved with it.

The output from each antenna is fed into its respective A.I.L. RF head and mixer. One local oscillator supplies the injection voltage to each of the four crystal mixers. The IF output of each mixer is amplified, detected, and fed into a gated amplifier feeding a deflection plate of the oscilloscope through a ganged attenuator. Further description of the system is best accomplished by analyzing its operation for an assumed incoming signal

Consider a horizontally polarized signal arriving off the left wing making an angle of 60° with respect to the nose of the aircraft (Fig. 16a). The amplitude of the voltage input to the RF head in each channel is directly proportional to the amplitude of the respective antenna pattern at that angle. Further, the magnitudes of the deflection voltages at the oscilloscope will be proportional to the amplitudes of the patterns at the designated angle of arrival (assuming matched gain channels). Therefore the beam of the oscilloscope will be deflected to an appropriate position near the number 1 deflection plate. Gating the outputs of the deflection plate amplifiers makes available a straight line indication on the scope face.

Because the antenna patterns are not circles, any bearings read on such a scope face marked off in degrees would be incorrect. However this situation is present for most fixed small aperture direction-finders whose patterns deviate from the conventional "perfect figure-eight". Generally this difficulty is resolved by calibrating the system (i.e. a curve of true bearing vs. indicated bearing at each frequency over the band).

It was evident in the operation of the model DF system that there are present sectors in the azimuth where bearing errors exist which cannot be corrected by calibration charts. These errors are due to two types of pattern variations and their existence can be anticipated from a study of the patterns where such variations occur.

One type variation is present for the leading edge, wing antenna patterns in the very low end of the band (Fig. 18). Here the amplitudes of the patterns about the aircraft nose do not decrease uniformly (i.e. with a slope of constant sign) from the pattern maximum. Specifically, there is a tendency toward lobing thereby causing changes in the direction of concavity in the curves. In these regions there exist two angles of arrival where the pattern amplitudes are the same so that the DF system indicates the same bearing. The effect causes errors in spot sectors about the aircraft nose but is not a limitation for angles of arrival off either wing tip. This is apparent from the slope of the antenna curves in the region about either wing tip.

The other source of error is due to the broadness or flatness of the amplitude patterns specifically about a pattern maximum. This condition is indicated in Fig. 19. In such sectors the detected amplitude remains a fairly constant signal so that the scope beam will be held in one spot (the amplitudes of the other antenna signals are down *considerably* and thereby have comparatively little effect on the beam's deflection). As a consequence of this pattern fault, additional sectors of indeterminacy result.

These pattern characteristics appear to limit the range of usefulness of the amplitude system to those sectors (off wing tips) where the patterns change rapidly with a slope of constant sign. The direction-finder could be calibrated accurately in a 40° sector off each wing tip.

There exists the possibility of reducing errors due to the flatness effect by using a pair of fuselage mounted antennas in place of the trailing edge tail elements (Figs 10a, 10b, and 10c). These patterns are somewhat sharper lobed and the position of the lobe is shifted nearer the wing tip and nearer the main lobe of the adjacent forward antenna. This lobe tilt indicates larger detected signals would be present on two scope plates and movement of the scope beam should be enhanced. One obvious disadvantage of these patterns is the lack of coverage in a sector off the aircraft tail.

The ultimate utility of the amplitude system may be for an instantaneous quadrant detection system to be used in conjunction with a phase comparison DF.

4. Conclusions on Aircraft RDF Systems

Two different RDF systems have been investigated and discussed in this report. They both use the same antenna configuration, viz., the wing-edge pair as used in the homing system, and a pair of tail-mount or fuselage-mount partial sleeves. Of the two systems, the amplitude comparison system seems to be the more instantaneous in operation, whereas the phase comparison system seems to be the more accurate. In both, the azimuthal range of accurate bearing information is substantially the same. With little equipment in addition to that which either system requires they could both be incorporated in one DF unit. Thus the advantages of each would be available.

Either of these RDF systems give a bearing that is accurate only in limited regions of azimuth, namely in the forward sector off the nose and in the sectors off each wing tip. It is believed that these sectors are the most important ones in the tactical use of the RDF system Nevertheless it must be concluded that the answers on the RDF problem obtained to date are only partially satisfactory and that they represent only an interim solution. Work on the aircraft RDF problem is continuing.

PART II

ILLUSTRATIONS

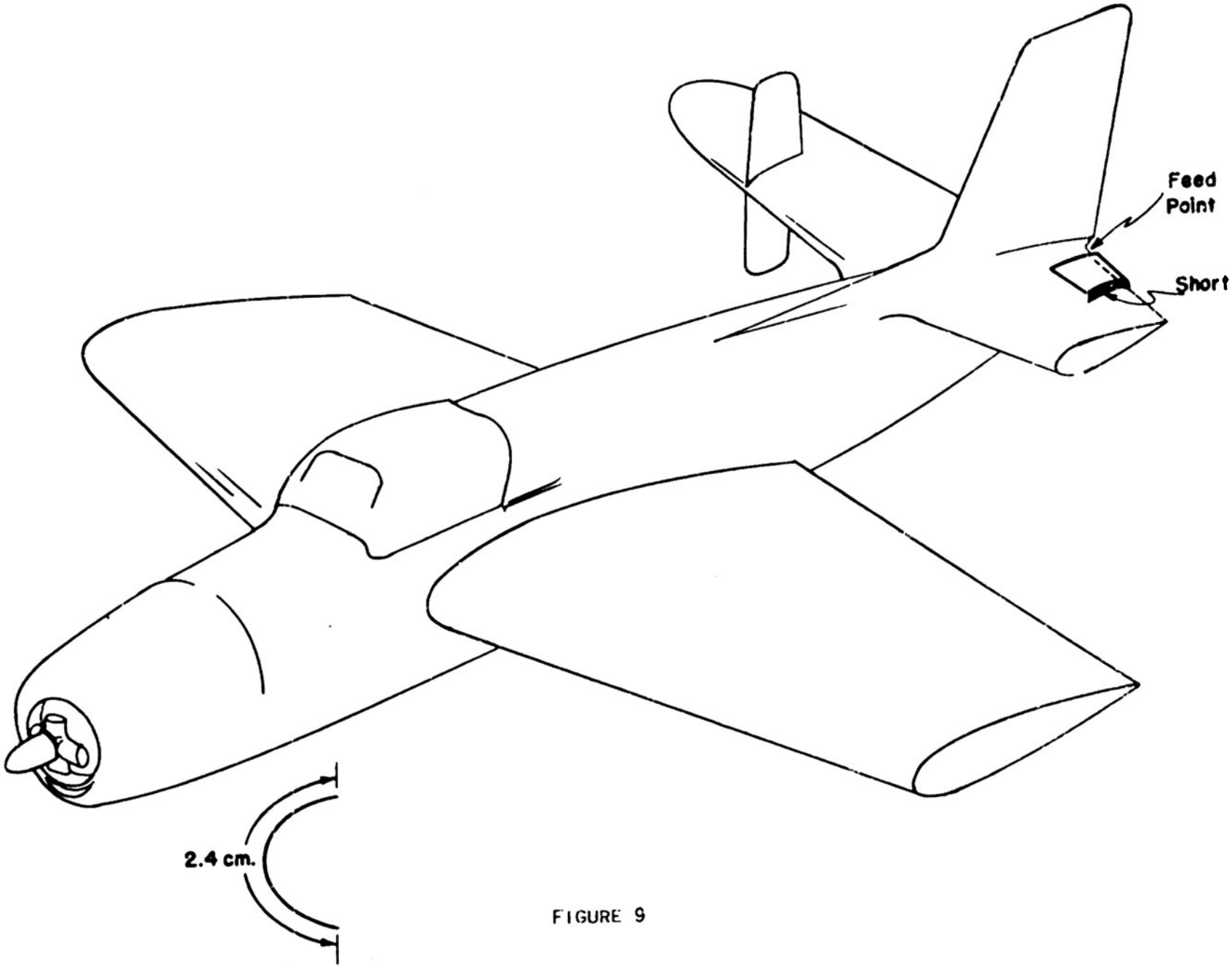

FIGURE 9

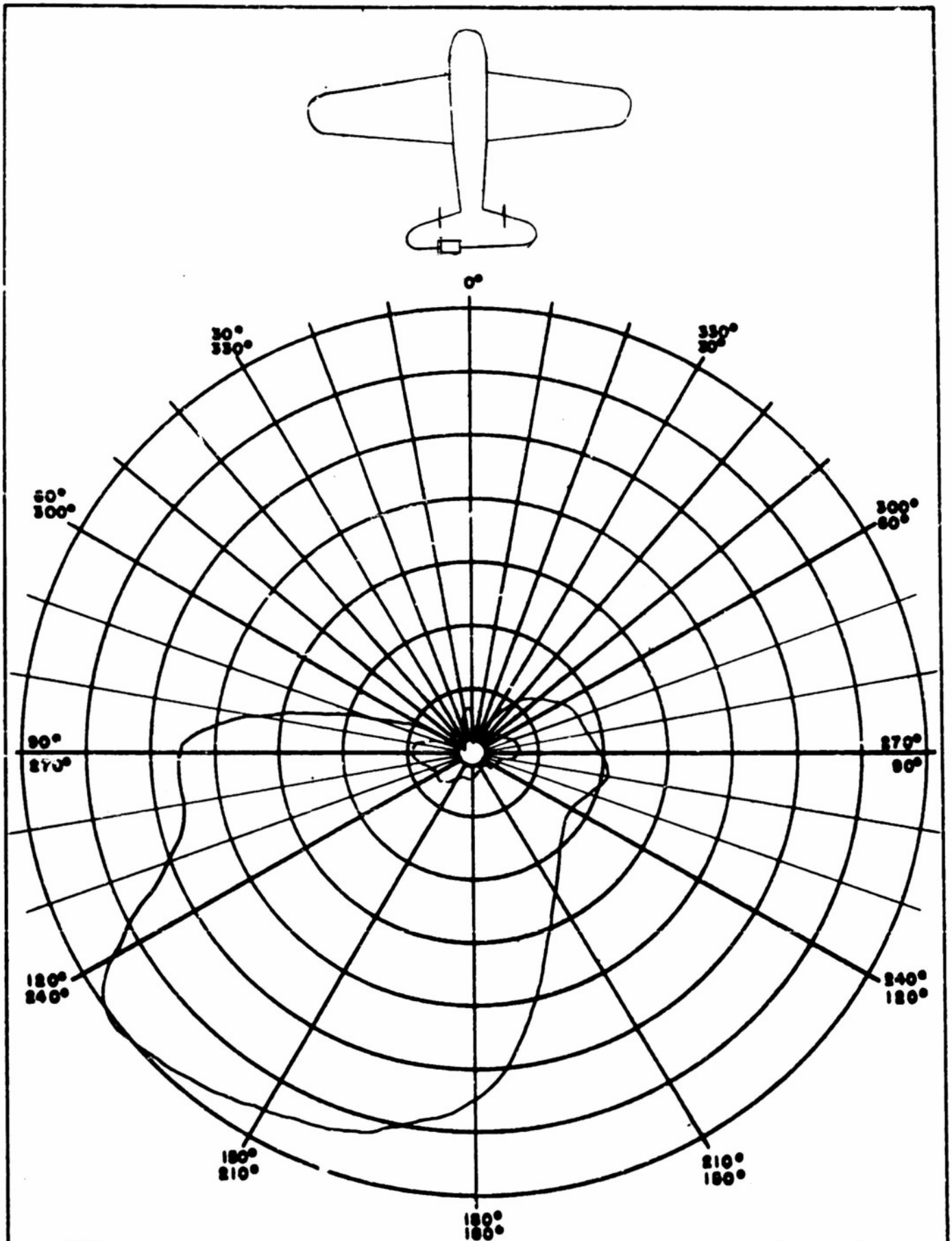

800 mc

——— Horizontal Polarization Pattern

- - - - - - - - Vertical Polarization Pattern

FIGURE 9a

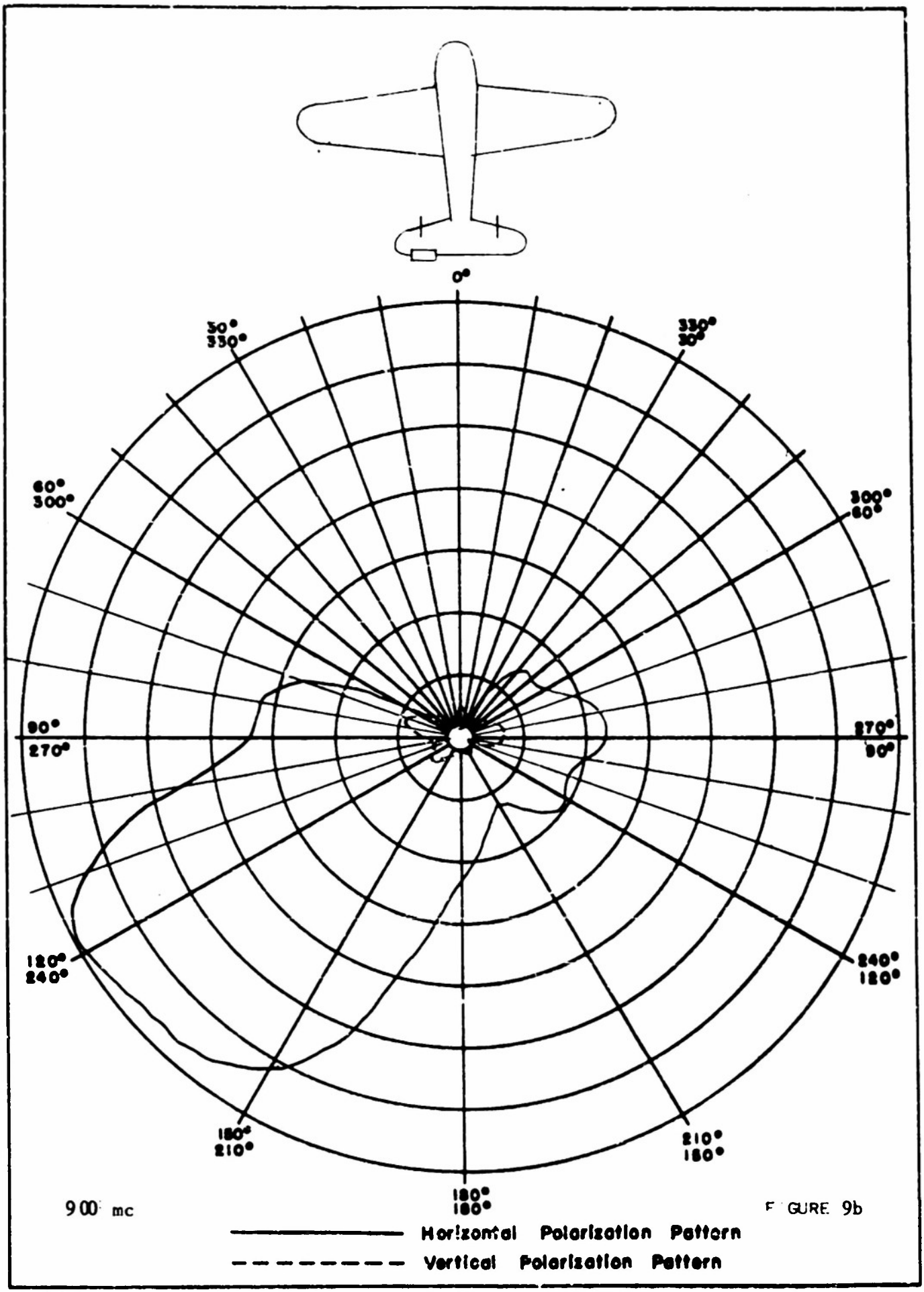
0°
30°
330°
60°
300°
90°
270°
120°
240°
150°
210°
180°
900 mc
Horizontal Polarization Pattern
Vertical Polarization Pattern

FIGURE 9b

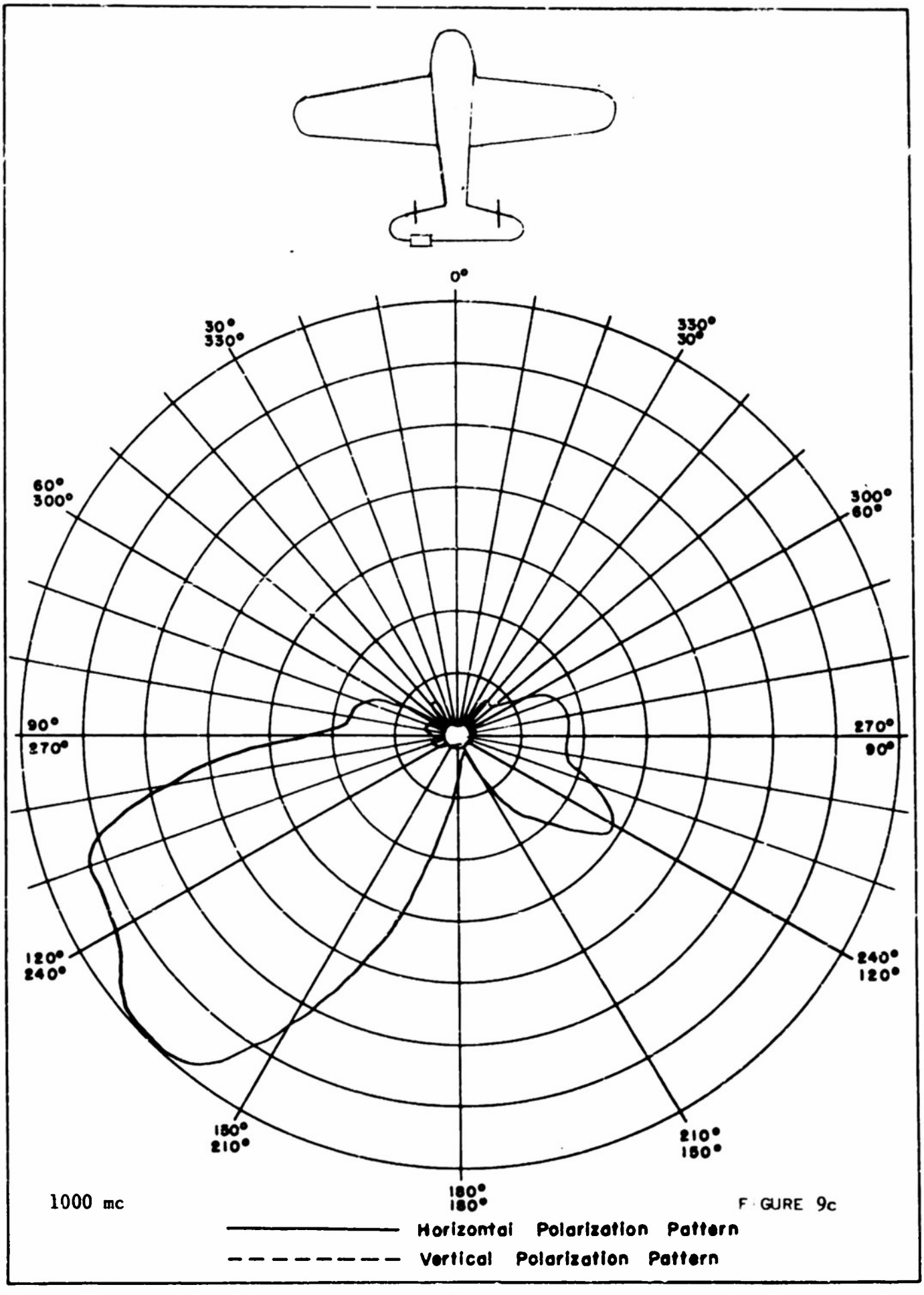
0°
30°
330°
330°
30°
60°
300°
300°
60°
90°
270°
270°
90°
120°
240°
240°
120°
150°
210°
210°
150°
180°
180°
1000 mc
Horizontal Polarization Pattern
Vertical Polarization Pattern

FIGURE 9c

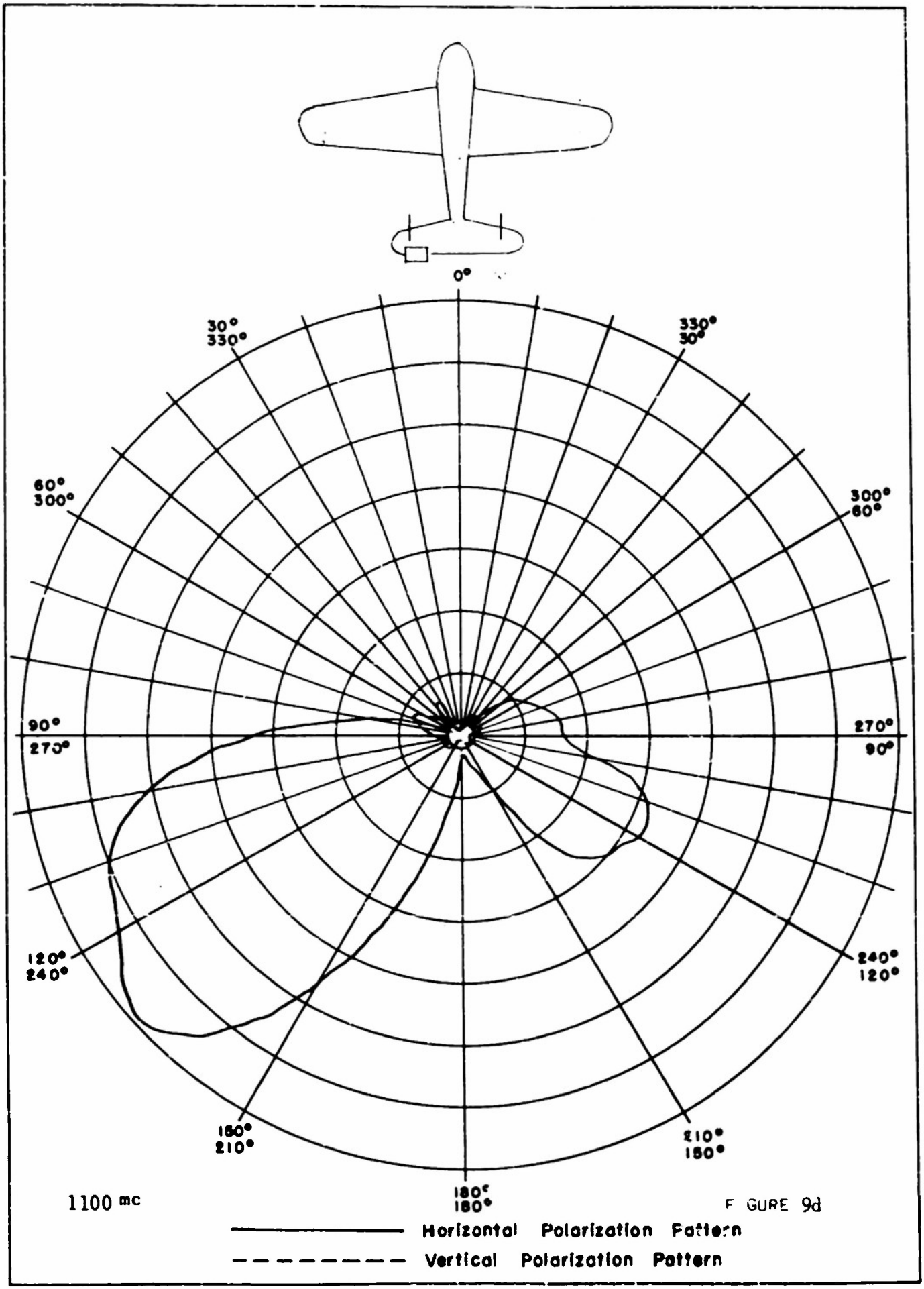
0°
30°
330°
330°
30°
60°
300°
300°
60°
90°
270°
270°
90°
120°
240°
240°
120°
150°
210°
210°
150°
180°
180°
1100 mc
Horizontal Polarization Pattern
Vertical Polarization Pattern

FIGURE 9d

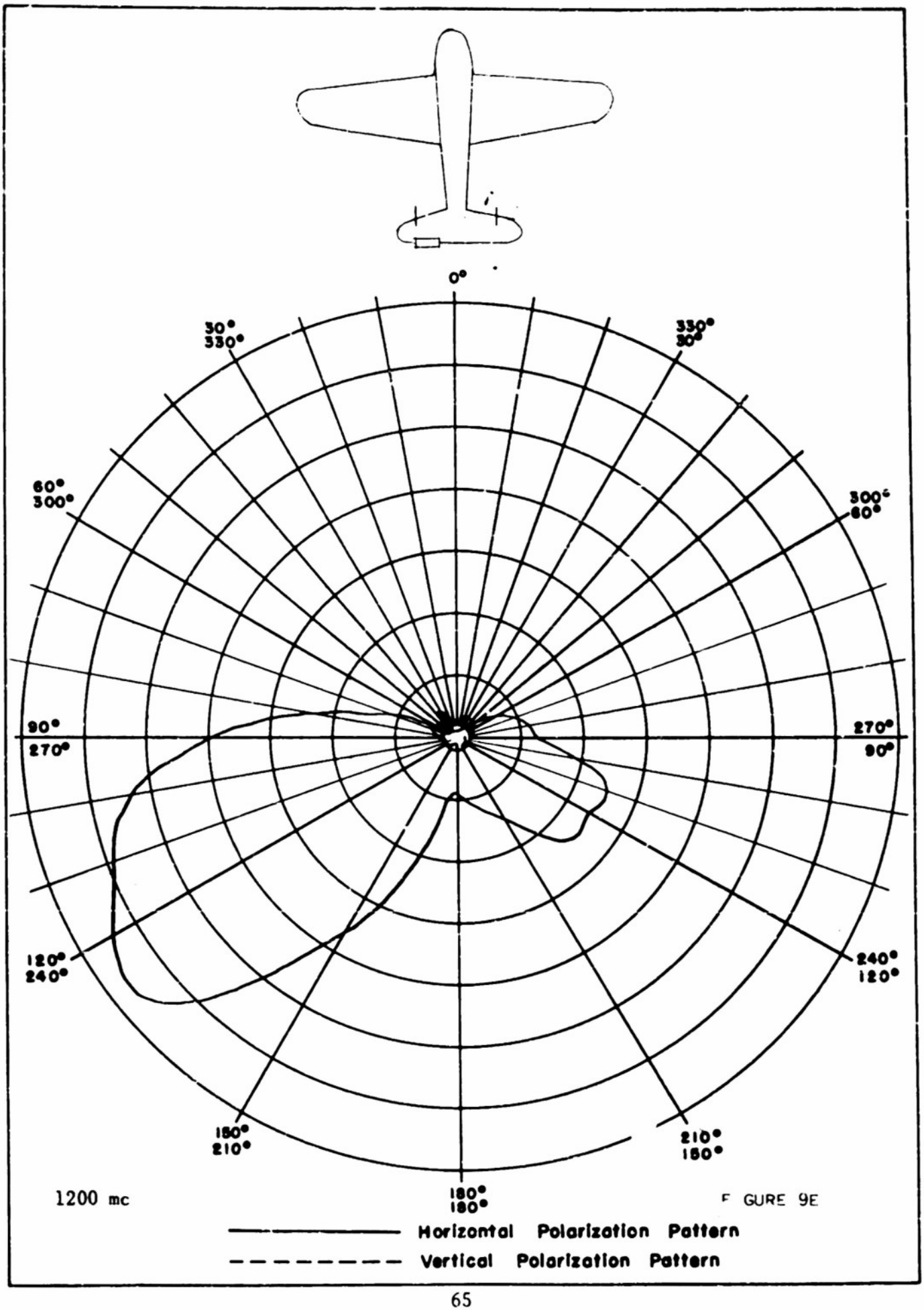
0°
30°
330°
330°
30°
60°
300°
300°
60°
90°
270°
270°
90°
120°
240°
240°
120°
150°
210°
210°
150°
180°
180°
1200 mc
FIGURE 9E
Horizontal Polarization Pattern
Vertical Polarization Pattern

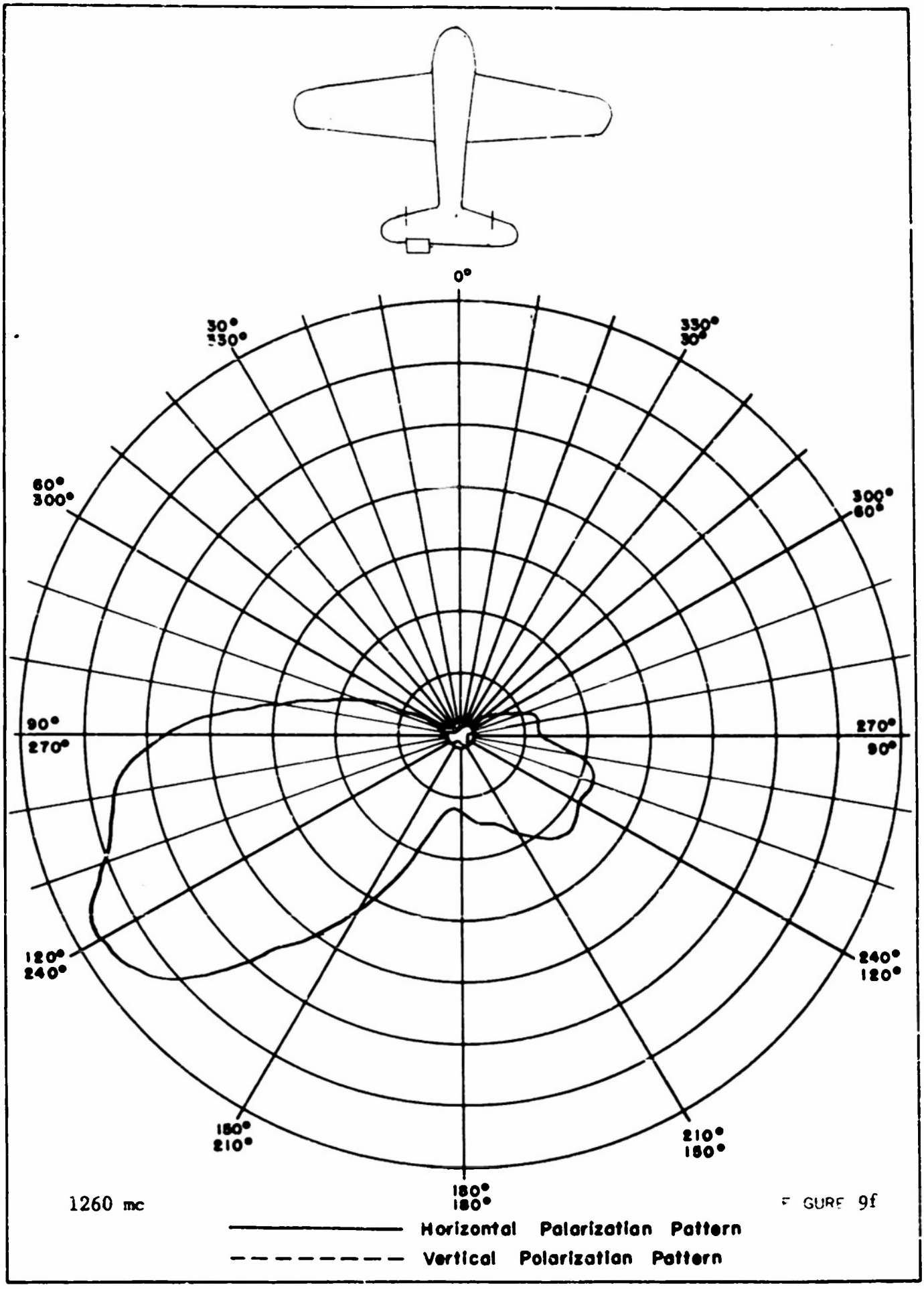
0°
30°
330°
330°
30°
60°
300°
300°
60°
90°
270°
270°
90°
120°
240°
240°
120°
150°
210°
210°
150°
180°
180°
1260 mc
Horizontal Polarization Pattern
Vertical Polarization Pattern

FIGURE 9f

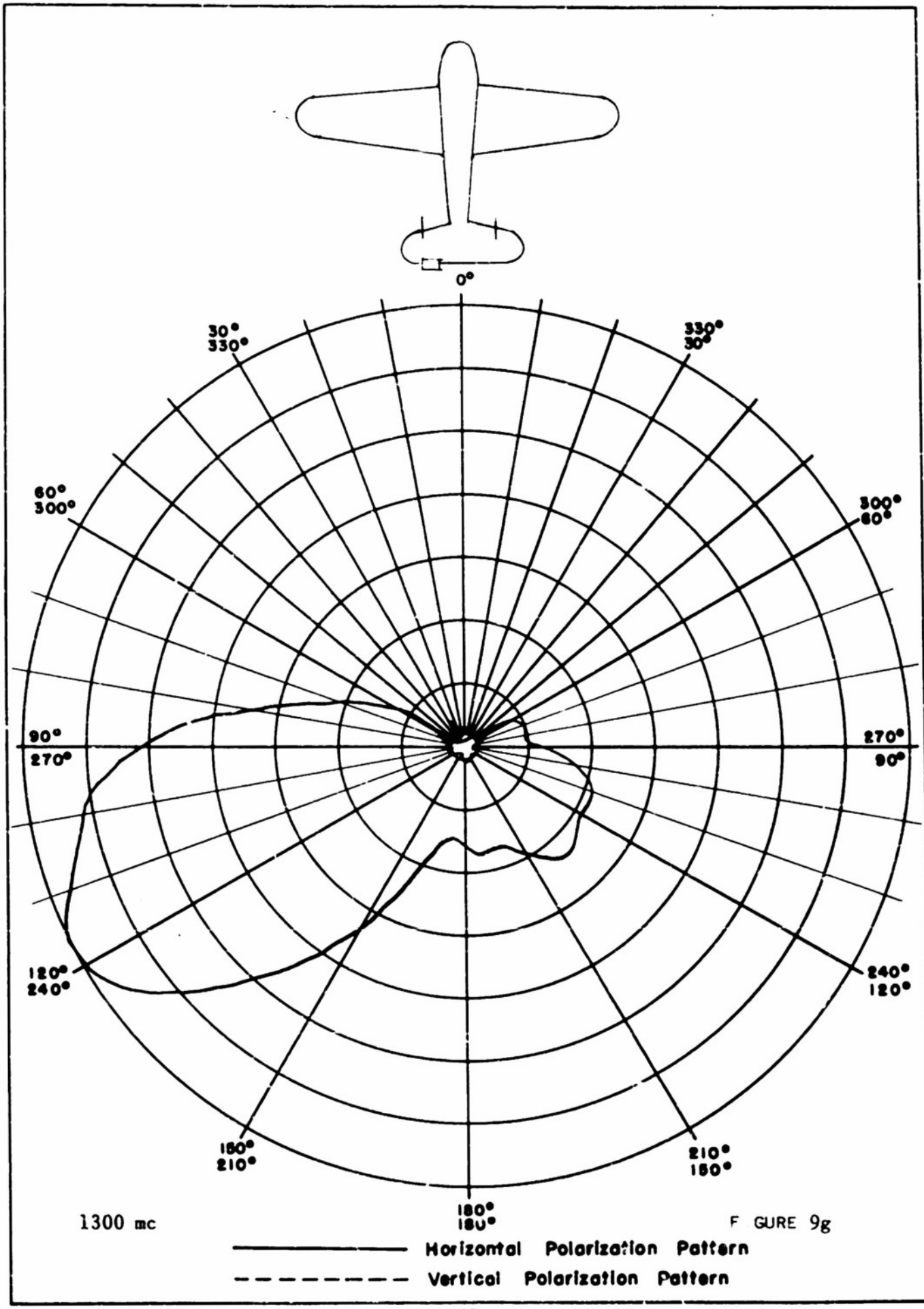
0°
30°
330°
330°
30°
60°
300°
300°
60°
90°
270°
270°
90°
120°
240°
240°
120°
150°
210°
210°
150°
180°
180°
1300 mc
Horizontal Polarization Pattern
Vertical Polarization Pattern

FIGURE 9g

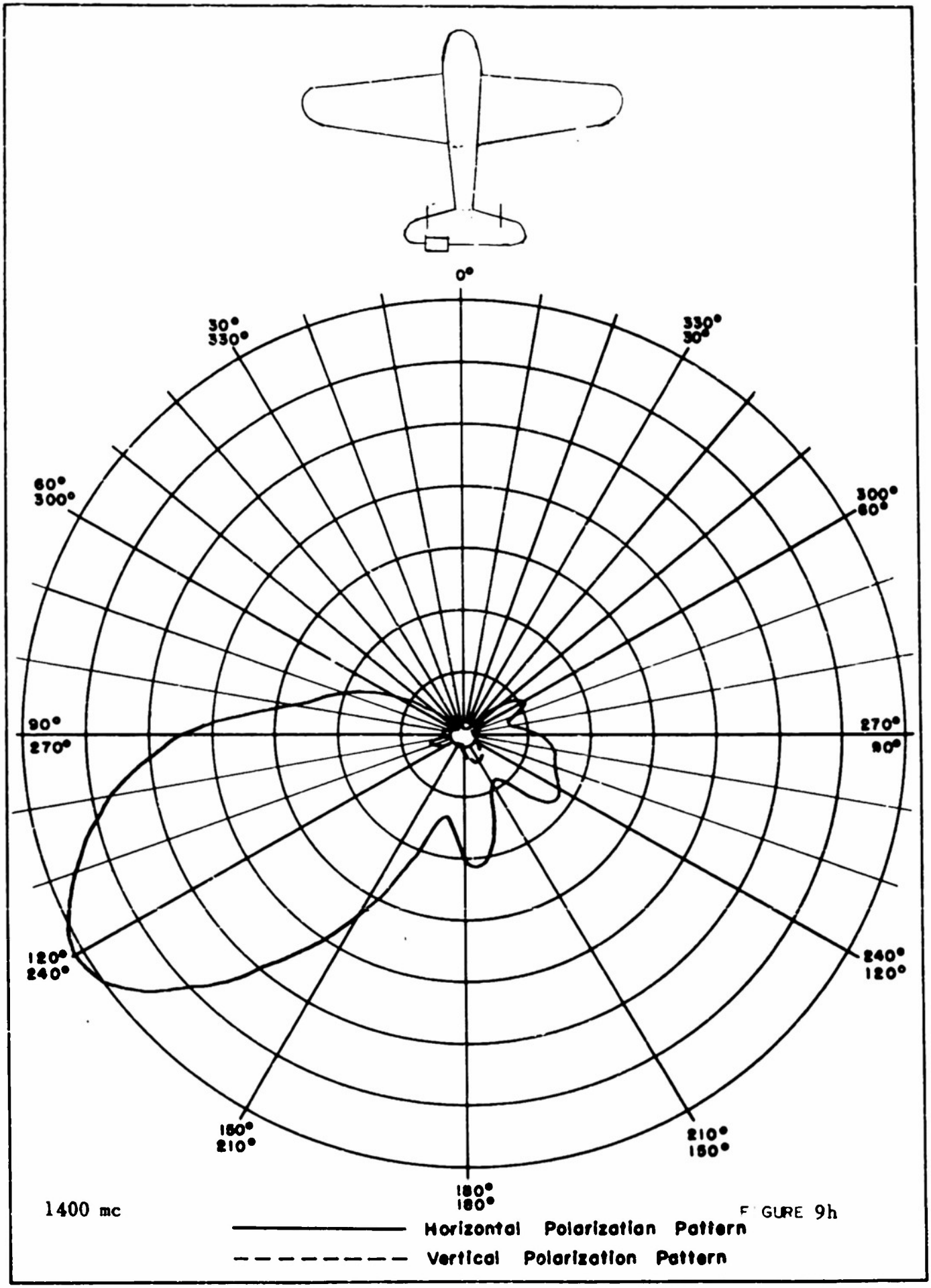
0°
30°
330°
330°
30°
60°
300°
300°
60°
90°
270°
270°
90°
120°
240°
240°
120°
150°
210°
210°
150°
180°
180°
1400 mc
Horizontal Polarization Pattern
Vertical Polarization Pattern

FIGURE 9h

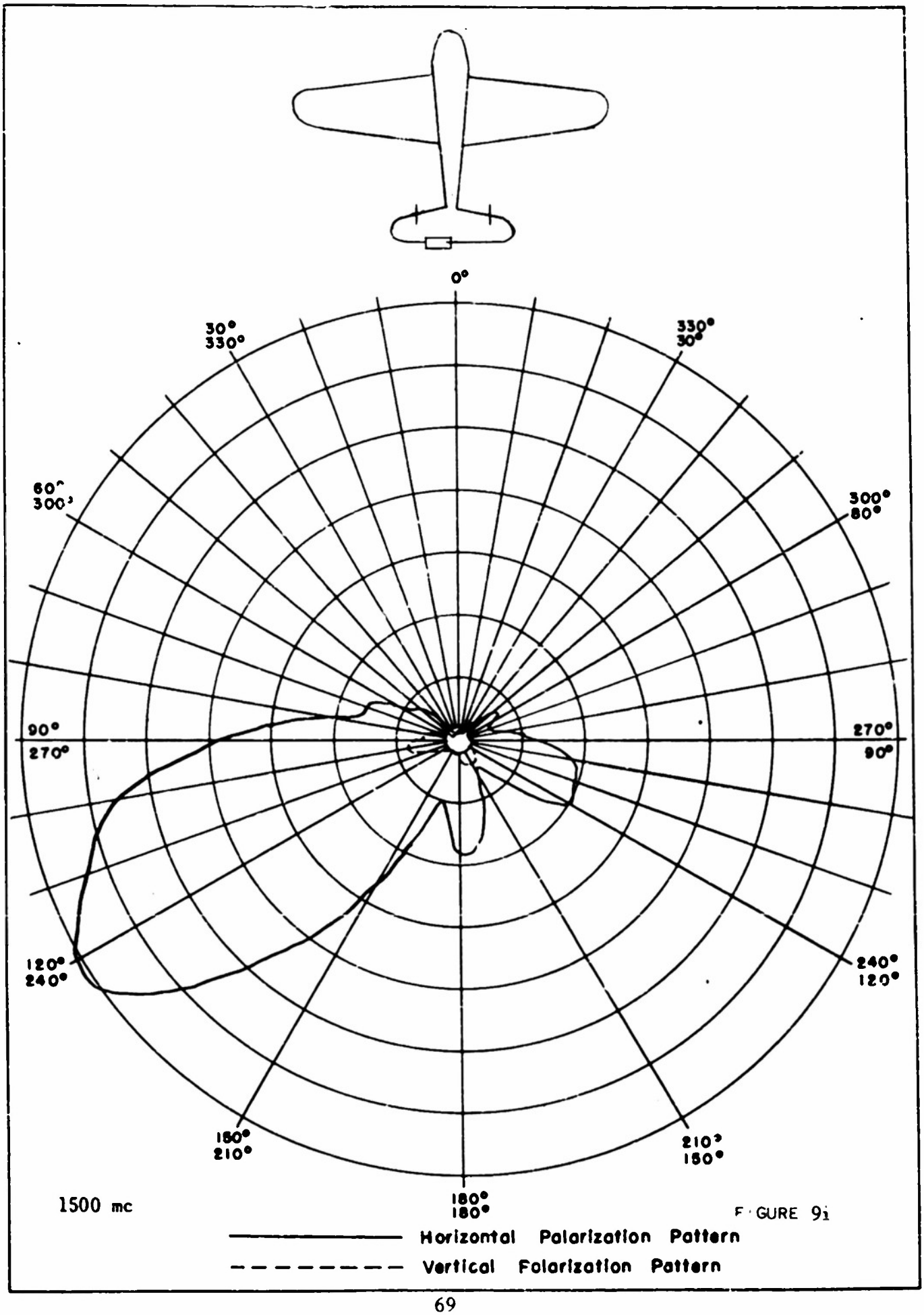
0°
30°
330°
330°
30°
60°
300°
300°
80°
90°
270°
270°
90°
120°
240°
240°
120°
150°
210°
210°
150°
180°
180°
1500 mc
Horizontal Polarization Pattern
Vertical Polarization Pattern

FIGURE 9i

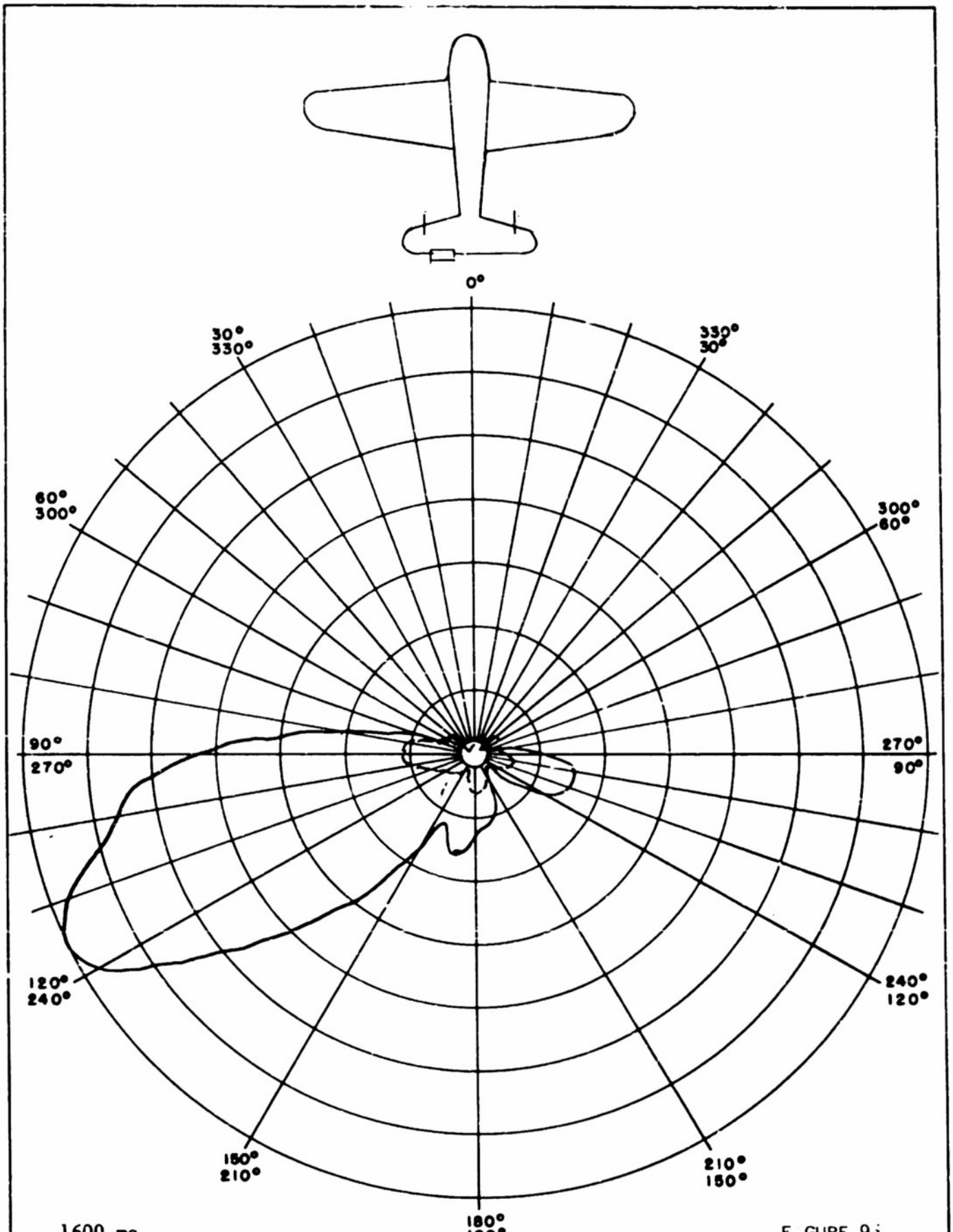

1600 mc

FIGURE 9j

Horizontal Polarization Pattern

Vertical Polarization Pattern

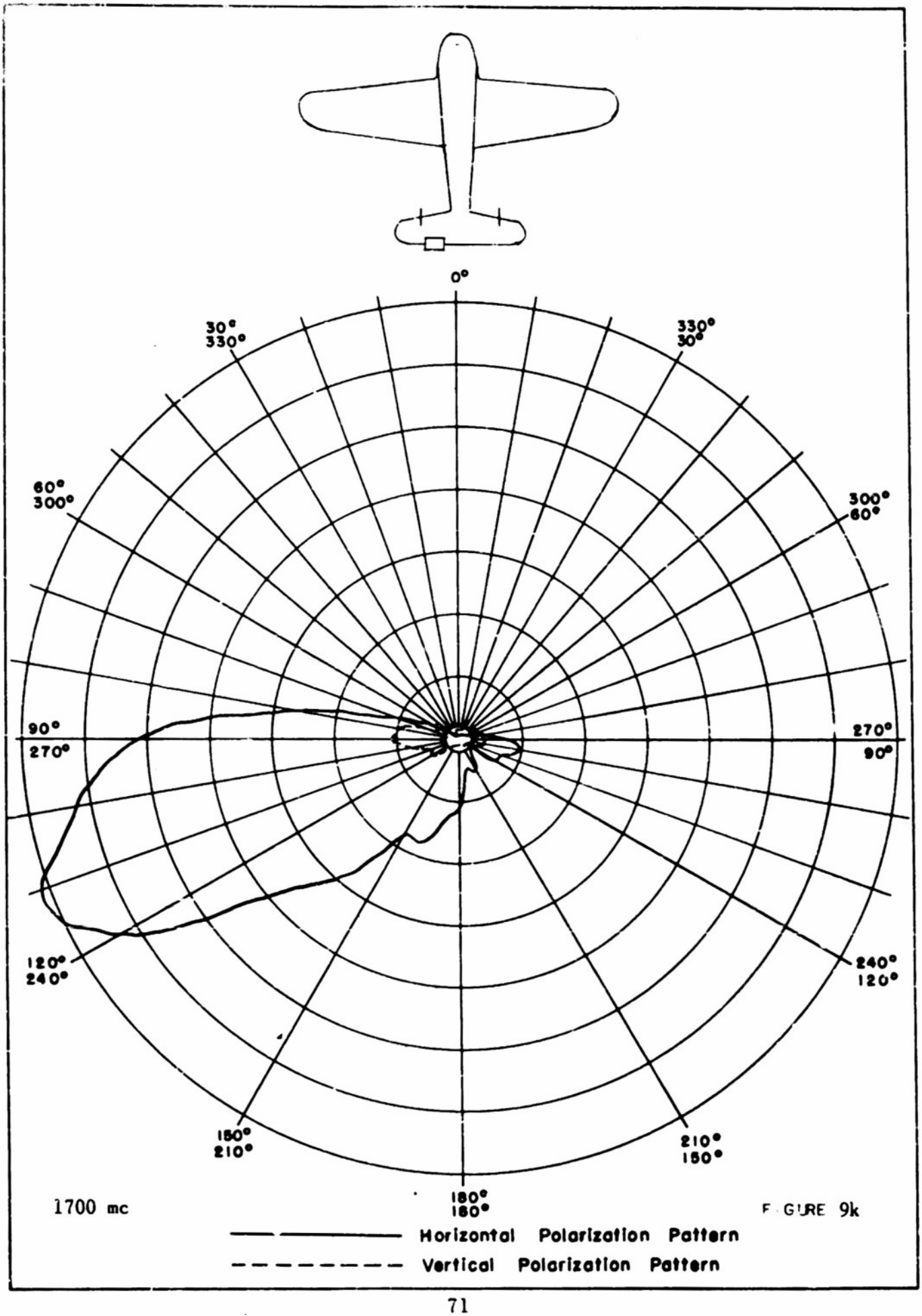

1700 mc

FIGURE 9k

——— Horizontal Polarization Pattern

- - - - - - - Vertical Polarization Pattern

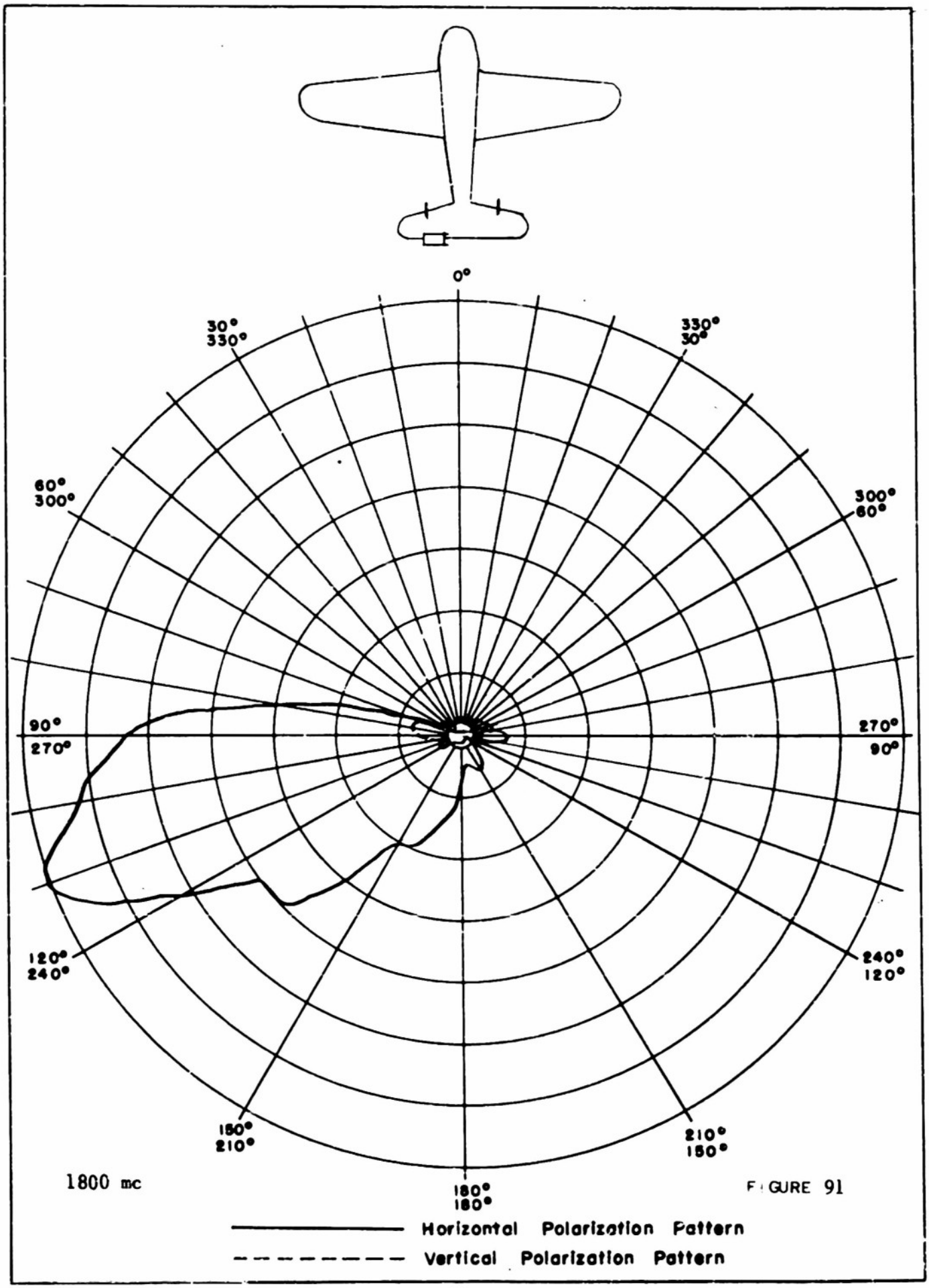
0°
30°
330°
330°
30°
60°
300°
300°
60°
90°
270°
270°
90°
120°
240°
240°
120°
150°
210°
210°
150°
180°
180°
1800 mc
Horizontal Polarization Pattern
Vertical Polarization Pattern

FIGURE 91

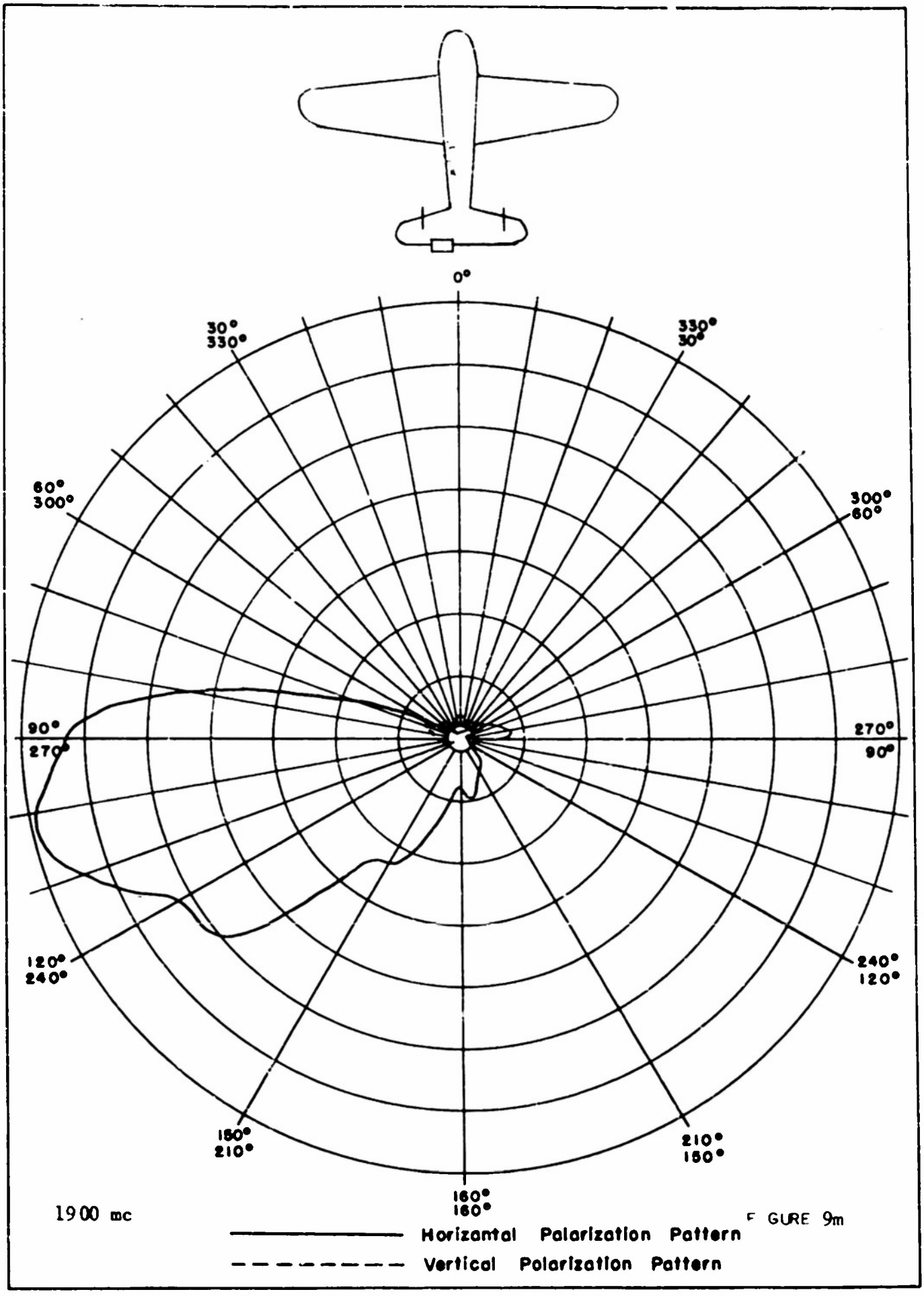

1900 mc

FIGURE 9m

Horizontal Polarization Pattern

Vertical Polarization Pattern

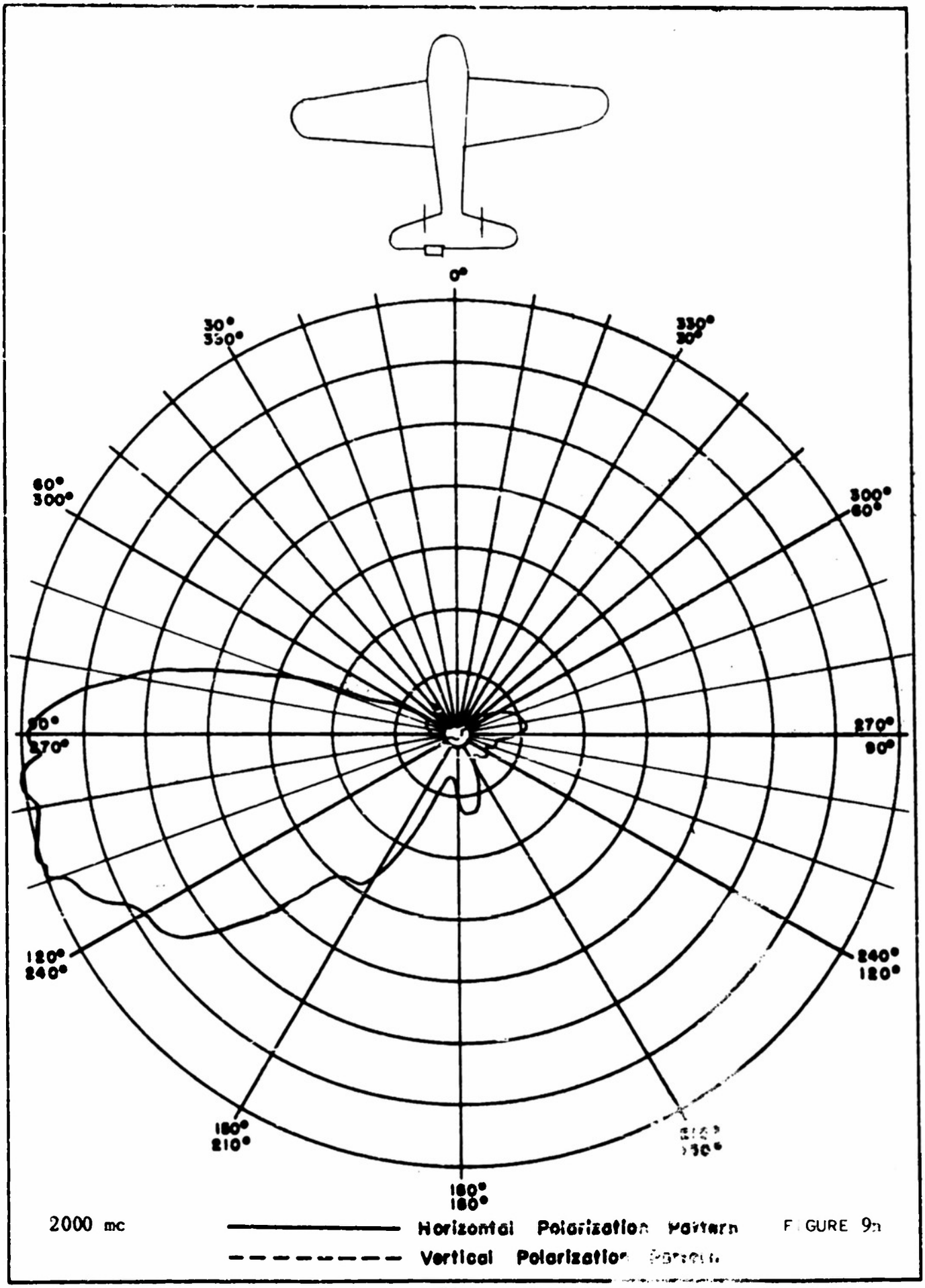
0°
30°
330°
60°
300°
90°
270°
120°
240°
150°
210°
180°
180°
2000 mc
Horizontal Polarization Pattern
Vertical Polarization Pattern

FIGURE 9n

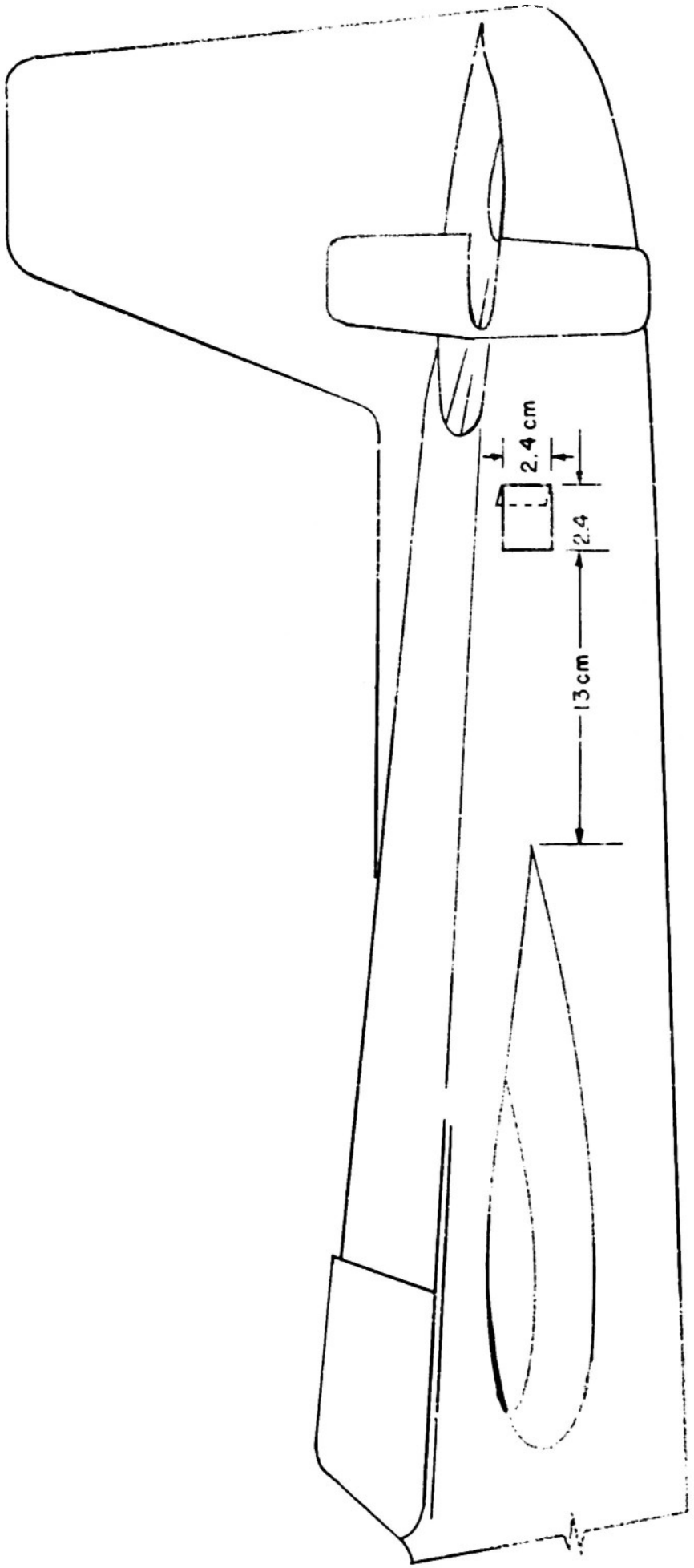

FIGURE 10

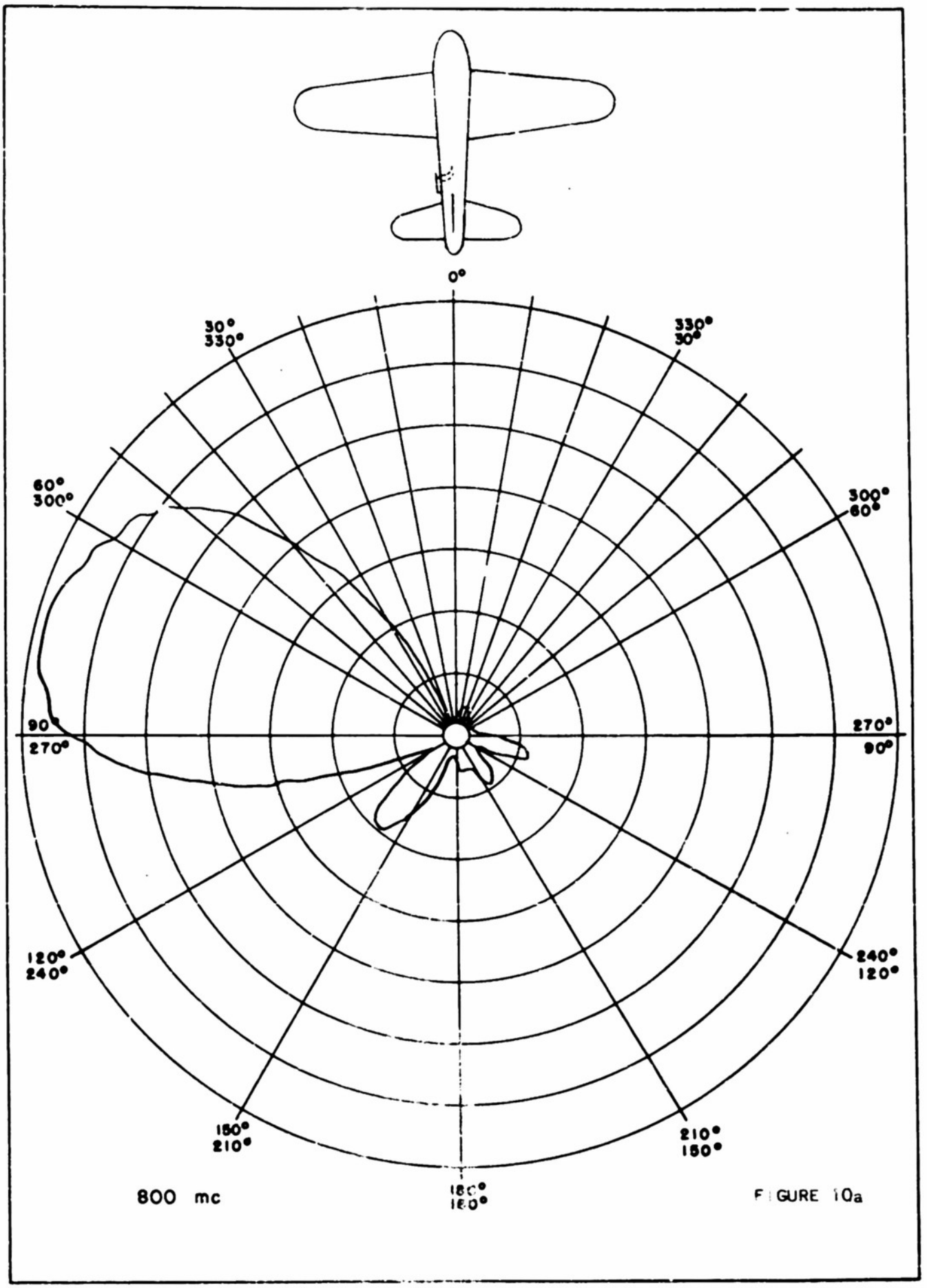

800 mc

FIGURE 10a

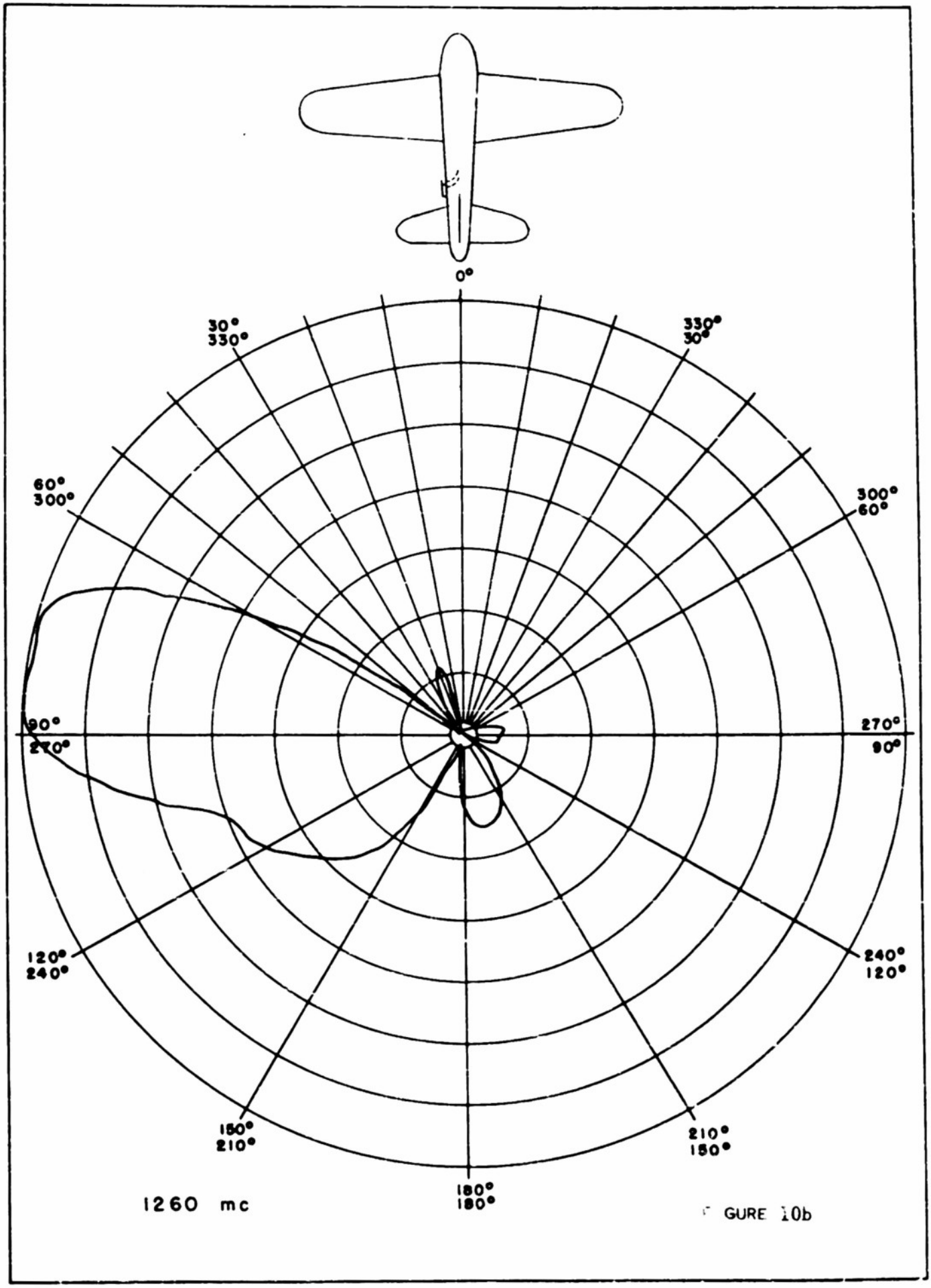
0°
30°
330°
330°
30°
60°
300°
300°
60°
90°
270°
270°
90°
120°
240°
240°
120°
150°
210°
210°
150°
180°
180°
1260 mc

FIGURE 10b

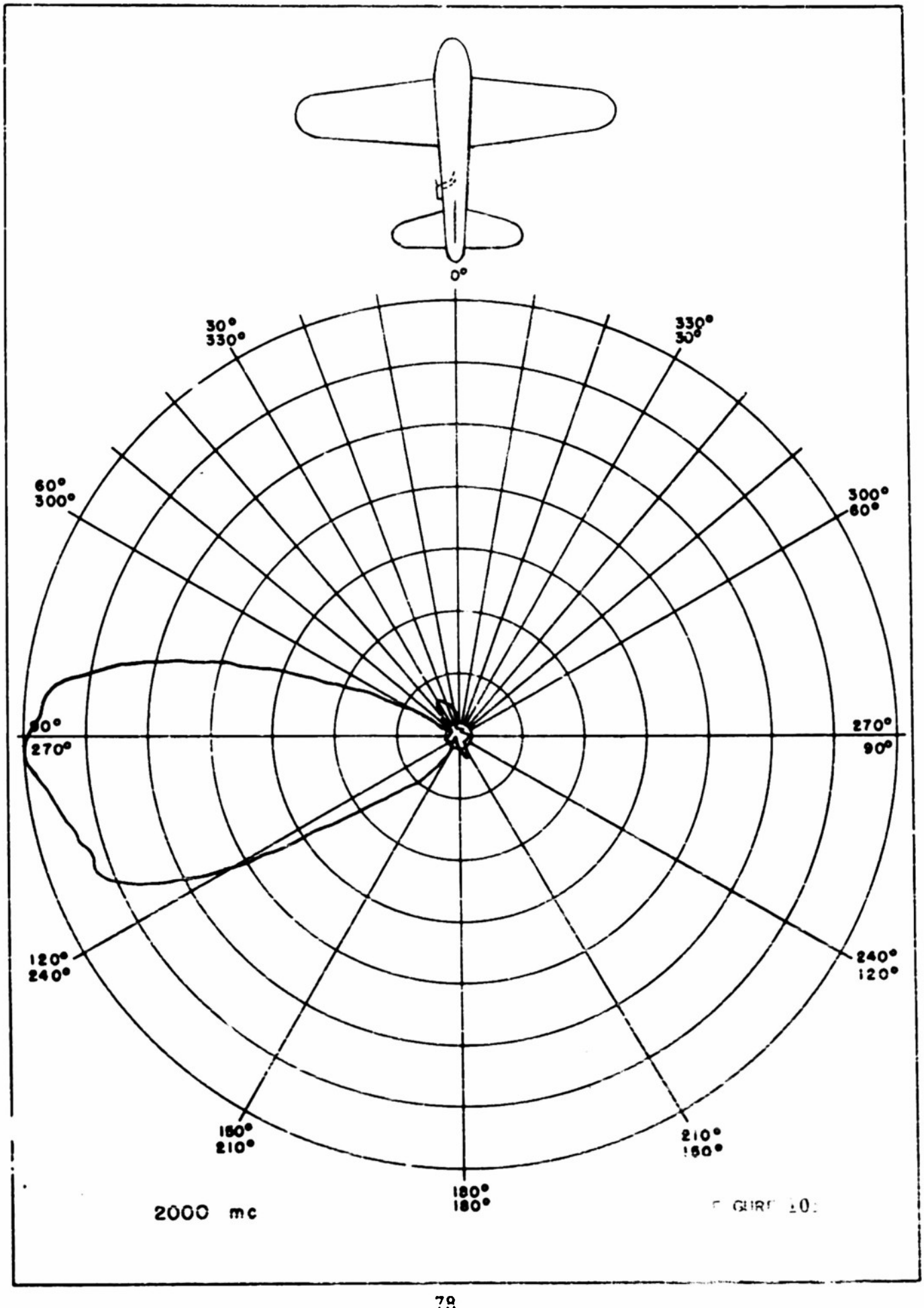

2000 mc

FIGURE 10

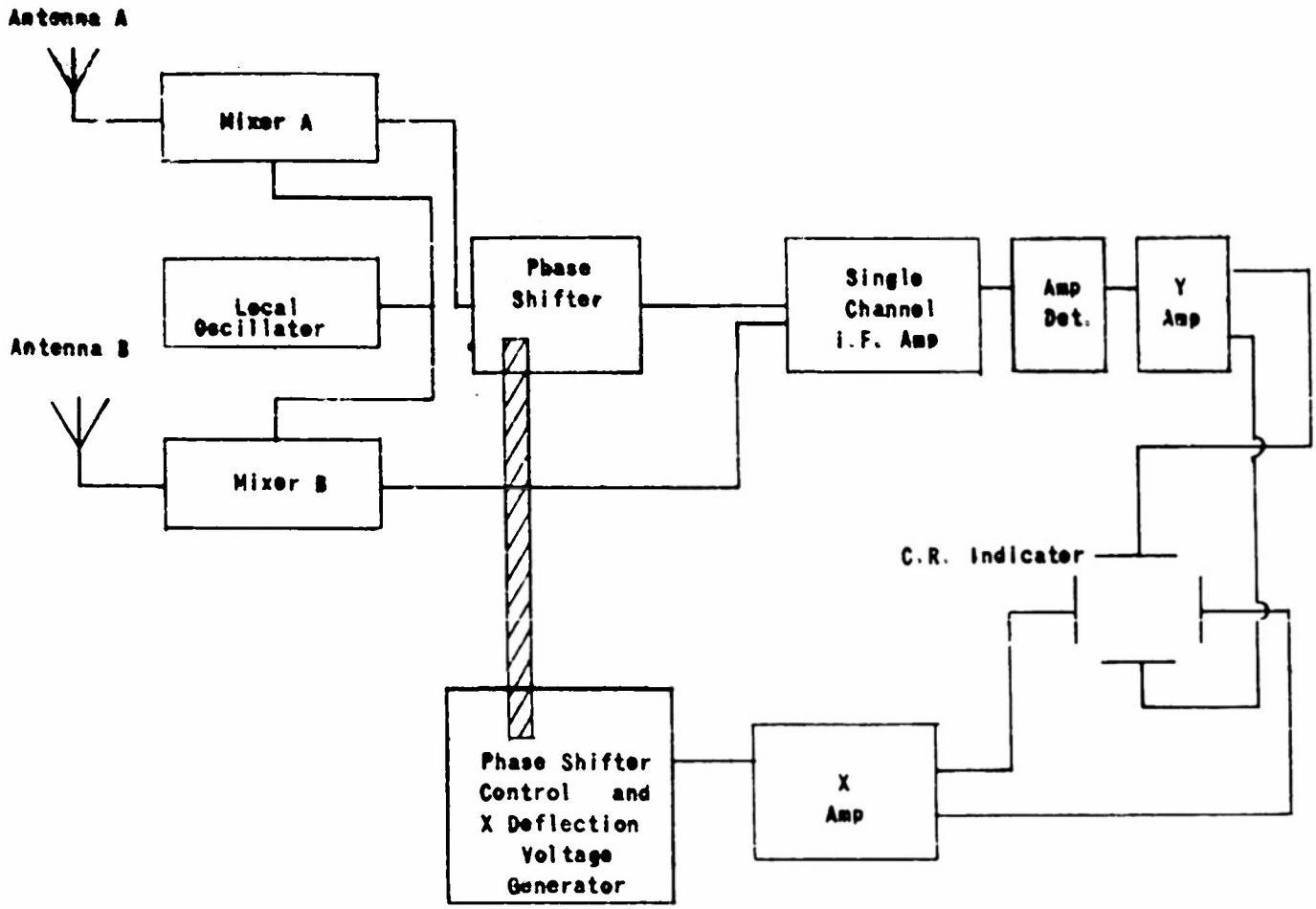

DF System Proposal

FIGURE 11

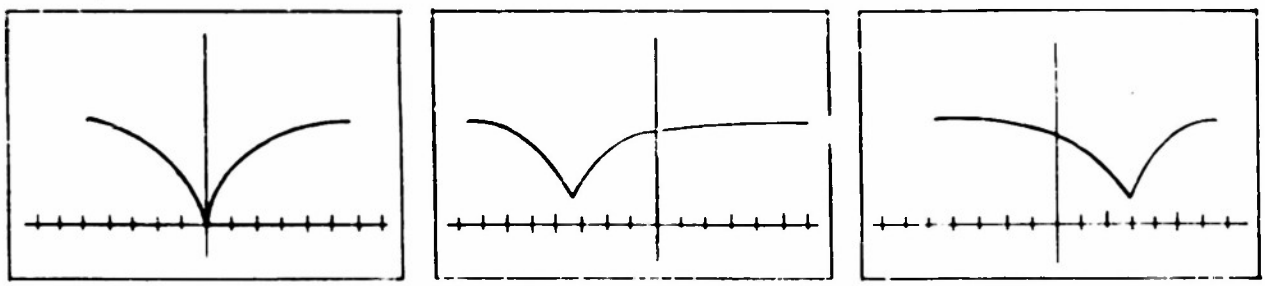

Transmitter Dead - Ahead

Transmitter to Left of Dead - Ahead

Transmitter to Right of Dead - Ahead

Appearance of Bearing Indicator

FIGURE 12

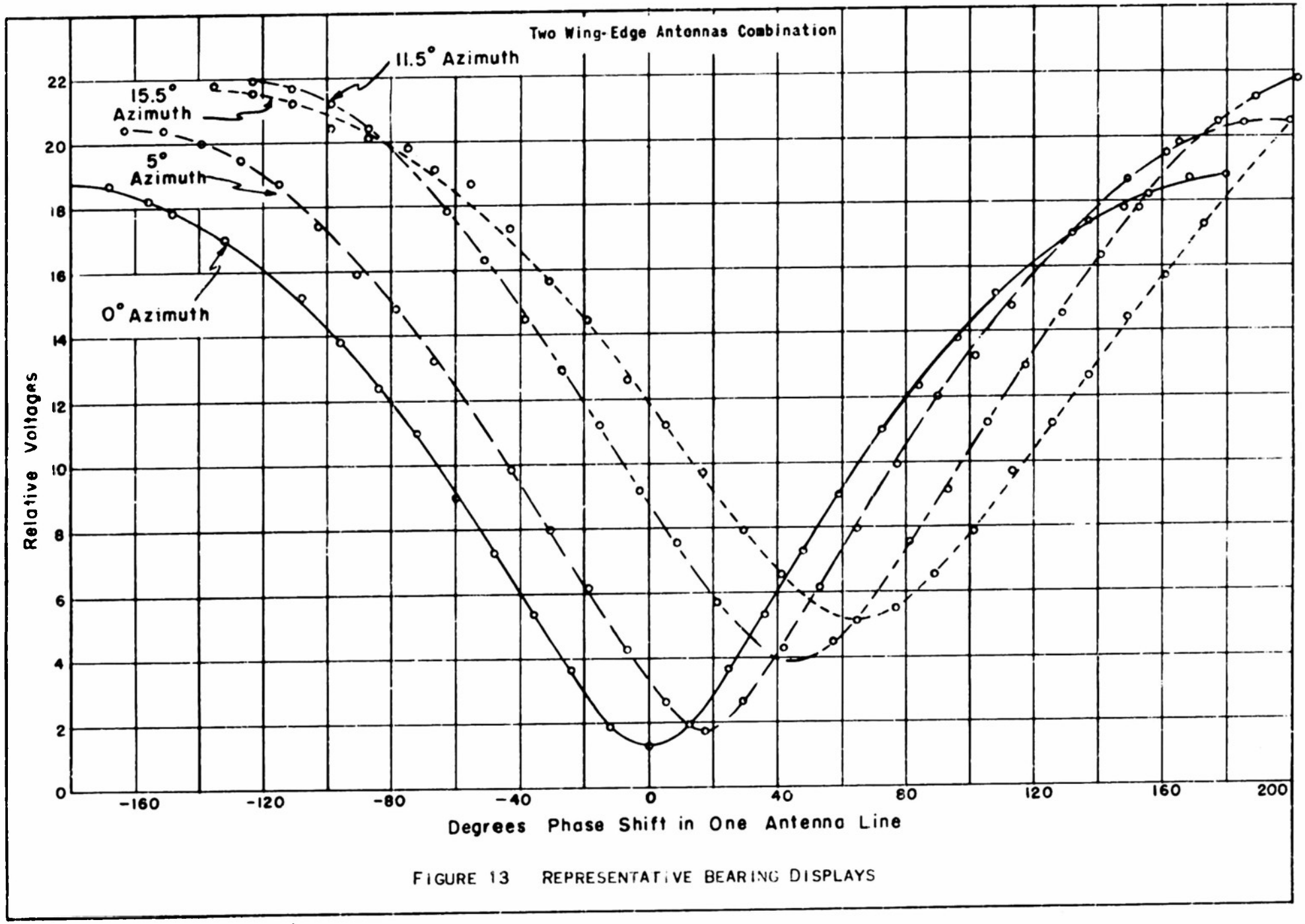

FIGURE 13 REPRESENTATIVE BEARING DISPLAYS

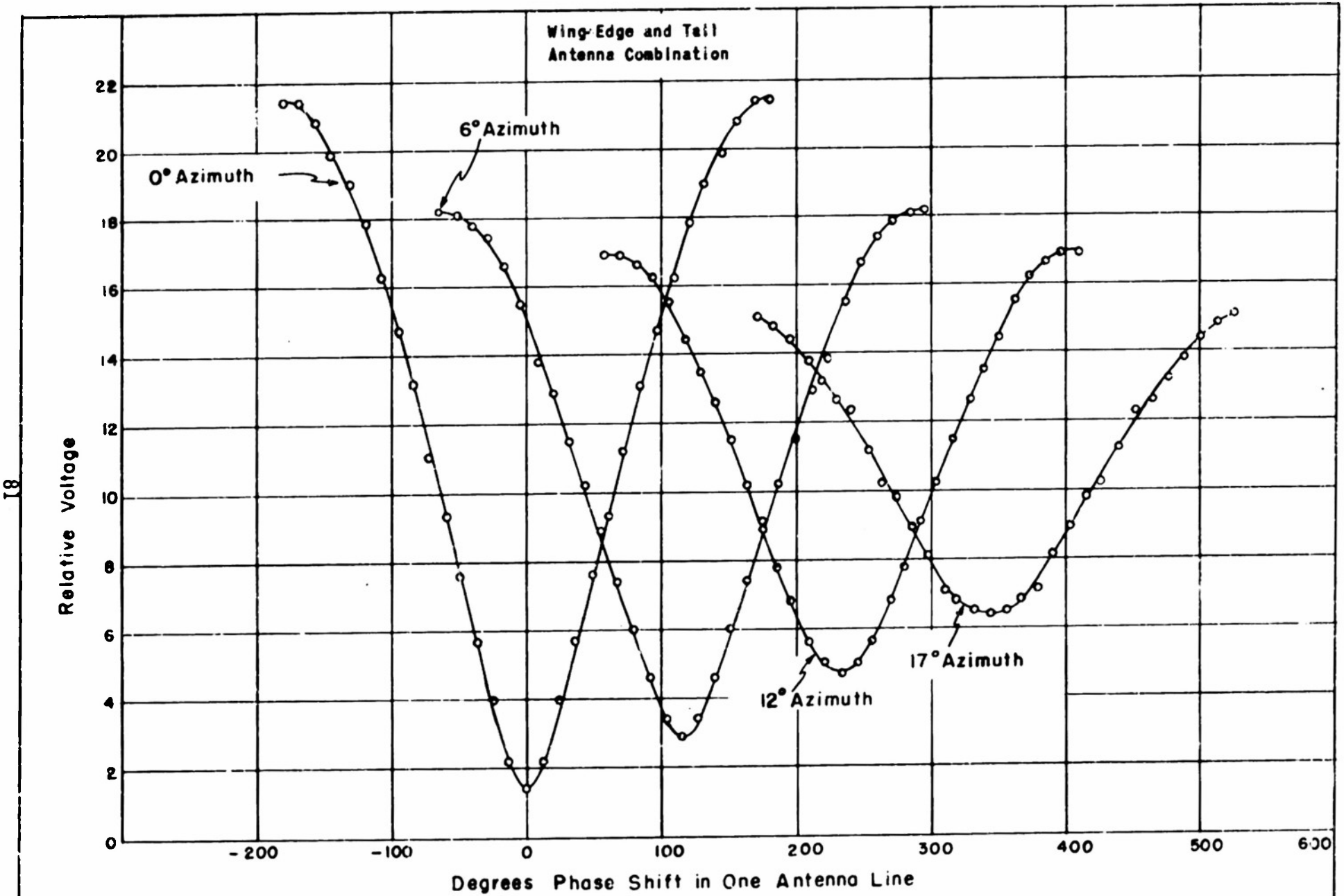

FIGURE 14 REPRESENTATIVE BEARING DISPLAYS

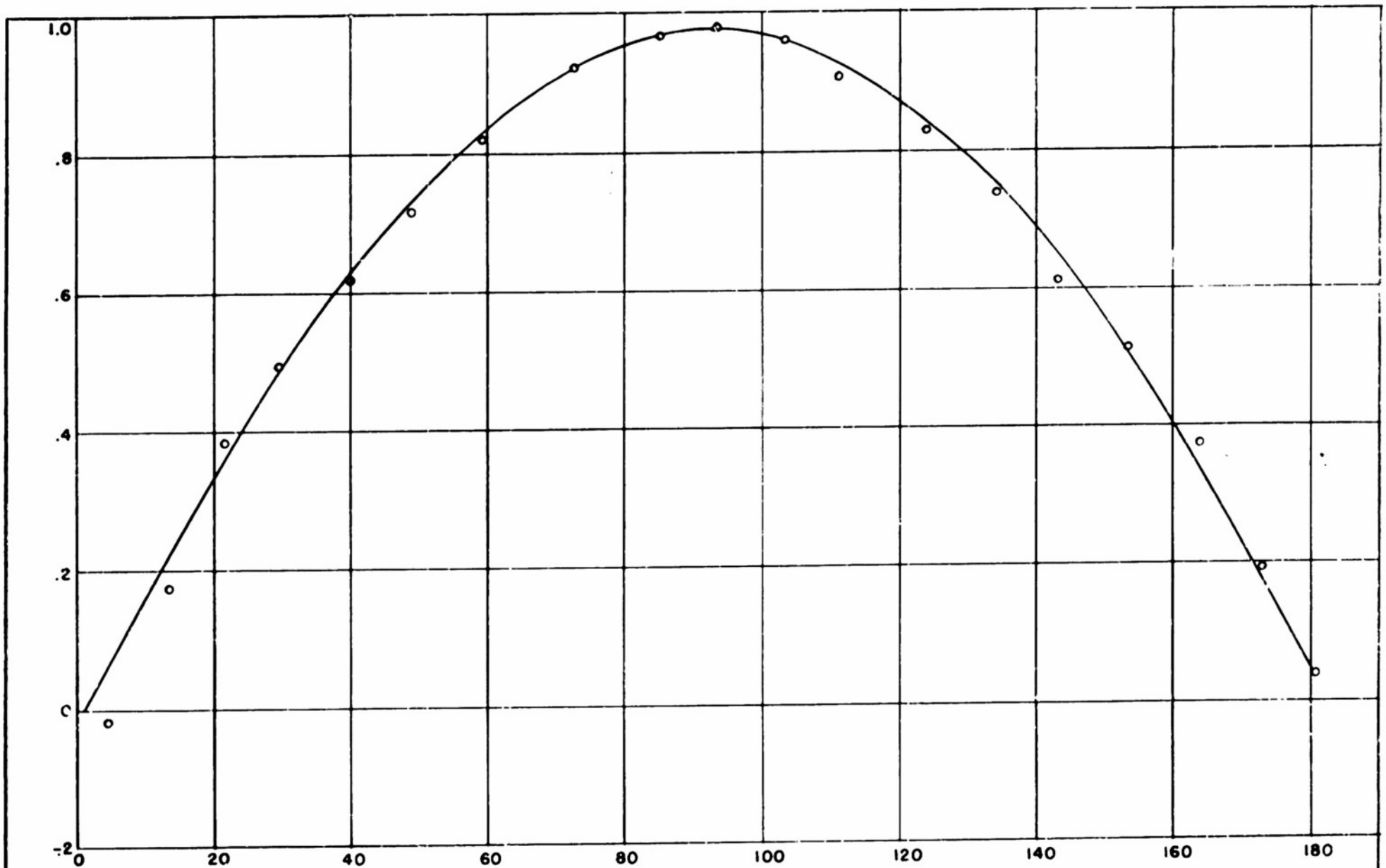

FIGURE 15 ANTENNA DIFFERENT A.. PHASE ADDING SCHEME ACCURACY CHECK MADE ON VERTICAL SLEEVE MONOPOLES
20 3 N BETWEEN ANTENNAS P 1250 MC λ 24 CM

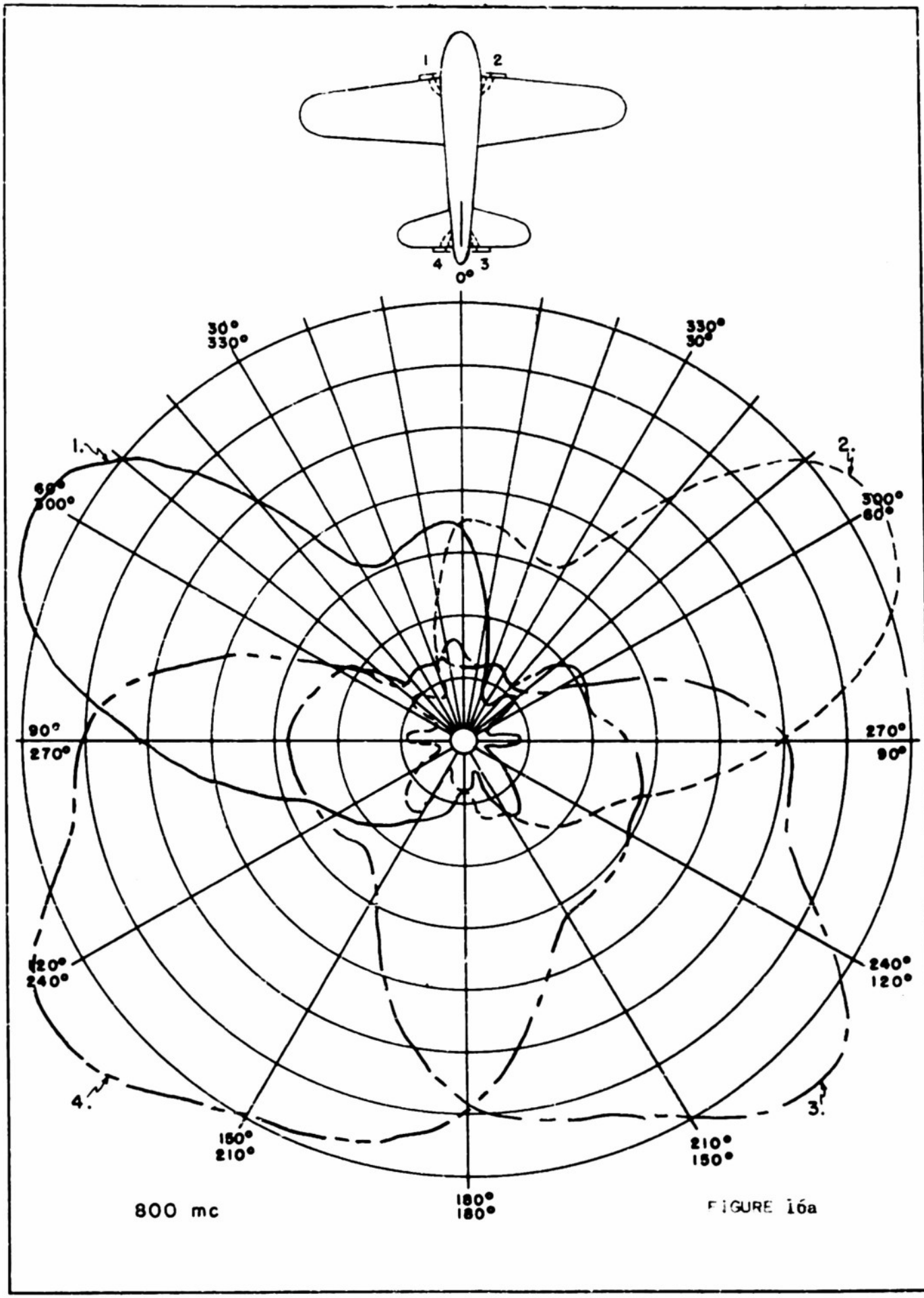

800 mc

FIGURE 16a

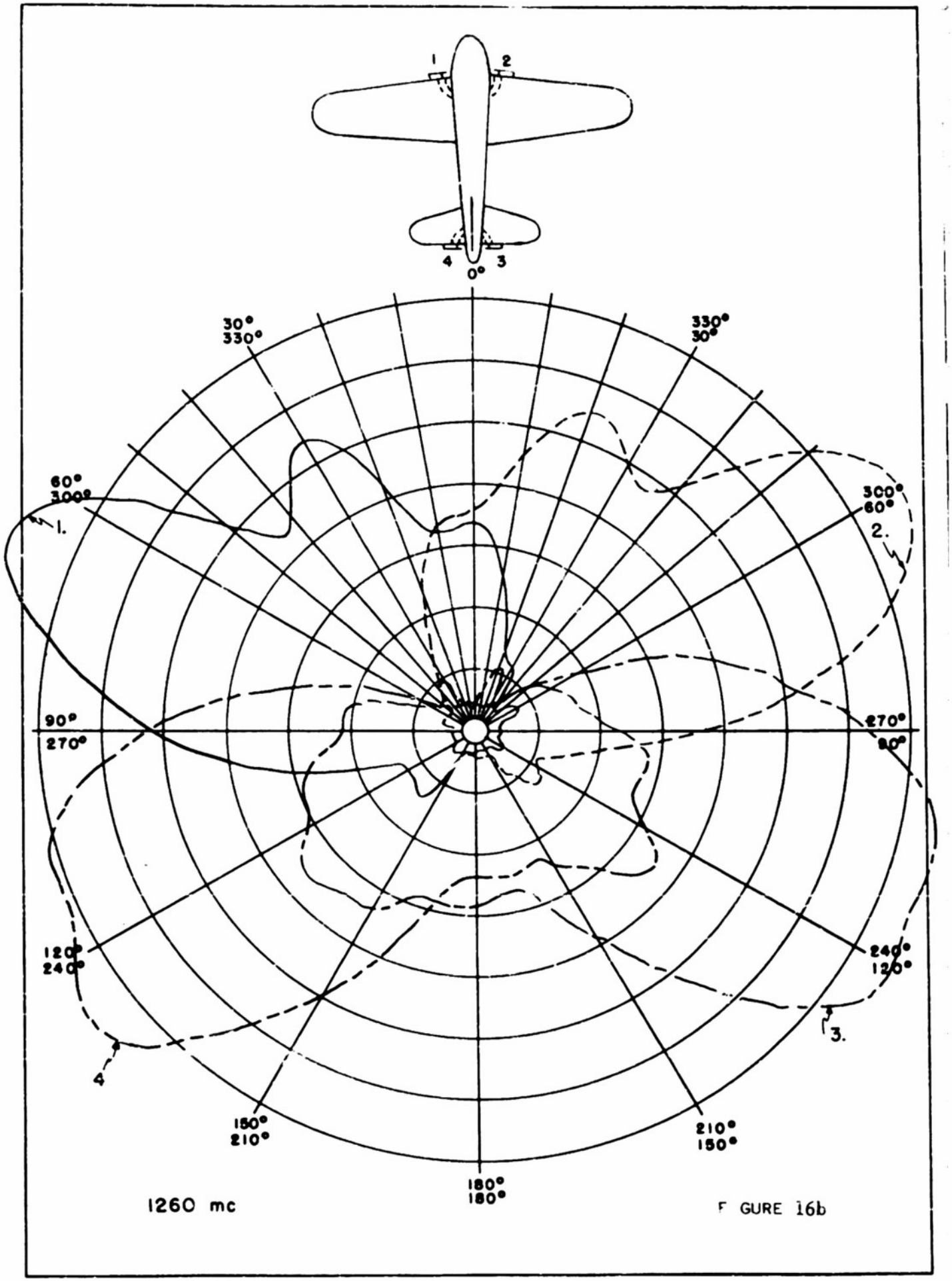

1260 mc

FIGURE 16b

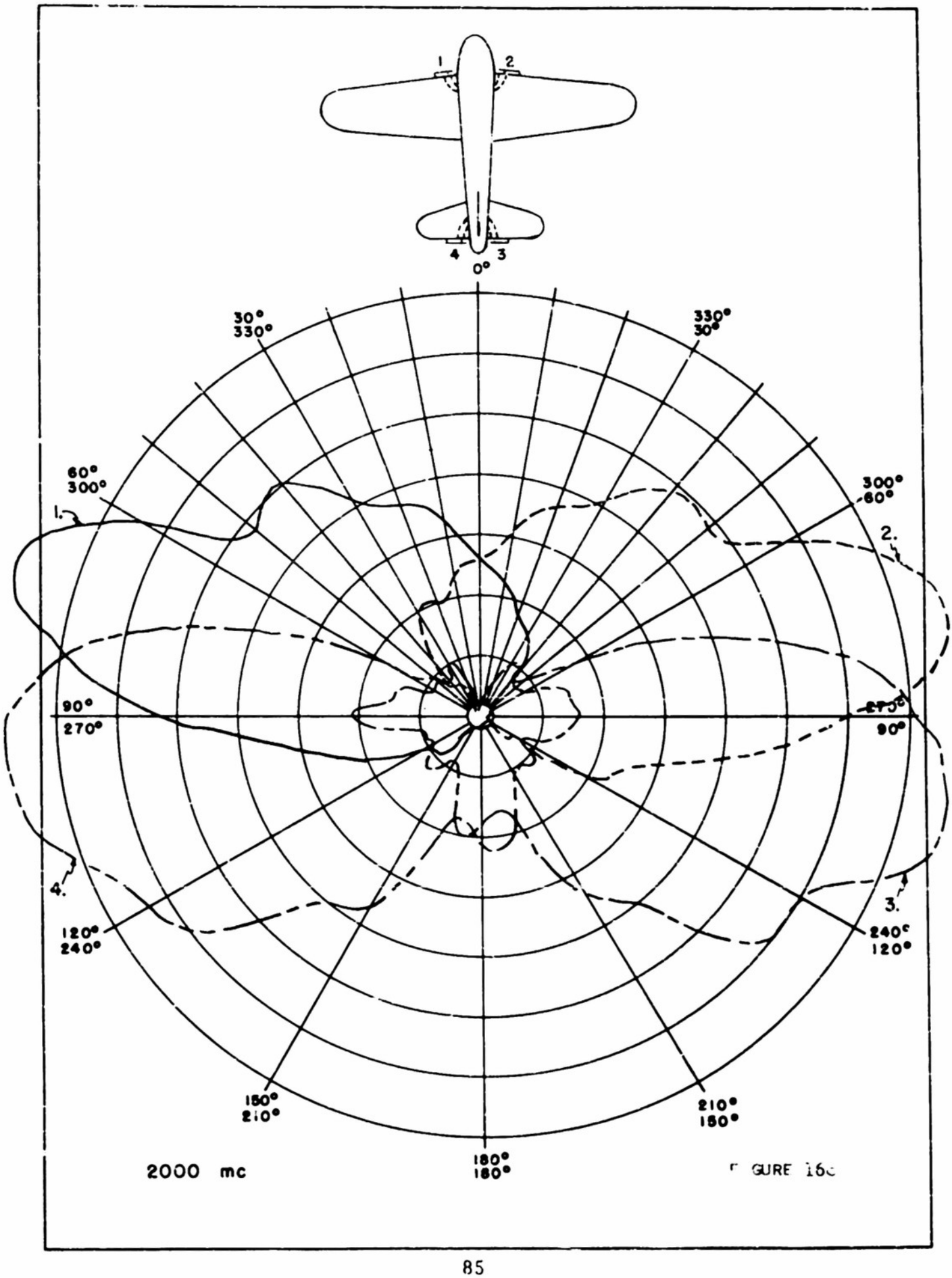

2000 mc

FIGURE 16c

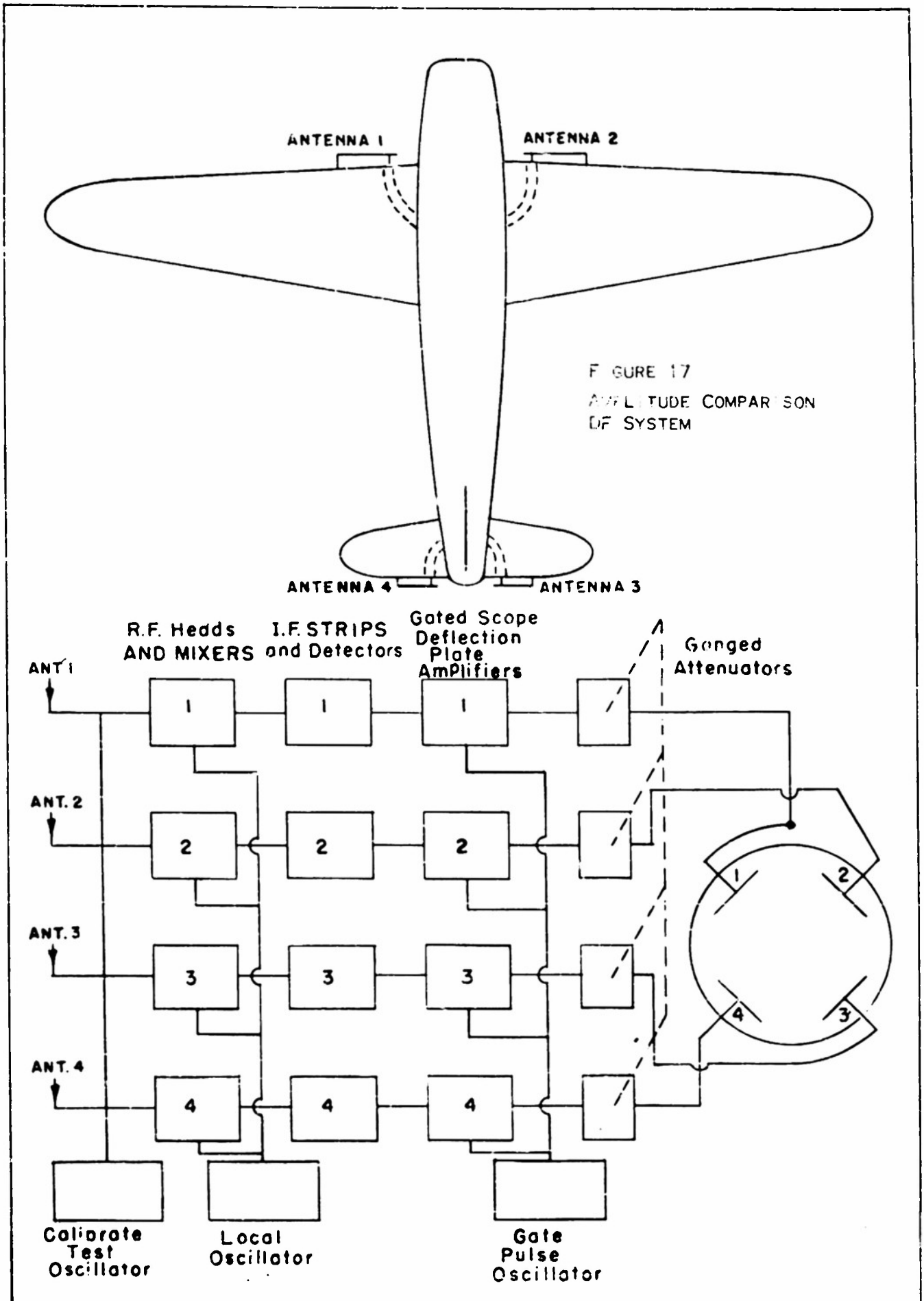

FIGURE 17

AMPLITUDE COMPARISON DF SYSTEM

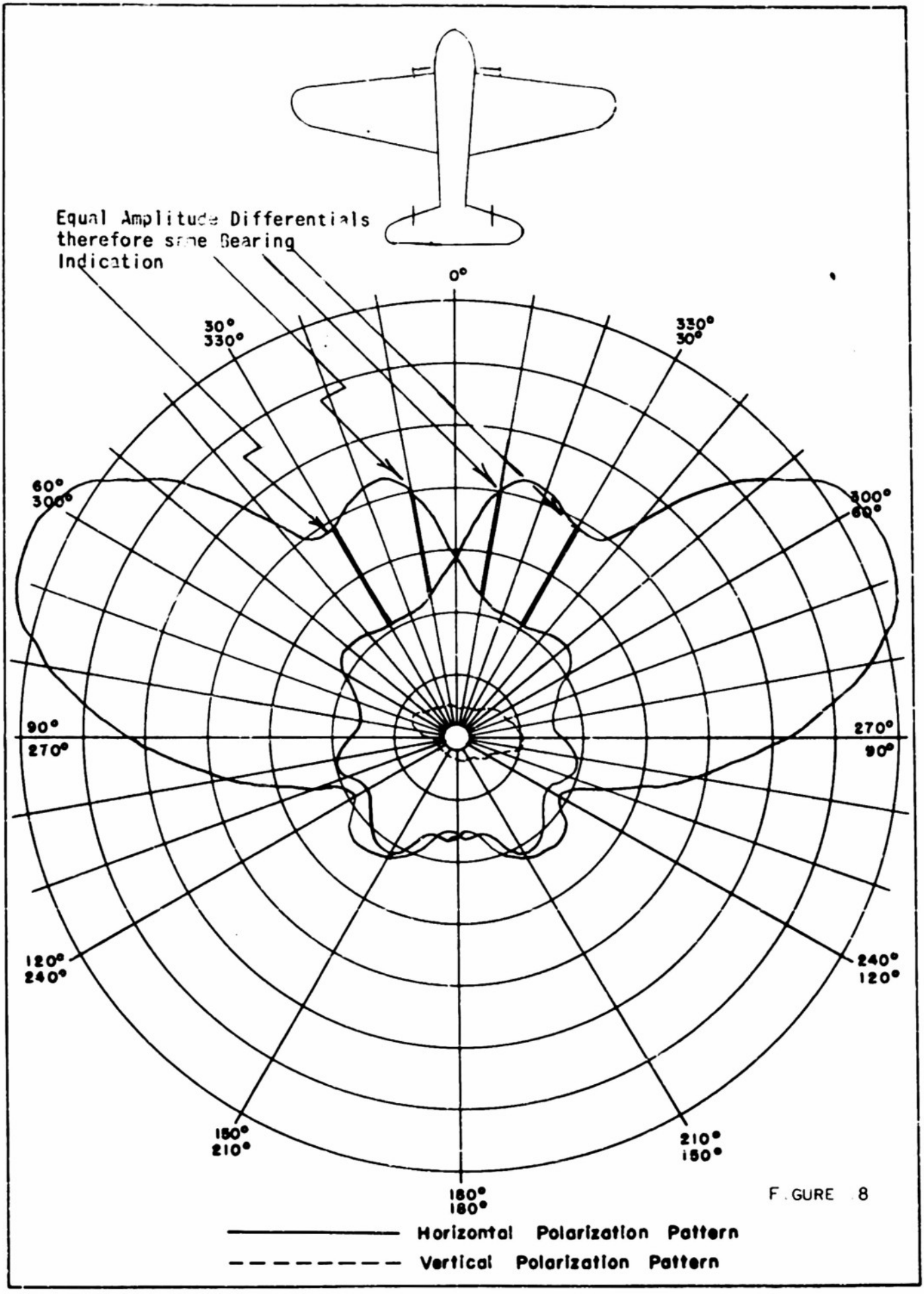
Equal Amplitude Differentials
therefore same Bearing
Indication
0°
30°
330°
330°
30°
60°
300°
300°
60°
90°
270°
270°
90°
120°
240°
240°
120°
150°
210°
210°
150°
180°
180°
Horizontal Polarization Pattern
Vertical Polarization Pattern

FIGURE 8

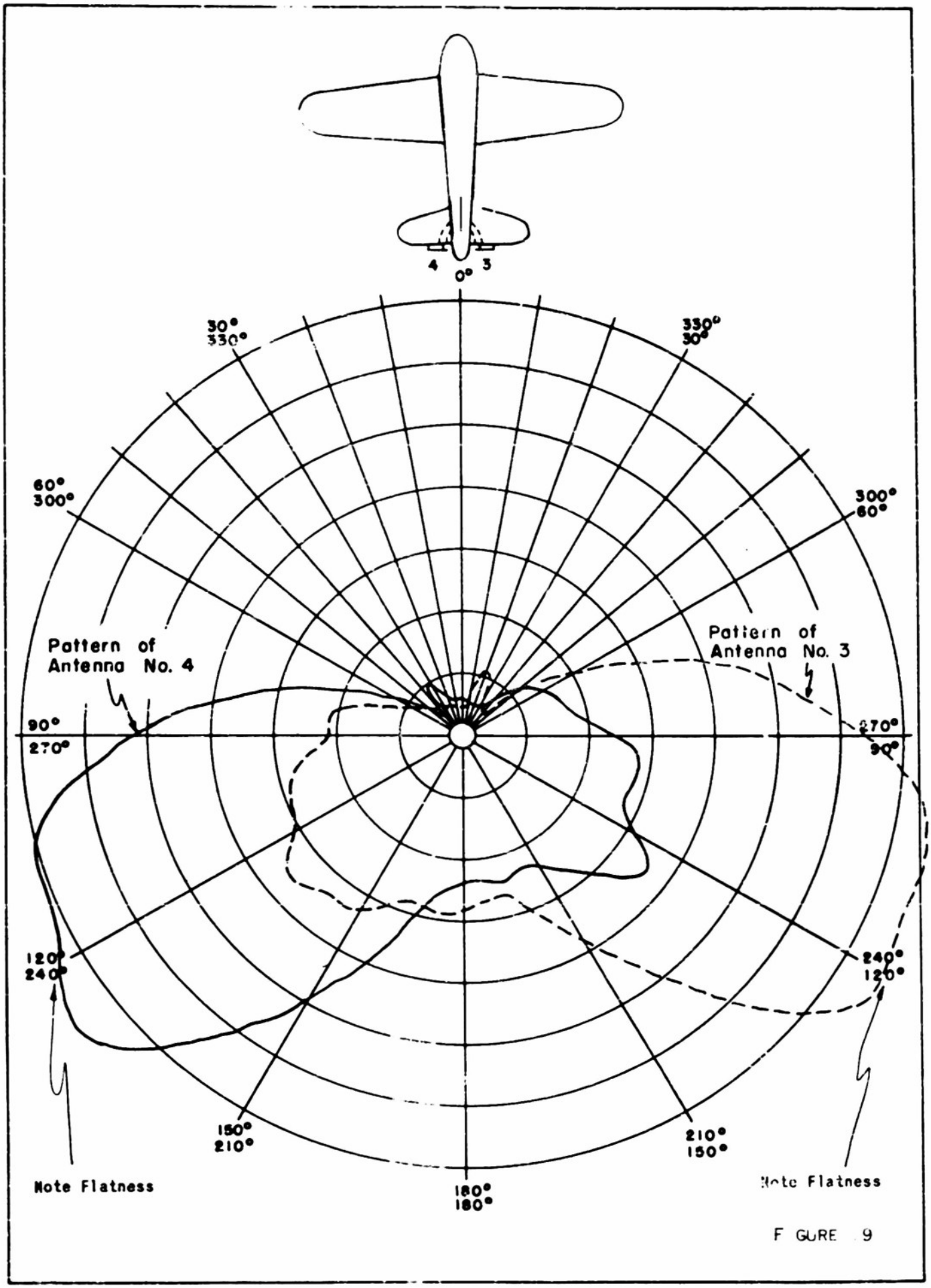
4
0°
3
30°
330°
330°
30°
60°
300°
300°
60°
Pattern of
Antenna No. 4
Pattern of
Antenna No. 3
90°
270°
270°
90°
120°
240°
240°
120°
150°
210°
210°
150°
180°
180°
Note Flatness
Note Flatness

FIGURE 9

APPENDICES

APPENDIX I
MODEL HOMING SYSTEMS

To aid in the evaluation of the usefulness of antennas in homing systems a working model of a conventional aural null A-N system has been constructed. A block diagram of the arrangement is given in Fig 20 The two antennas to be used for homing are mounted on the aircraft model A bolometer detector with tuning stub is connected to each. The detector output cables are led from the model through separate amplifiers to a single pole double throw micro-switch which is actuated by a cam The cam is so shaped that the switch connects the input of the display oscilloscope vertical deflection amplifier to each antenna in the sequential fashion diagrammed below

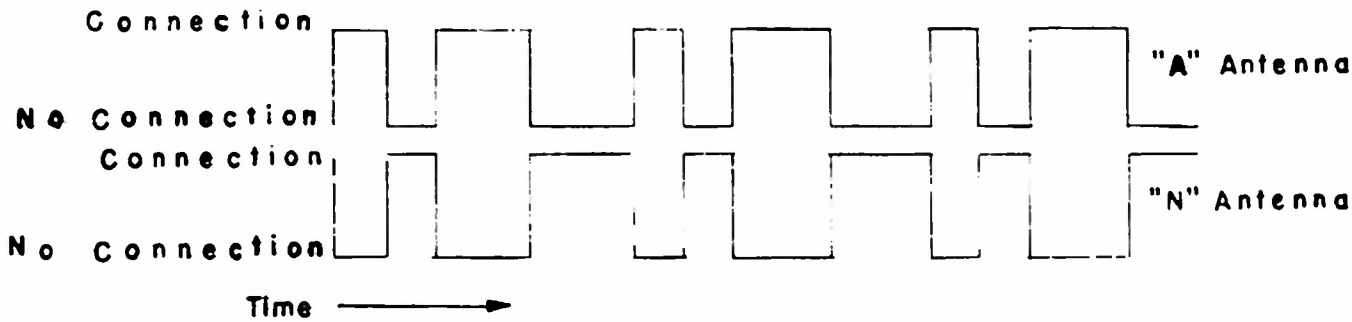

FIGURE 20a

In this manner the 1000 cps modulation from the detector output of the one antenna is modulated with an "A" signal while the corresponding output of the other antenna is modulated with an "N" signal. The "A" and "N" signals are so timed that the 1000 cps tones from the two antennas coalesce into a steady tone when the antenna outputs are equal in magnitude. This condition is present when the aircraft is on course. When the output of either antenna exceeds the other, an "A" or an "N" keyed tone predominates, depending on which antenna output is the greater. This case corresponds to an off course position of the aircraft.

The tower upon which the model is placed is rotatable through 360° by the tower drive. Synchronized to this drive is a potentiometer connected to a battery so that a direct voltage proportional to the angular position of the tower is available. This voltage is amplified in the oscilloscope horizontal deflection amplifier and applied to the oscilloscope horizontal deflection plates. Centering and gain controls are at hand by means of which the beam of the oscilloscope can be located at the center of its horizontal traverse across t e oscilloscope face when the aircraft model is head on, and the travel of the beam in inches per degree rotation of the model can be chosen at will For the

purposes of this report two different rates of travel were used; the one spread the 120° centered at the nose of the model across the oscilloscope face; the other spread the entire 360° rotation of the model across the tube face, again centered on the nose

The rotation rate of the cam actuating the A-N switch was initially chosen to produce 22.5 characters per minute which is about the rate of the aircraft beacon stations. This rate was used in the photographs showing 360° model rotation A rate six times higher was used in the photographs showing 120° model rotation to give a finer presentation. The model rotation rate is 1 RPM so 22.5 characters appear in the 360° rotation photographs The 120° photographs were taken at the same tower rotation rate but six times the character rate, so 45 characters appear in the trace.

A description of tests of wing-edge antennas in a model homing system, A-N and of propeller modulation effects on wing-edge antennas is given in Sections A and B which follow.

A. Tests of Wing-edge Antennas in a Model Homing System, A-N

The value of having a working model of a typical homing system, which is in this case on aural null A-N system, is two-fold. It aids in determining the usefulness of antennas proposed for homing applications which otherwise has been described in terms of relative sensitivity and definition. It provides a clear graphic summary of the homing antennas' operation over the entire 360° of azimuth in the form of oscilloscopic photographs.

All the photographs presented in Figs. 21a through 21g show the response of the aural null A-N system utilizing the wing-edge antennas as function of angular position of the aircraft in the azimuthal plane. The center of each trace corresponds to head-on position of the aircraft. In the photographs labeled 360° rotation the ends of the trace correspond to tail-on position of the aircraft, i.e., the entire azimuthal plane is presented. In Figs. 21f and 21g an expanded presentation appears in which the forward 120° (60° to each side of head-on position) is shown.

Figures 21a through 21e present the homing response patterns of the wing-edge antennas on the accurate scale model. There are two photographs taken every 100 mcs through the band of interest. At every frequency shown the vertical deflection amplifier was adjusted in gain to produce the convenient sized display shown for horizontally polarized waves. The vertical polarization pattern was then taken with no change made in the system except a rotation through 90° of the driving dipole in the focus of the parabolic reflector which illuminates the aircraft. The pairs of photographs taken at each frequency therefore give the true relative behavior of the homing antennas with respect to horizontally and vertically polarized waves in all azimuthal directions.

Attention is drawn to the fact that the envelopes of these response patterns deviate from the shapes of the corresponding antenna patterns presented. The antenna patterns yield relative electric field intensities as per custom. They are obtained by the use of square law detectors (bolometers) in conjunction with a square root extracting amplifier. It was thought that in practice square law detectors would be used without such an amplifier. The responses of these detectors, and consequently the homing response patterns shown, vary as the square of the received electric field intensity. This detector response characteristic would seem to be of value in increasing the definition of homing system antennas.

It is apparent from the photographs that response of the wing-edge antennas to vertically polarized waves is negligible.

Figures 21f and 21g give horizontal and vertical polarization responses of the wing-edge antennas mounted on the accurate scale model and taken at 5 different frequencies throughout the band for the forward 120° of azimuth. As result of the A-N keying and the tower rotation rates employed in the 360° rotation photographs, one character occupies some 16° of angular rotation and the on-course coalescence of the tones is obscured. To better present this coalescence, only the forward 120° is now shown with the A-N keying rate so increased that one character

occupies 2.67° of rotation Referring to Figs. 21f and 21g one notes that the horizontal polarization response seem to consist of two patterns superimposed, the one being modulated by the keying rate, the other being a solid pattern. Actually what occurs is the following: The aircraft is rotated from 60° off head-on course in the one quadrant through head-on course to 60° off head-on course in the next quadrant. The A-N switch connects first the one antenna to the indicator and then the other. At 60° off head-on course one antenna has a high response and the other has a low response. The ratio of maximum deflection to minimum deflection of the beam is high. Turning towards head-on course this ratio diminishes until it reaches unity on course Turning past head-on course position the ratio increases from unity upwards as the antenna responses begin to differ in magnitude again To the one side an "A" signal is observed, to the other an "N" signal The angular range in which the deflection ratio is very near unity is readily picked out as the range wherein the envelopes of the "two" patterns touch one another

In the operating of the model system it has been observed that the aural indication of head-on course is at least as sharp as the visual presentation indicates.

B Propeller Modulation Effects on Wing-Edge Antennas

Figures 22a through 22d comprise a group made during the investigation of propeller modulation effects on the wing-edge antennas mounted on the crude model described in Report ADF-3 Because these antennas are mounted on the leading edges of the wing about 0.5 cm from the fuselage, the effects of the propeller on the homing system operation must be considered A small electric motor was mounted in the model and a scaled-to-size aluminum propeller attached thereto. The photographs present the operation of the A-N homing system over 360° of azimuth at four frequencies, the edges and center of the band and the frequency in the neighborhood of which the propeller would be expected to resonate. At each frequency the polarization of the impinging electric field was made horizontal, 45° and vertical; and for each case a photograph is presented showing the system operation with and without the propeller rotating The band of interest for this model was 950 mcs to 2350 mcs rather than 800 mcs to 2000 mcs for the accurate scale model due to the difference in size The propeller resonance frequency, calculated on the basis of its operating as a dipole of fatness commensurate with its dimensions, was 1410 mcs The propeller rotation speed was about 20 RPS The headphone monitor as well as the oscilloscope indicator was used during the tests.

In no case was any propeller modulation effect noted either visually or aurally. A sputtering noise was audible in the headphones as the propeller was driven, but this was traced to brush noise in the motor (a universal wound AC-DC motor) by rapidly connecting and disconnecting the motor voltage while the propeller continued to rotate.

This useful result, that propeller modulation effects on the wing-edge homing antennas were not detectable in the model studies described, is considered in Appendix II It is pointed out there that the four

bladed propeller used on this model aircraft together with a certain symmetry in the antenna mounting with respect to the propeller could be the important factors contributing to this result.

Propeller modulation studies were not made on the rudder mounted homing antennas as their distance from the propeller should render its effects upon them negligible.

Horizontal Polarization

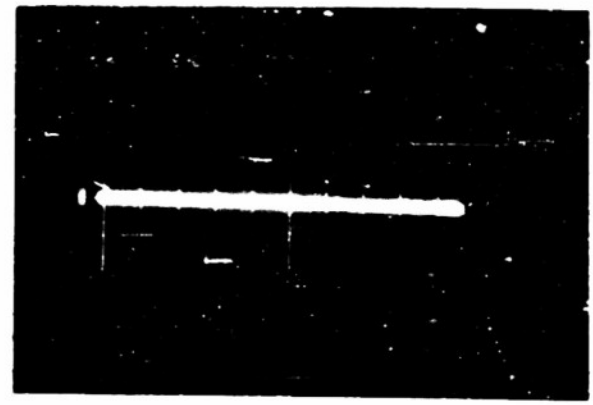

Vertical Polarization

800 mc, 360° Rotation

Horizontal Polarization

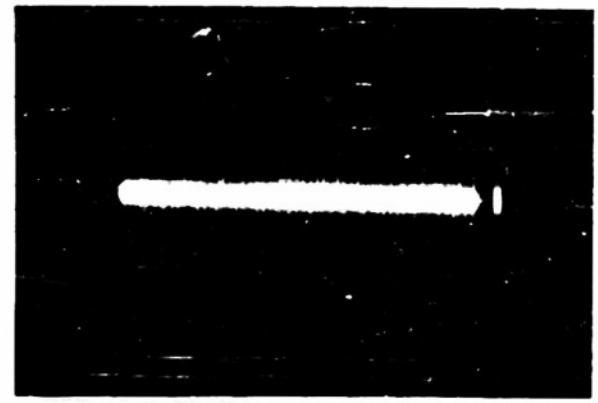

Vertical Polarization

900 mc, 360° Rotation

Horizontal Polarization

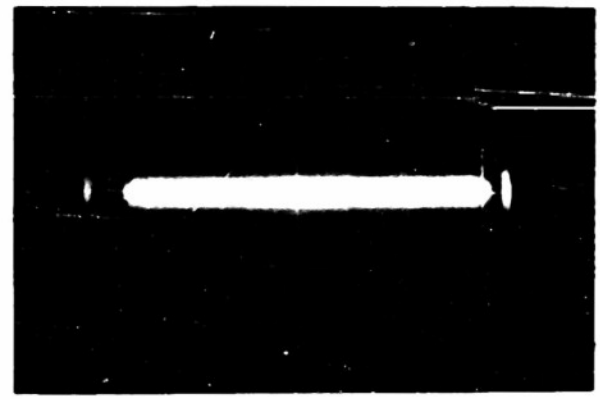

Vertical Polarization

1000 mc, 360° Rotation

FIGURE 21a

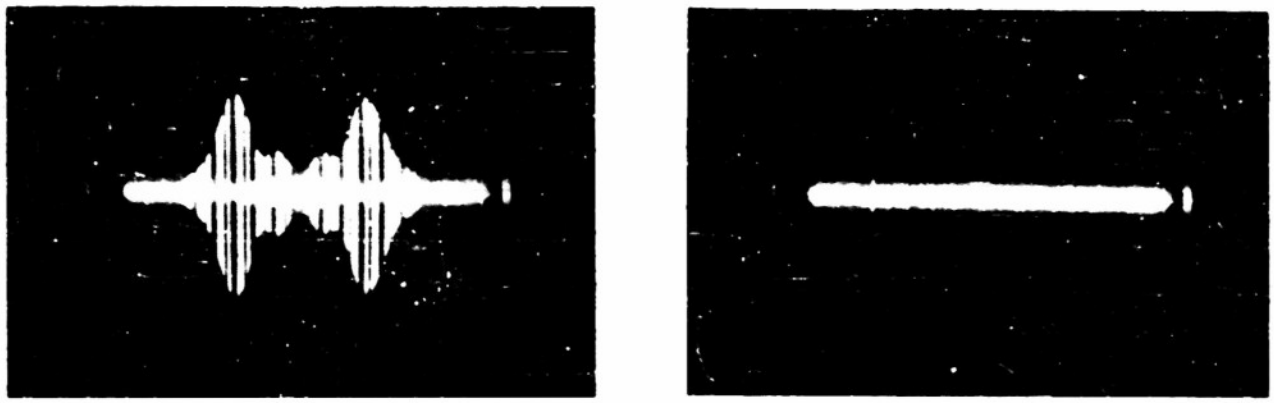

1100 mc. 360° Rotation

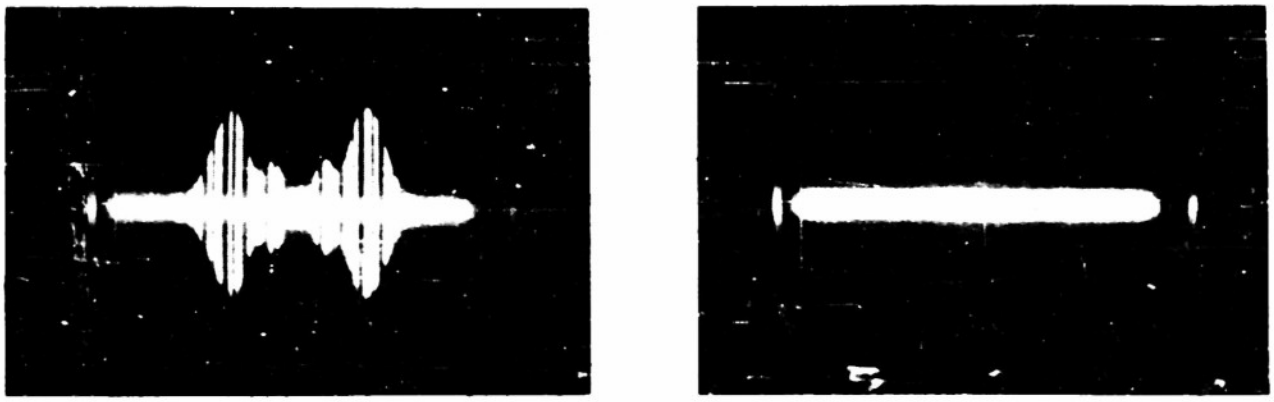

1200 mc. 360° Rotation

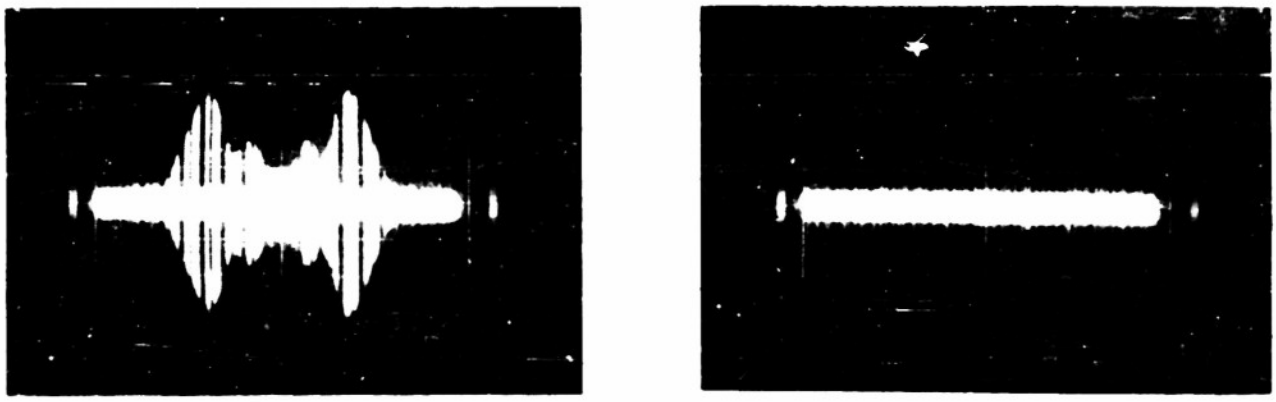

1270 mc. 360° Rotation

FIGURE 21b

Horizontal Polarization

Vertical Polarization

1400 mc, 360° Rotation

Horizontal Polarization

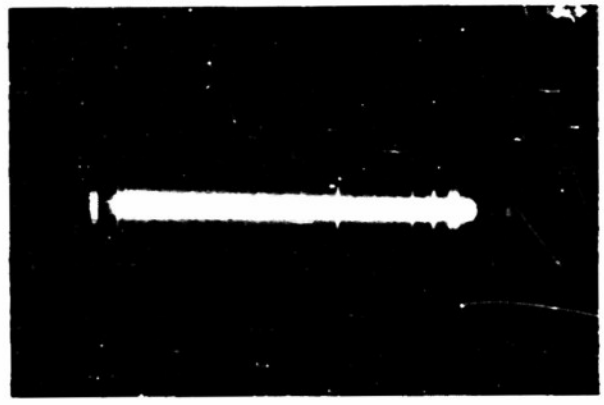

Vertical Polarization

1500 mc, 360° Rotation

Horizontal Polarization

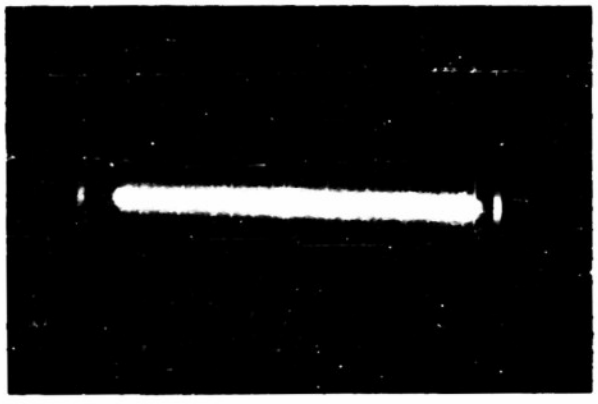

Vertical Polarization

1600 mc, 360° Rotation

FIGURE 21c

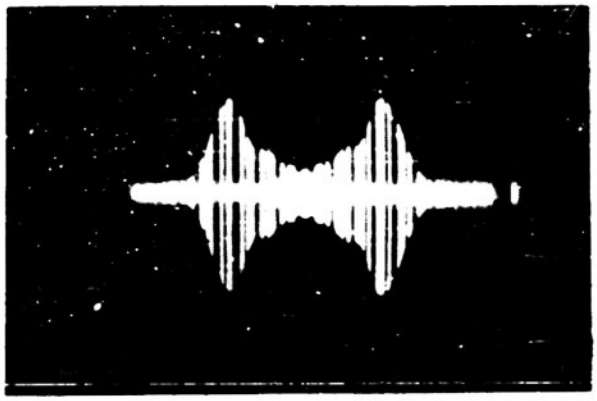

Horizontal Polarization

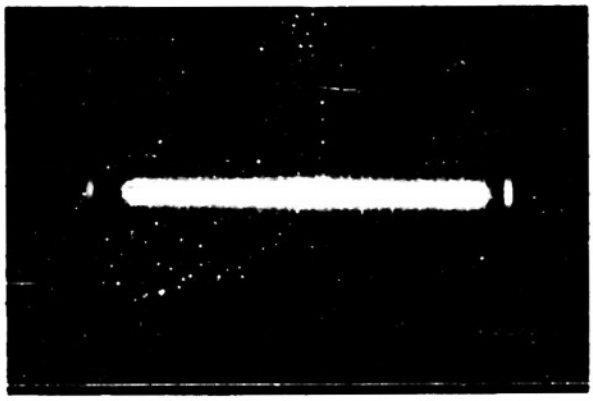

Vertical Polarization

1700 mc, 360° Rotation

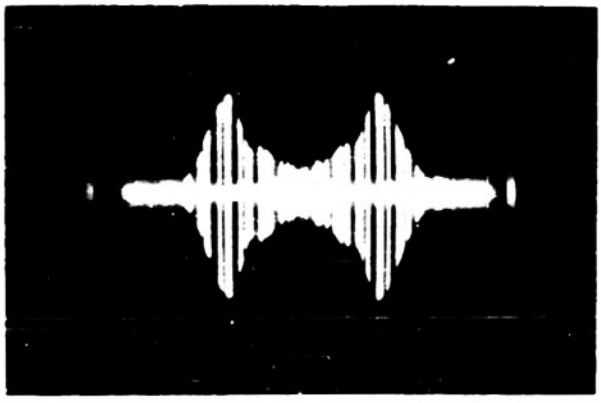

Horizontal Polarization

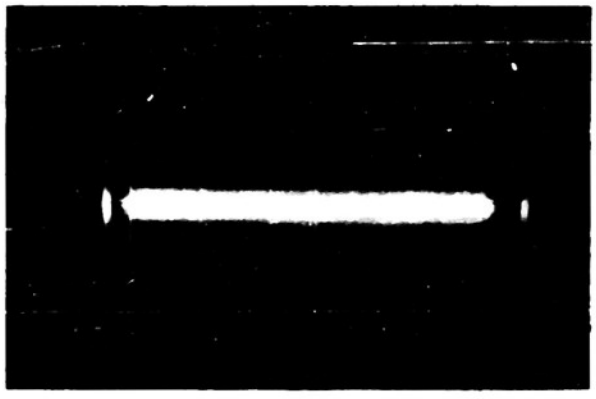

Vertical Polarization

1800 mc, 360° Rotation

FIGURE 21d

Horizontal Polarization

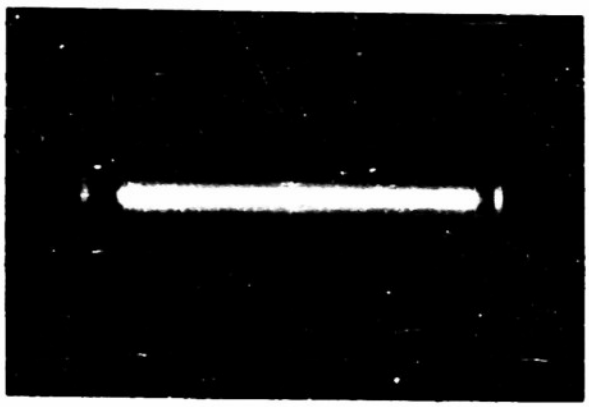

Vertical Polarization

1900 mc, 360° Rotation

Horizontal Polarization

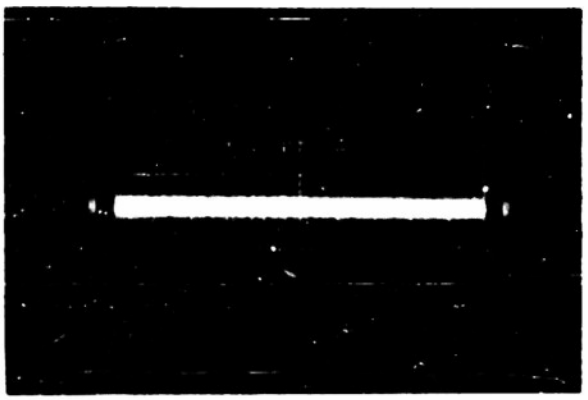

Vertical Polarization

2000 mc, 360° Rotation

FIGURE 21e

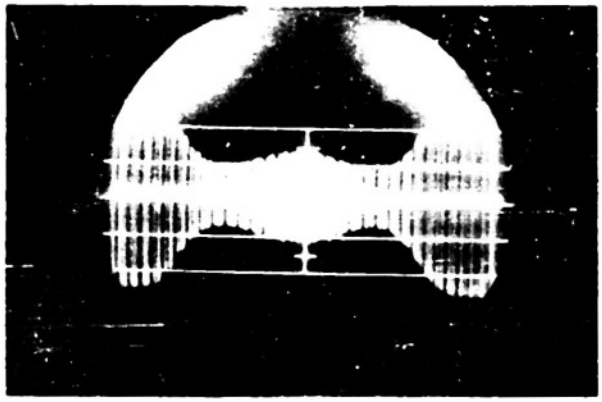

Horizontal Polarization

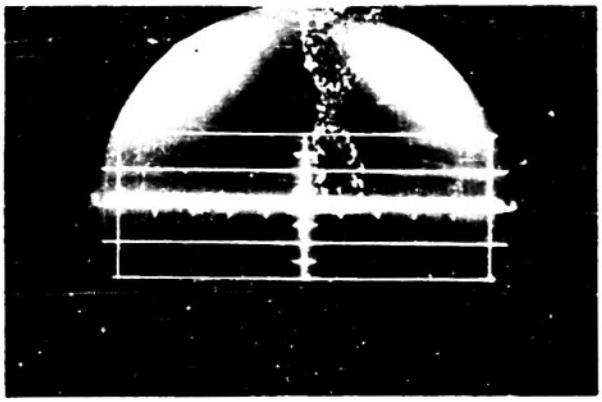

Vertical Polarization

800 mc, 120° Rotation

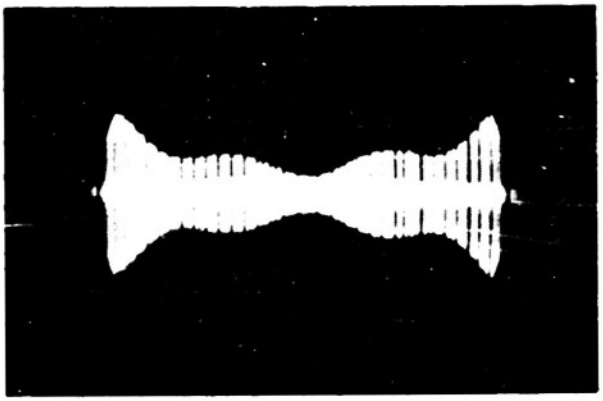

Horizontal Polarization

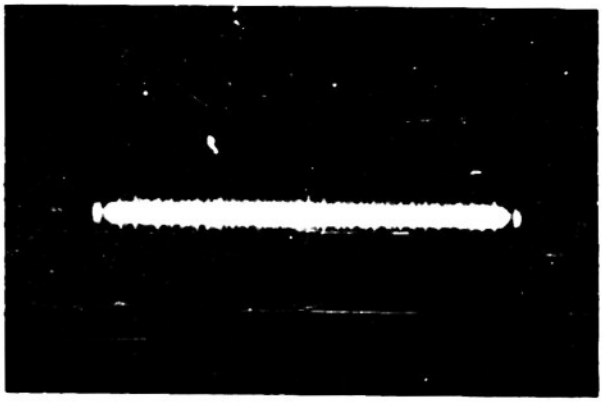

Vertical Polarization

1100 mc, 120° Rotation

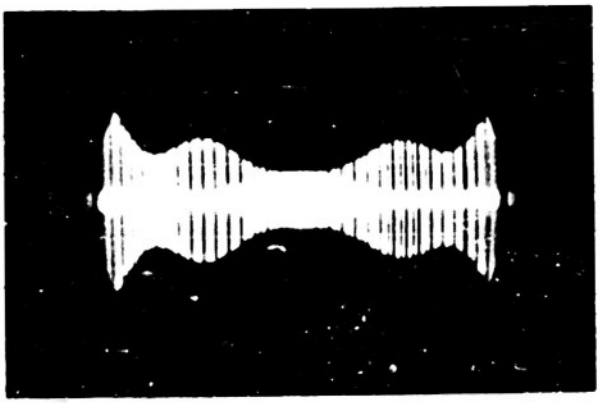

Horizontal Polarization

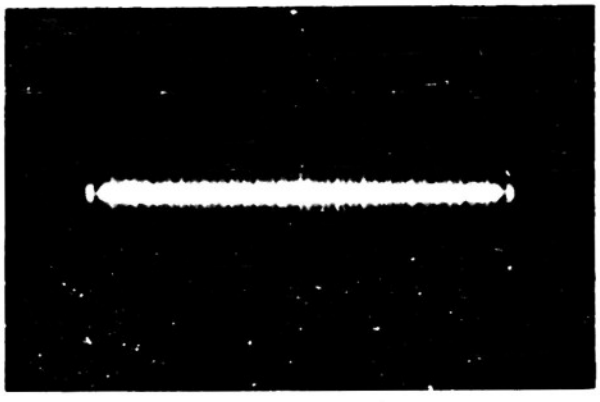

Vertical Polarization

1270 mc, 120° Rotation

FIGURE 21f

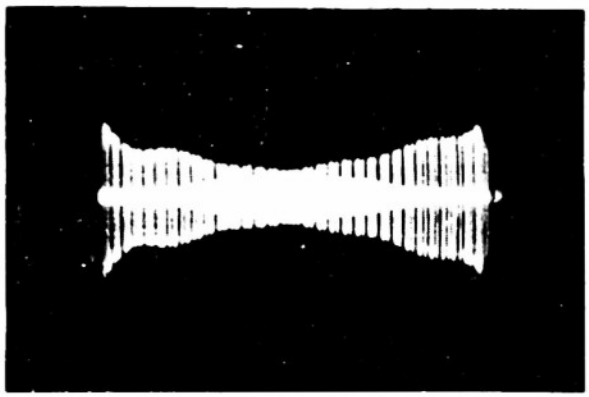

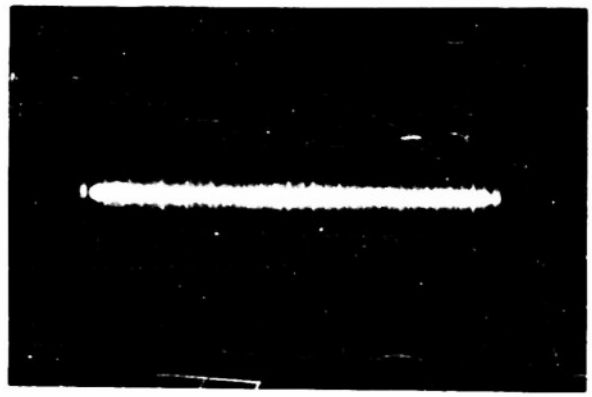

1700 mc. 120 Rotation

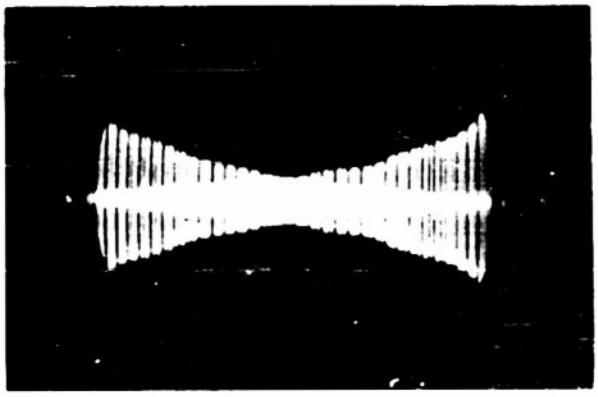

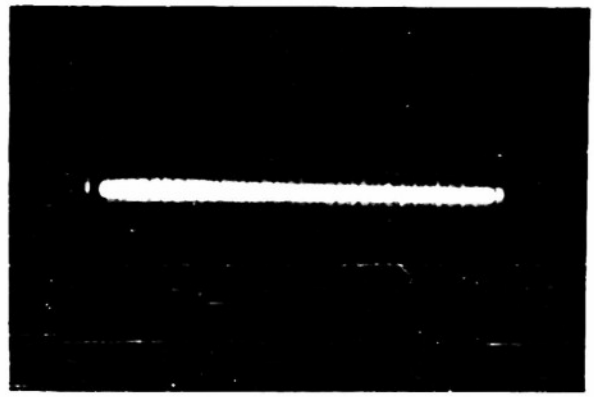

2000 mc. 120 Rotation

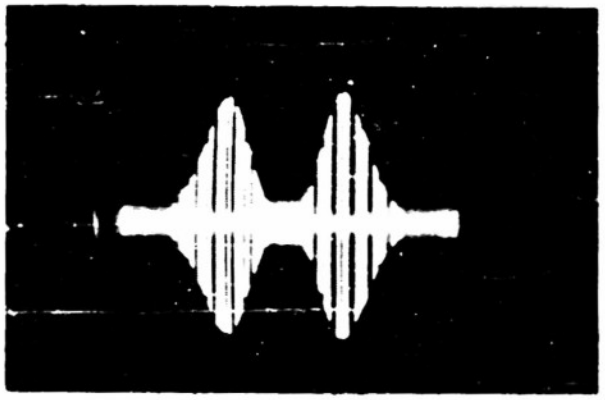

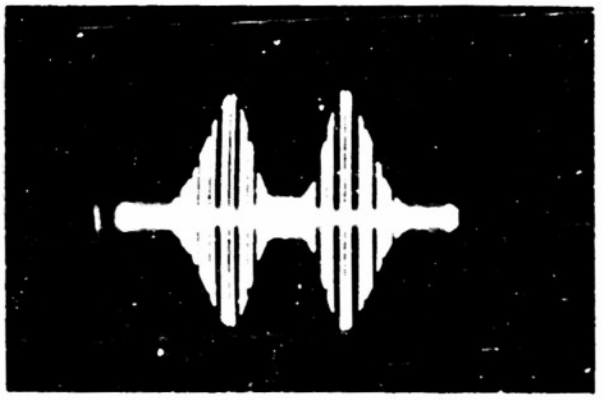

950 mc, Horizontal Polarization, 360° Rotation

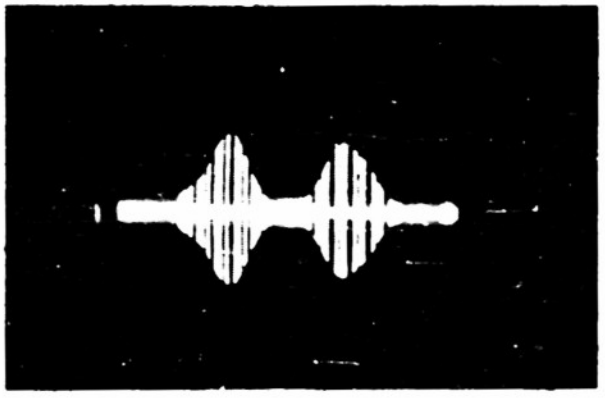

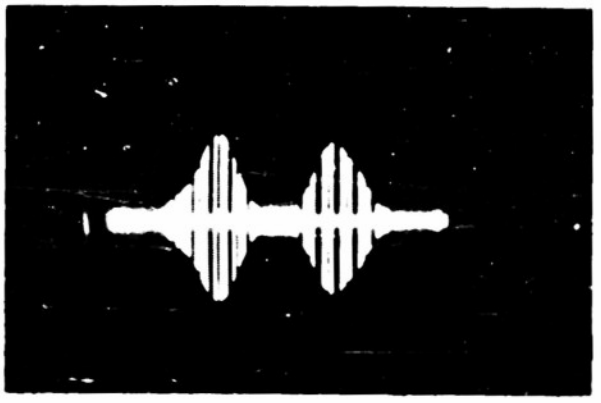

950 mc, 45° Polarization, 360° Rotation

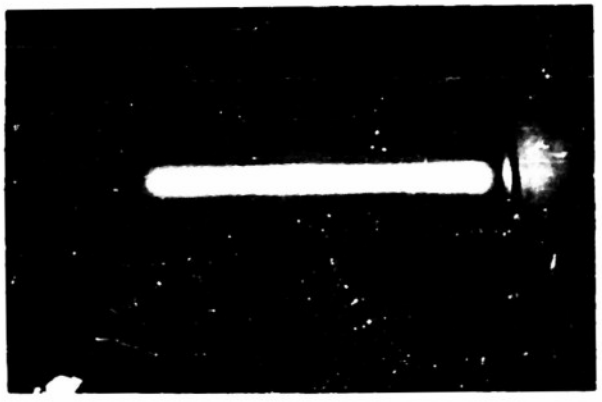

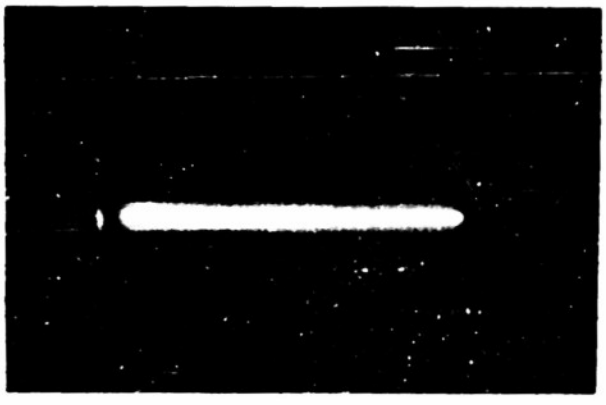

950 mc, Vertical Polar zation, 360° Rotation

FIGURE 22a

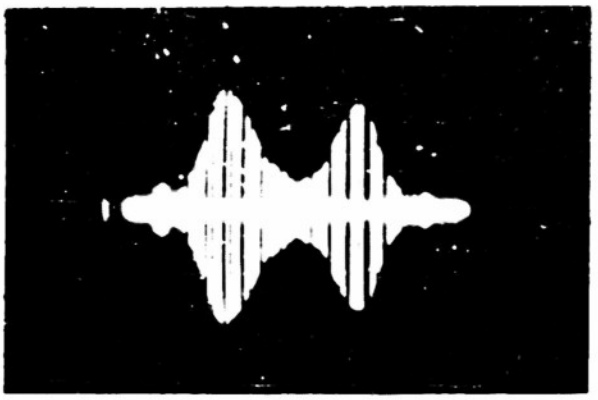

Without Propeller Modulation

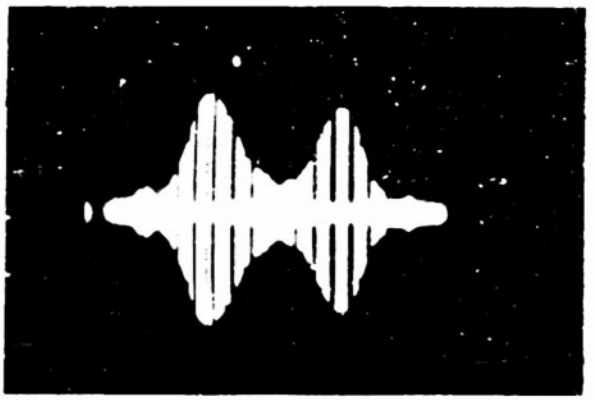

1410 mc. Horizontal Polarization. 360 Rotation

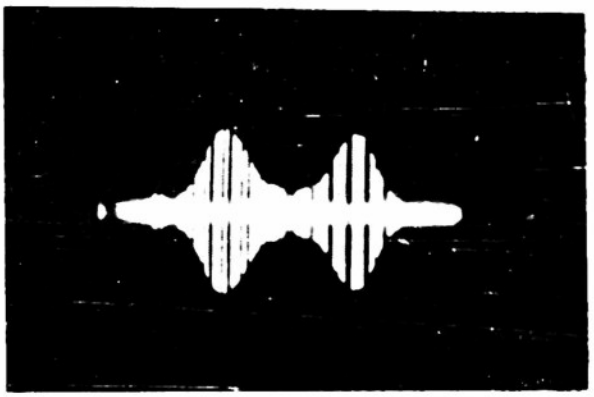

Without Propeller Modulation

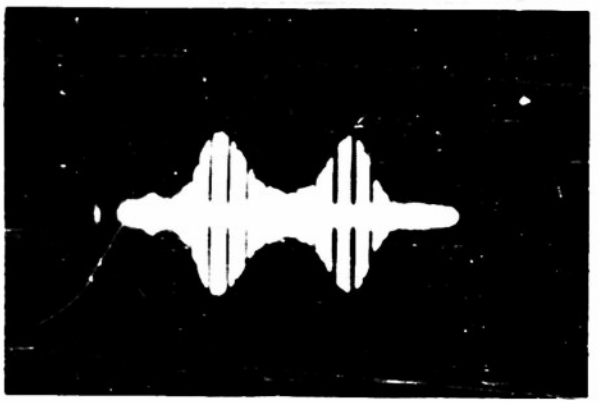

1410 mc. 45° Polarization. 360 Rotation

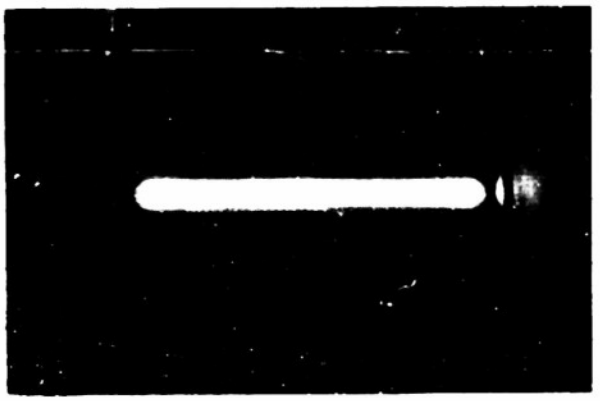

Without Propeller Modulation

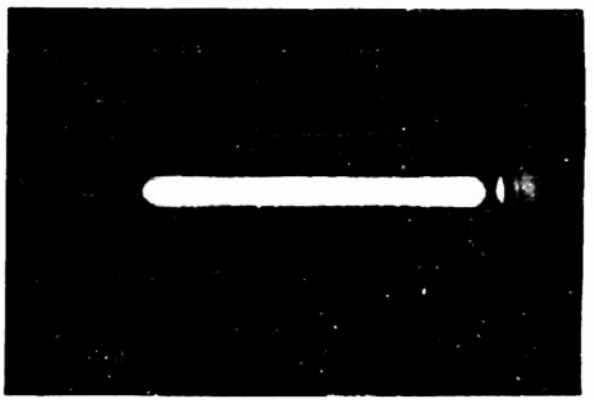

1410 mc. Vertical Polarization. 360 Rotation

FIGURE 22b

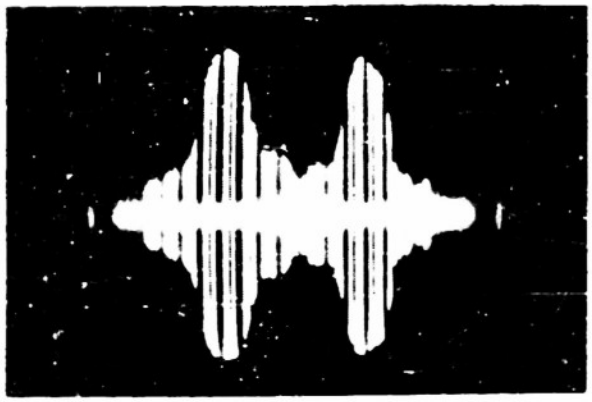

Without Propeller Modulation

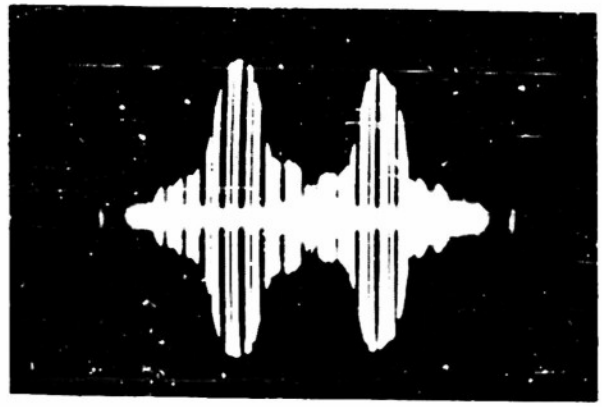

With Propeller Modulation

1500 mc, Horizontal Polarization, 360 Rotation

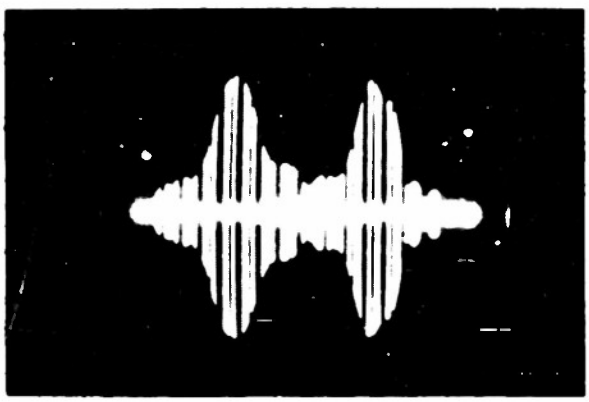

Without Propeller Modulation

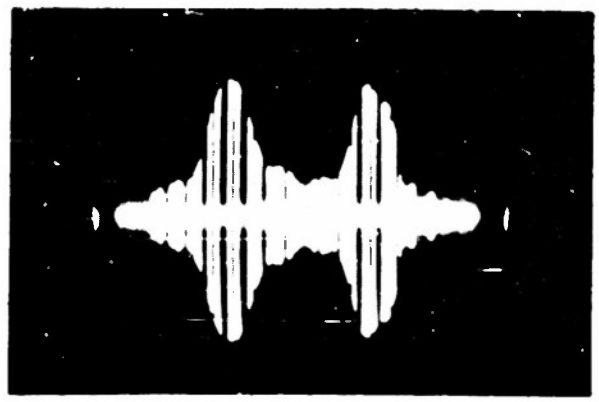

With Propeller Modulation

1500 mc, 45° Polarization, 360° Rotation

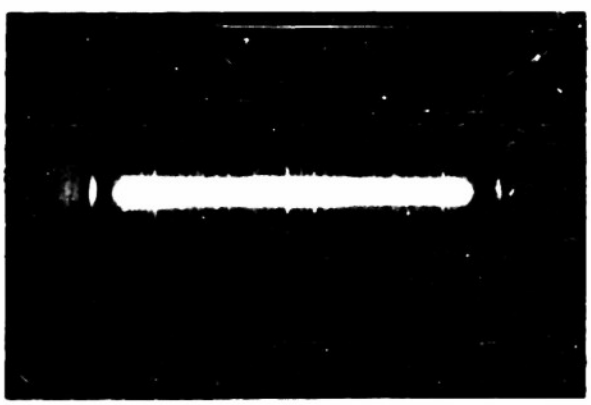

Without Propeller Modulation

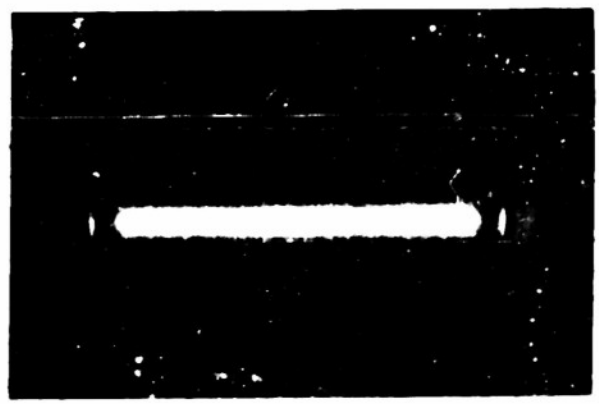

With Propeller Modulation

1500 mc, Vertical Polarization, 360 Rotation

FIGURE 22c

Without Propeller Modulator

With Propeller Modulator

2350 mc. Horizontal Polarization. 360 Rotation

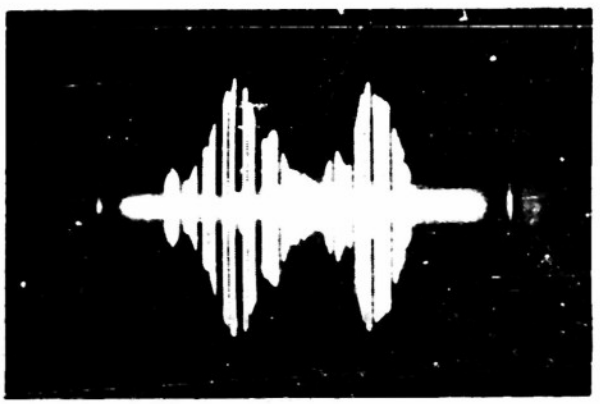

Without Propeller Modulator

With Propeller Modulator

2350 mc. 45 Polarization. 360 Rotation

Without Propeller Modulator

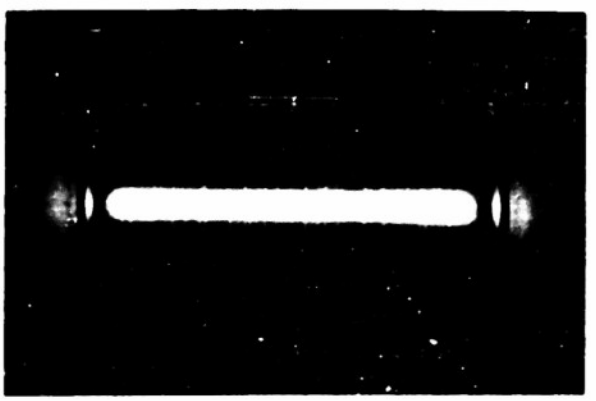

With Propeller Modulator

2350 mc. Vertical Polarization. 360 Rotation

FIGURE 22d

APPENDIX II

FACTORS CONTRIBUTING TO THE SUPPRESSION OF PROPELLER MODULATION IN THE WING-EDGE ANTENNAS

In the frequency band of 40 mcs to 100 mcs the aircraft structure plays a predominate role in shaping the patterns of antennas attached to it because of the currents flowing on its surface when it is immersed in the electromagnetic field. In the particular case of the wing-edge antenna, experiments indicate that the leading edge of the wing and the fuselage extending from the wing forward to the nose behave somewhat in the manner of a corner reflector with the "antenna" itself providing a convenient means of coupling to the surface currents. In view of this it is difficult to assay quantitatively how and to what extent the propeller would affect the antenna's operation. Having experimentally observed in the model studies that the propeller effects are negligible on the wing-edge antenna, a qualitative explanation of this is attempted in this section.

Refer to Fig. 23. Let is be assumed that the received field is vertically polarized as shown by E_v. At an instant the propeller is in the arbitrary position indicated. At point 1 on the propeller, distant d units from the hub, a current element di_{1V} flows. Similarly, at point 2 on blade 2 a current element di_{2V} flows. The parts of the blades shielded from the quadrant of the aircraft shown by the nose of the fuselage are not considered. Point A is located on the vertical gap of the antenna. The voltage present across this gap excites the antenna and provides its driving force. Let the contributions to this gap voltage by the current elements di_{1V} and di_{2V} be dV_{A1} and dV_{A2} respectively.

The current element di_{1V} is proportional to the received field.

$$di_{1V} = K_1 E_V \cos \varphi$$

and similarly

$$di_{2V} = K_1 E_V \sin \varphi.$$

The antenna gap responds only to horizontally polarized fields. di_{1V} contributes to the gap voltage by the amount

$$dV_{A1} = K_2 di_{1V}\, \varepsilon^{-j\beta r_1} \sin \varphi = K_1 K_2 E_V\, \varepsilon^{-j\beta r_1} \sin \varphi \cos \varphi$$

and also

$$dV_{A2} = K_2 di_{2V}\, \varepsilon^{-j\beta r_2} \cos \varphi = K_1 K_2 E_V\, \varepsilon^{-j\beta r_2} \sin \varphi \cos \varphi$$

The total contribution to the gap voltage by the two current elements is

$$dV_A = dV_{A1} + dV_{A2} = K_1 K_2 \sin \varphi \cos \varphi (di_{1V}\, \varepsilon^{-j\beta r_1} - di_{2V}\, \varepsilon^{-b\beta r_2}).$$

By symmetry of the propelier blades

$$|di_{1V}| = |di_{2V}|$$

At $\varphi = 45°$, $r_1 = r_2$, and because of the small ratio of d to r_1 in the region where the propeller is not shielded by the fuselage, $r_1 \approx r_2$ there.

We can then write $dV_A \approx 0$.

Consider the case where the received field is horizontally polarized and given by E_h. Resulting from this field are di_{1h} and di_{2h}

$$di_{1h} = K_1 E_h \sin \varphi$$

$$di_{2h} = K_1 E_h \cos \varphi$$

These currents elements would produce at the gap the voltages

$$dV_{A1} = K_2 di_{1h} e^{-j\beta r_1} \sin \varphi = K_1 K_2 E_h \varepsilon^{-j\beta r_1} \sin^2 \varphi$$

$$dV_{A2} = K_2 di_{2h} e^{-j\beta r_2} \cos \varphi = K_1 K_2 E_h \varepsilon^{-j\beta r_2} \cos^2 \varphi$$

At

$$\varphi = 45°, \quad r_1 = r_2$$

and

$$dV_A = dV_{A1} + dV_{A2} = K_1 K_2 E_h \varepsilon^{-j\beta r_1} (\sin^2 \varphi + \cos^2 \varphi)$$

which is independent of φ. Therefore, to the extent that r_1 does not deviate much from r_2, the propeller adds a contribution to the gap voltage which is independent of its rotation rate when the field is horizontally polarized.

Following the foregoing line of reasoning, entirely equivalent results are obtained if it is assumed that the antenna is sensitive only to vertically polarized waves with the difference that, in this case, with a vertically polarized field the propeller contributes a constant amount to the antenna voltage while with a horizontally polarized field the propeller contributes nothing to the voltage.

The limitations of this analysis are obvious but it may serve to point out the design factors which tend to minimize the effects of the propeller upon the performance of the wing-edge antennas.

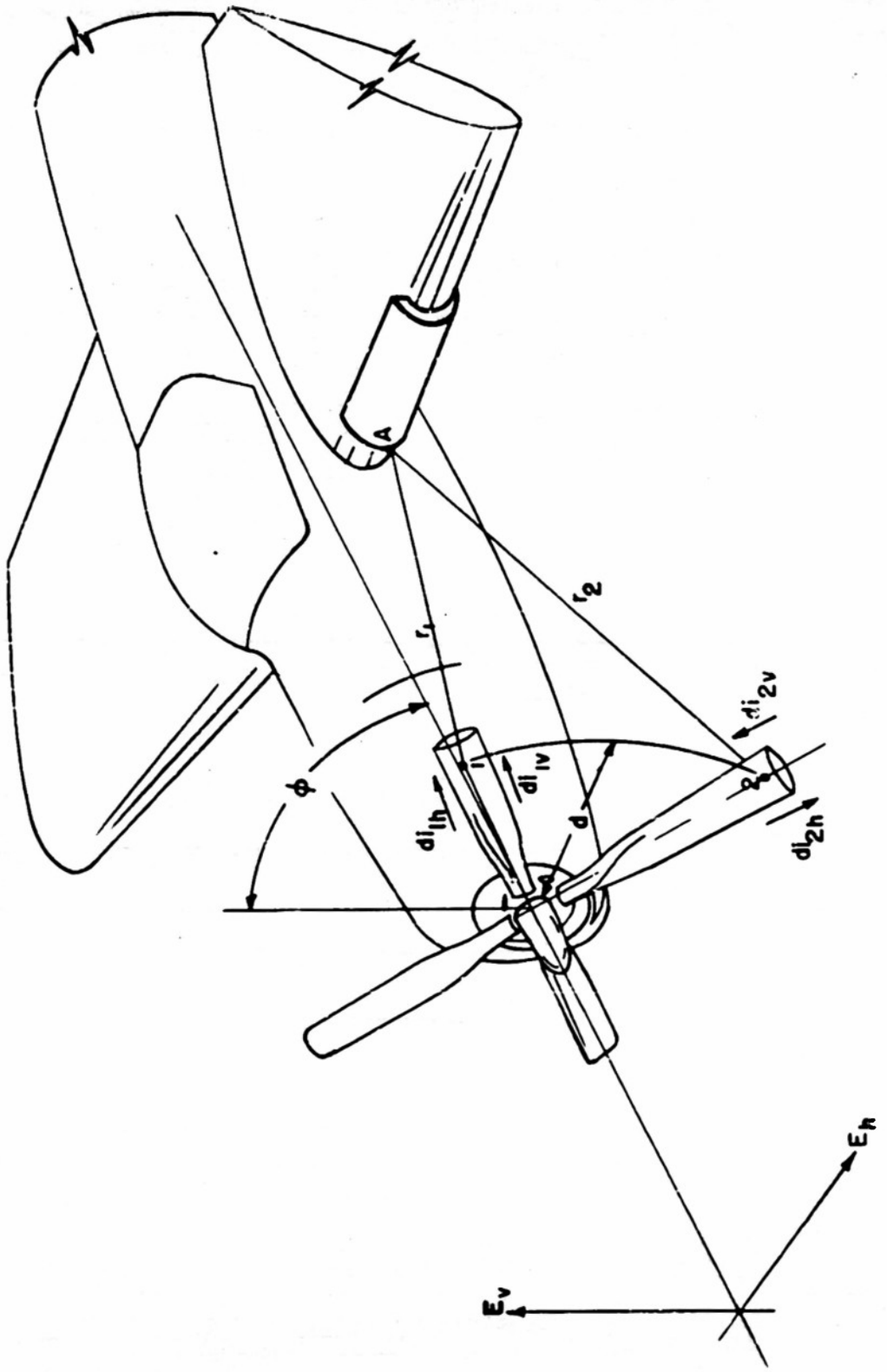

FIGURE 23

APPENDIX III

Phase Shift Homing System Proposal

Figure 11 is a block diagram of a possible homing system with C.R. tube indicator. This system is capable of handling pulsed signals; it is not a null system. It provides directional information - in fact it can be calibrated to provide angular off-course information for use in homing on a transmitter while flying in a strong crosswind.

The antennas used are the wing edge sleeves mounted close to the fuselage. The output of the tuning head of each is fed into its own mixer, one of which is connected directly to a local oscillator, the other is connected through a phase shifter to the local oscillator. The two mixer outputs are added and sent to a conventional IF amplifier and amplitude detector. The detector output is amplified and impressed across the vertical plates of an oscilloscope tube. The X deflection voltage is derived from the unit which supplies the phase shifter control. Suppose the phase shifter unit provides a phase shift in the oscillator voltage directly proportional to a control voltage from the control unit. Let this control voltage also be applied to the horizontal plates of the indicator tube. Then there exists a one to one correspondence between horizontal position of the scope beam and degrees of phase shift present between the oscillator voltages fed to the two mixers. Let the control voltage be of sinusoidal wave shape. Then the beam of the indicator tube will be constantly swept horizontally while its position vertically will depend upon the combined output of the differentially connected antenna pair. A cusp shaped figure will be formed as sketched for three positions of the transmitter with respect to the center line of the aircraft in Fig. 12. The location of the cusp gives the transmitter location. The horizontal scope axis can be calibrated to give the deviation in degrees between the transmitter and the center line of the plane for positions in the two forward quadrants.

In more detail:

Referring to Fig. 24 the antenna voltages are

$$V_A = F_{(\varphi)} \cos (\omega_s t - d' \sin \varphi)$$

$$V_B = F_{(-\varphi)} \cos (\omega_s t + d' \sin \varphi + \pi)$$

$$d' = \frac{2\pi}{\lambda} d \qquad \omega_s = \text{angular velocity of received wave.}$$

$F_{(\varphi)}$, $F_{(-\varphi)}$ antenna patterns - mirror images in $\varphi = 0$ line.

The oscillator voltage fed to the mixers is

$$V_o \cos \omega_o t \qquad \text{to mixer B}$$

$$V_o \cos(\omega_o t + \theta_{(t)}) \qquad \text{to mixer A}$$

where θ_t is the controlled phase shift added in the one oscillator-to-mixer line. Square law mixers are assumed; the outputs of angular velocity in neighborhood of $\omega_o - \omega_s = \omega_i$ are the only components which the IF amplifier will transfer.

From mixer A

$$V_{mA} = K_m V_o F_{(\varphi)} \cos (\omega_i t + d' \sin \varphi - \theta_{(t)})$$

from mixer B

$$V_{mB} = K_m V_o F_{(-\varphi)} \cos (\omega_i t - d' \sin \varphi - \pi).$$

The amplified sum of these is taken from the IF strip

$$V_{IF} = KV_o [F_{(\varphi)} \cos (\omega_i t + d' \sin \varphi - \theta_{(t)}) + F_{(-\varphi)} \cos(\omega_i t - d' \sin \varphi - \pi)]$$

This voltage is amplitude detected, further amplified, and fed to the vertical scope plates. Examination of the above expression shows that when the arguments of the two terms differ by π radians the magnitude of the voltage is

$$V_{IF} = KV_o (F_{(\varphi)} - F_{(-\varphi)})$$

which is zero at $\varphi = 0$ and is a minimum for other values of φ. We are interested in values of φ less than $\frac{\pi}{2}$.

The minimum occurs for

$$(\omega_i t + d' \sin \varphi - \theta_{(t)}) = (\omega_i t - d' \sin \varphi - \pi) + \pi$$

or

$$\theta_{(t)} = 2d' \sin \varphi$$

which shows that the value of $\theta_{(t)}$ to produce a minimum in the envelope of the DF output voltage is dependent on φ and on $d' = \frac{2\pi}{\lambda} d$.

As was suggested earlier a possible useful form of $\theta_{(t)}$ is

$$\theta_m \sin \omega_s t.$$

Then

$$\theta_m \sin \omega_s t = 2d' \sin \varphi$$

Suppose

$$\theta_m = 2d'$$

The horizontal sweep on the scope is proportional to $\theta_m \sin \omega_s t$ and is so synchronized that when $\omega_s t = 2\pi n$ with n integral, the beam is at center of the tube.

The vertical position of the beam is proportional to the envelope of the detected voltage.

It is easily seen now that the position of the cusp on the indicator face is directly determined by φ. The horizontal axis can be calibrated in degrees and the angle φ directly read off.

Since

$$\theta_m = 2d'$$

and

$$d' = \frac{2\pi d}{\lambda_{os}} \left(1 + \frac{\Delta f_s}{f_{os}} \right)$$

where f_{os}, λ_{os}, correspond to the center of the band, it is seen that an adjustment on θ_m is necessary over the tuning range to allow the indicator to be directly calibrated. This control should be readily obtained from the main tuning condenser assembly of the receiver.

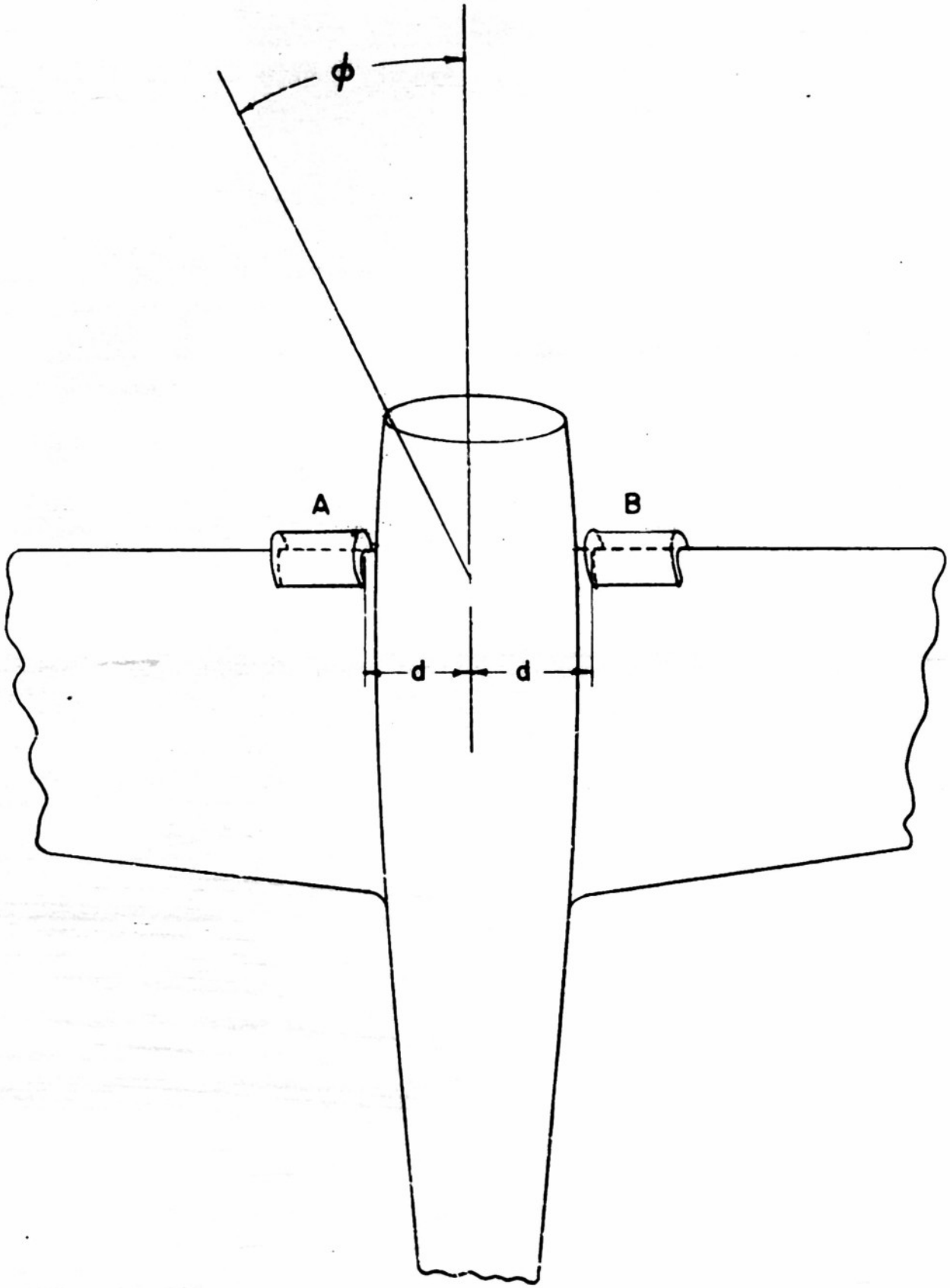

FIGURE 24

APPENDIX IV
ALTERNATE PROPOSAL - HOMING

The problems of aircraft homing and direction finding are two closely related subjects Hence it is not difficult to devise a system suitable for the solution of one problem and then to adapt this basic system with some changes toward solution of the second problem

Such is the case for the system to be discussed in this proposal Its basic application appears more suitable for homing although with modification the system has application for limited DF coverage The limited coverage disadvantage stems from the same primary limitation (the antenna system) which restricted the useful coverage of the phase comparison and amplitude comparison system previously described. In contrast, however, the system to be proposed makes use of both the signal phase and amplitude information that is available.

Refer to Figs. 25a, 25b and 25c which show the field intensity patterns for two wing-edge antennas mounted on opposite wings near the fuselage and connected in parallel. Because the antennas are in electrical antiphase, this connection produces a sharp null straight forward Further, Figs. 26a, 26b. and 26c are the field intensity patterns for the same antennas connected in-phase (by use of broadband balun) and this connection produces a broad maximum forward. The data indicates the possibility of using these "sum" and "difference" patterns in an inversion presentation system. That is, the electrical difference between the two resultant patterns will show a maximum indication for a signal arriving from head on and the indication will decrease for other angles of arrival within a useful sector. The useful sector is restricted to that region in which the unit antenna patterns contain a common area. This condition limits the usefulness of the system to a 60° sector about the aircraft nose. A block diagram for the homing network is shown in Fig. 27.

The system requires two IF channels matched in gain but whose phase characteristics are immaterial. They each are controllable in gain by an AGC detector and amplifier operating from the one IF channel. Thus gain of both channels is held to the same value and that value is sufficient to give a full scale indication of the meter when the ship is head on into the transmitter. In this case there is no signal at the output of Channel I. As the ship deviates from head on into the transmitter the signal magnitude in channel I increases and subtracts at the indicator to bring the needle back from full scale indication. The meter scale can be calibrated in degrees off head on. One disadvantage of this arrangement is lack of sense. The local osciliator could be keyed into the two mixers in an A-N fashion and the meter shunted with a pair of head phones to give an aural indication of sense with a visual indication of bearing deviation with respect to the transmitter.

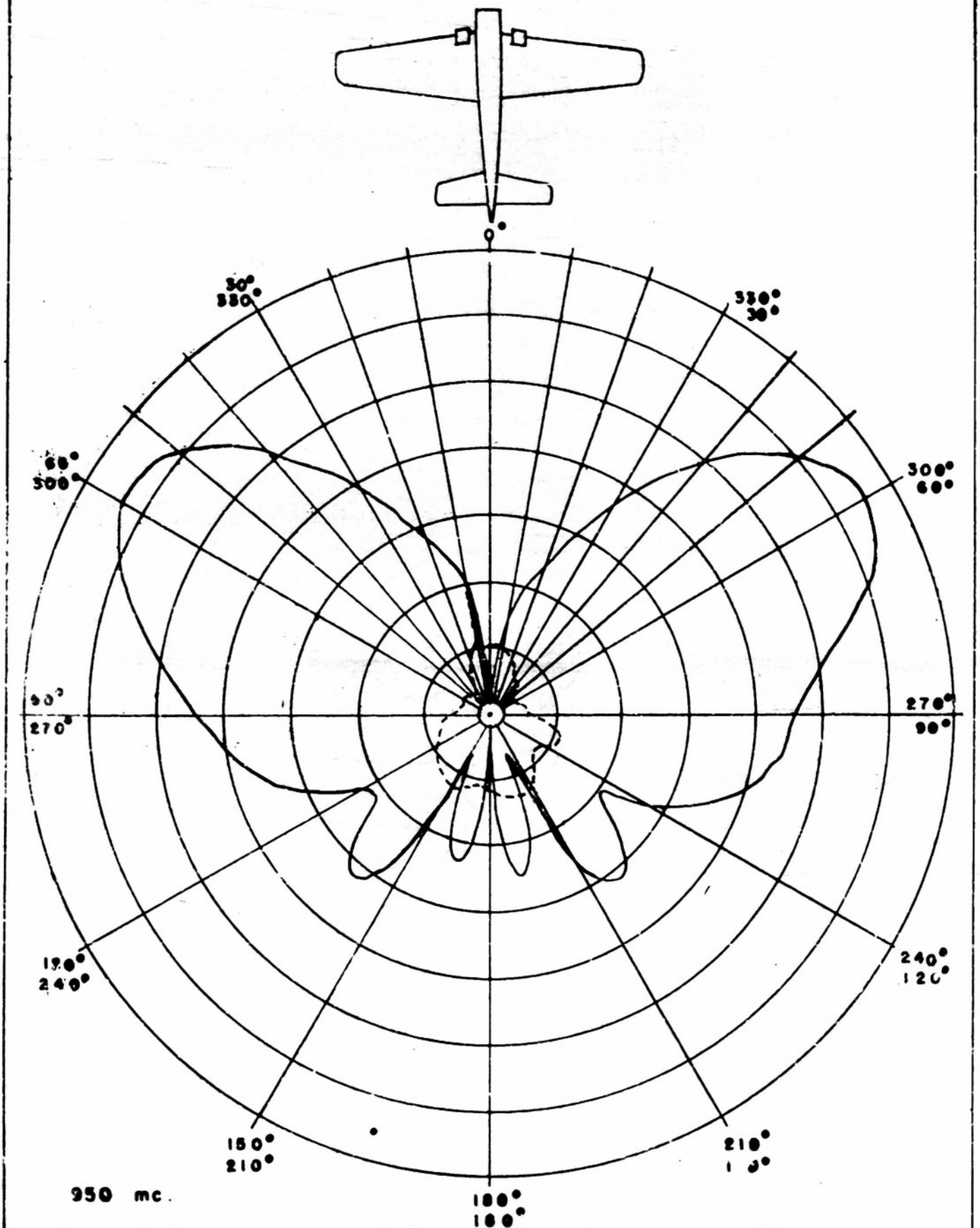
0°
30°
330°
60°
300°
90°
270°
120°
240°
150°
210°
180°
950 mc.
Horizontal Polarization Pattern
Vertical Polarization Pattern

FIGURE 25a

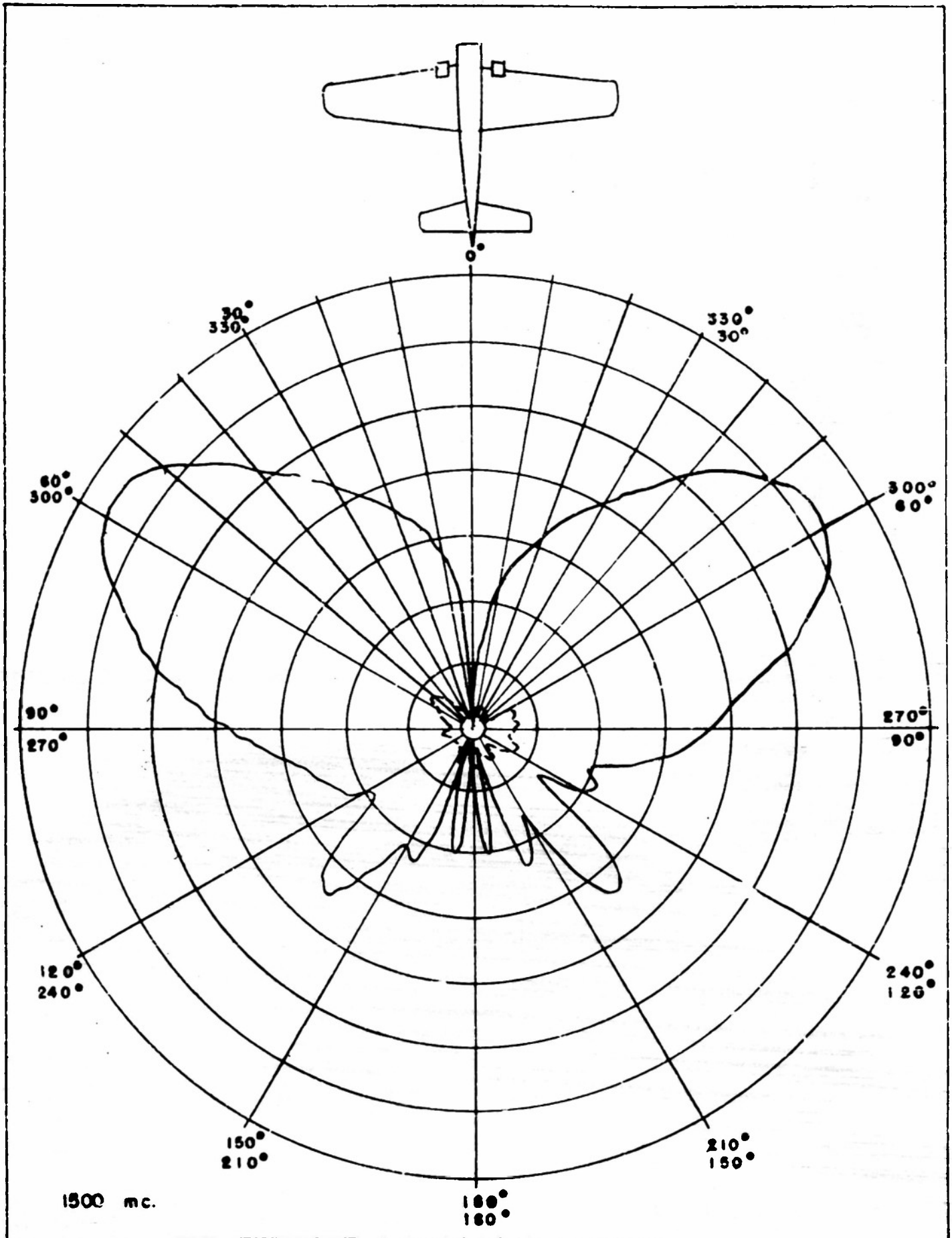
0°
30°
330°
330°
30°
60°
300°
300°
60°
90°
270°
270°
90°
120°
240°
240°
120°
150°
210°
210°
150°
180°
180°
1500 mc.
Horizontal Polarization Pattern
Vertical Polarization Pattern

FIGURE 25b

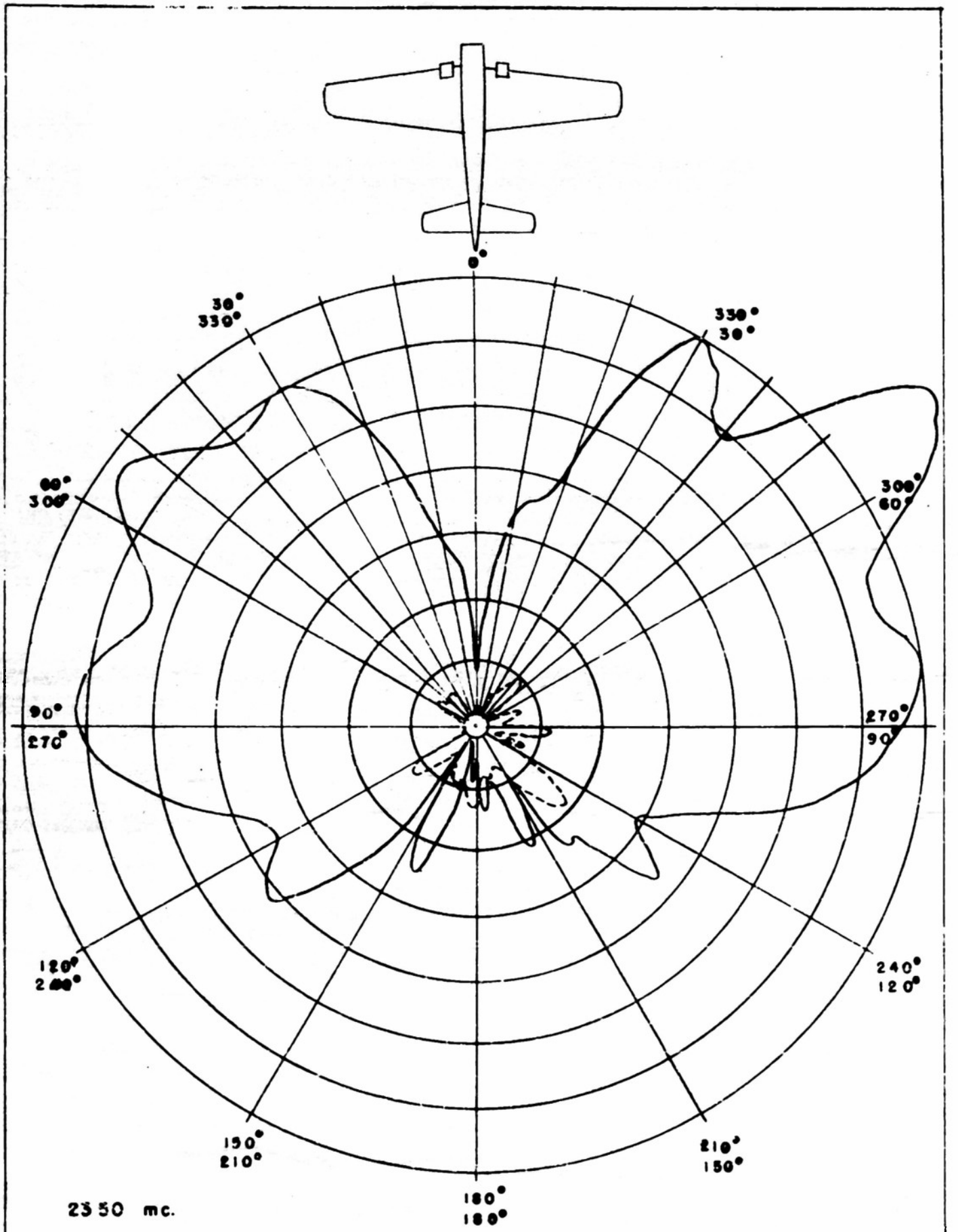
0°
30°
330°
330°
30°
60°
300°
90°
270°
270°
90°
120°
240°
240°
120°
150°
210°
210°
150°
180°
180°
2350 mc.
Horizontal Polarization Pattern
Vertical Polarization Pattern

FIGURE

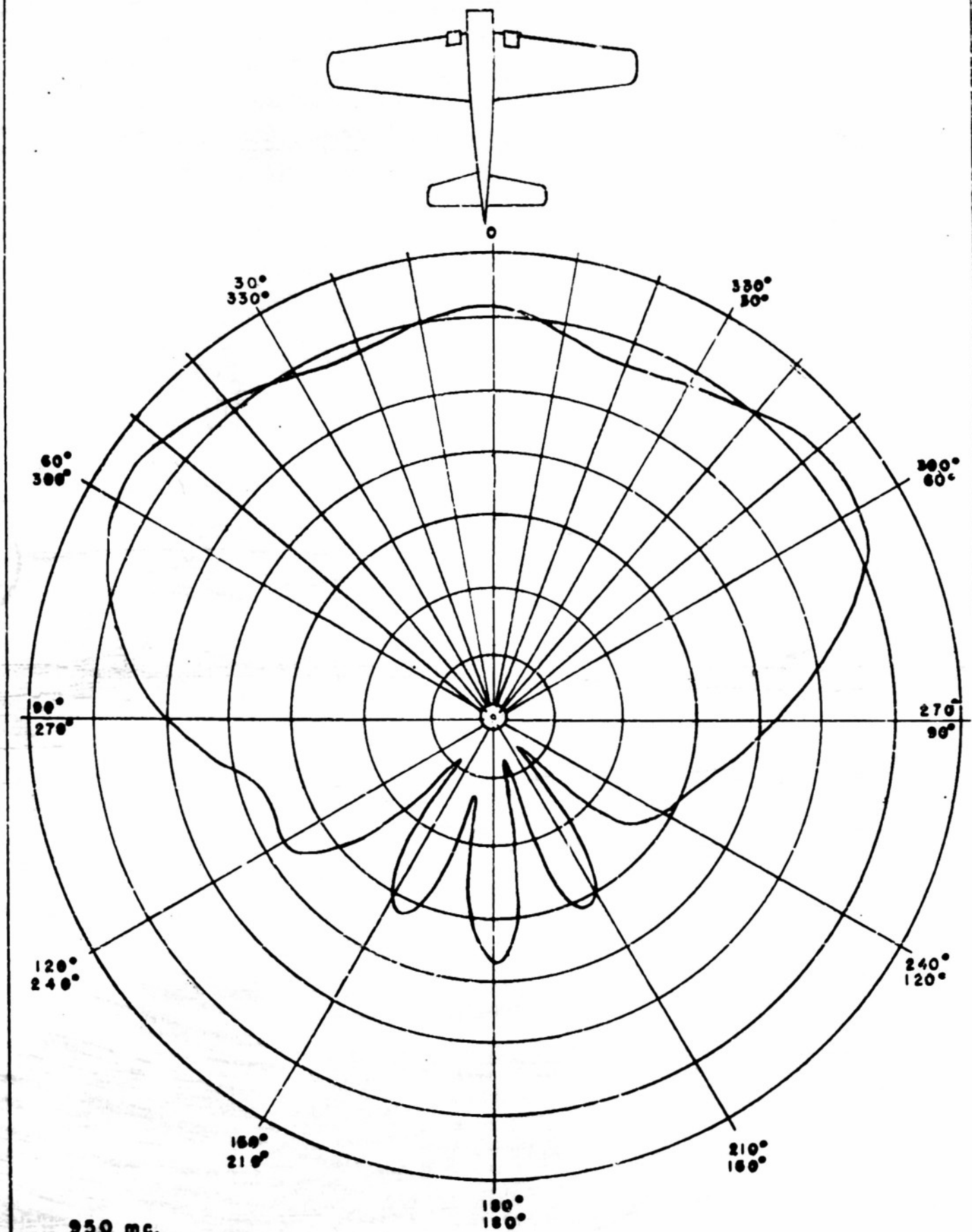
0
30°
330°
330°
30°
60°
300°
300°
60°
90°
270°
270°
90°
120°
240°
240°
120°
150°
210°
210°
150°
180°
180°
950 mc.
Horizental Polarization Pattern

FIGURE 26g

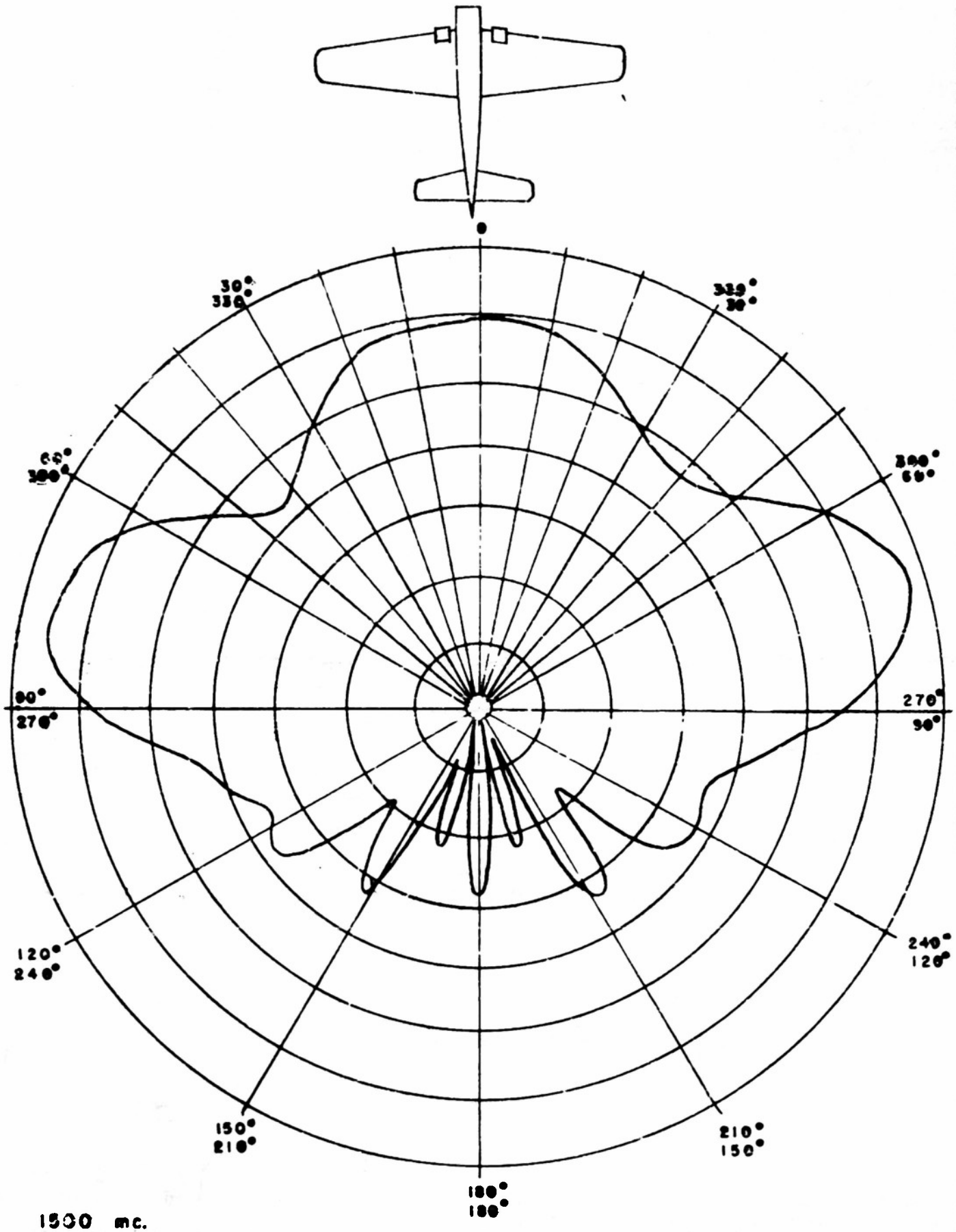

1500 mc.

——————— Horizontal Polarization Pattern

FIGURE 26b

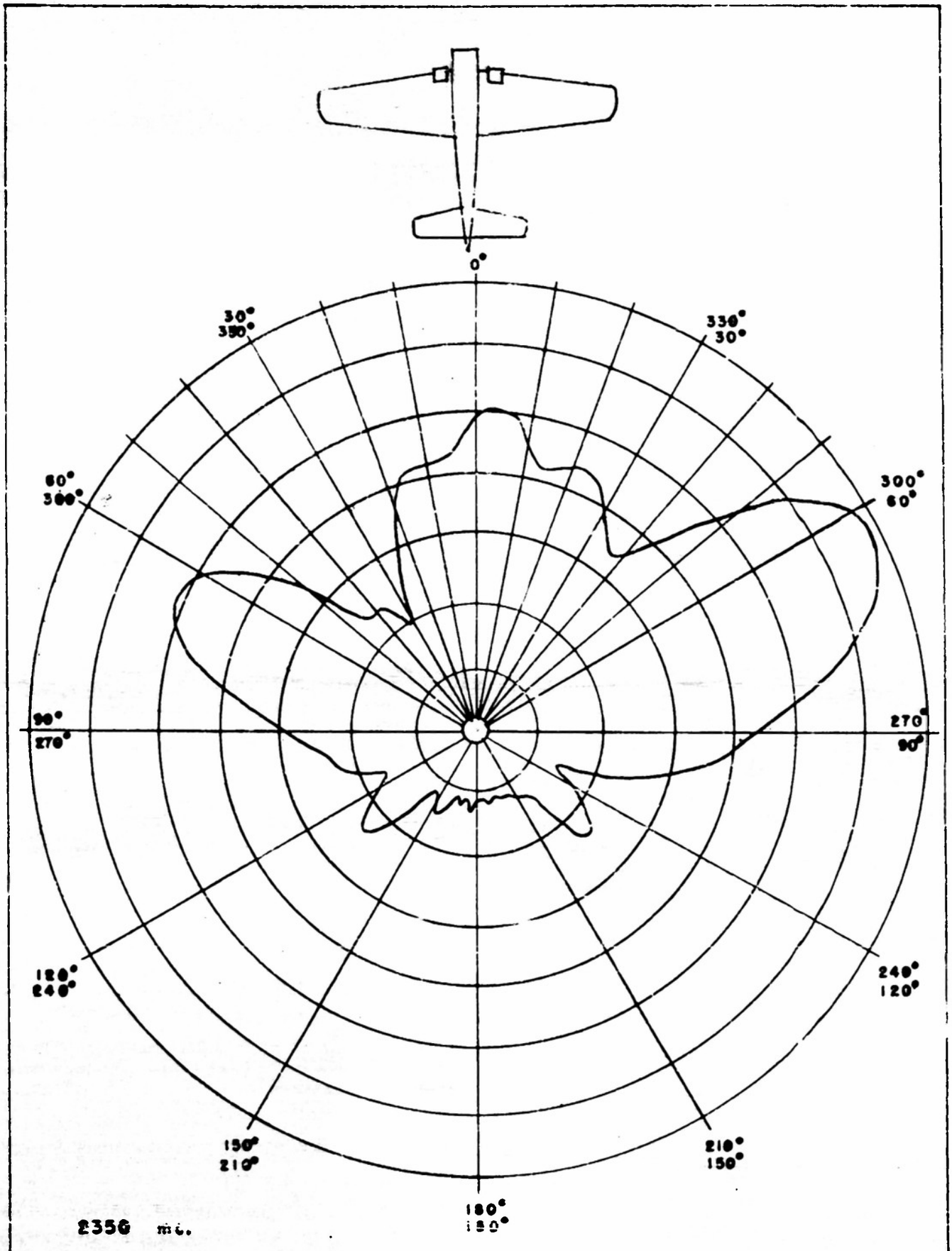

Horizontal Polarization Pattern

FIGURE 28c

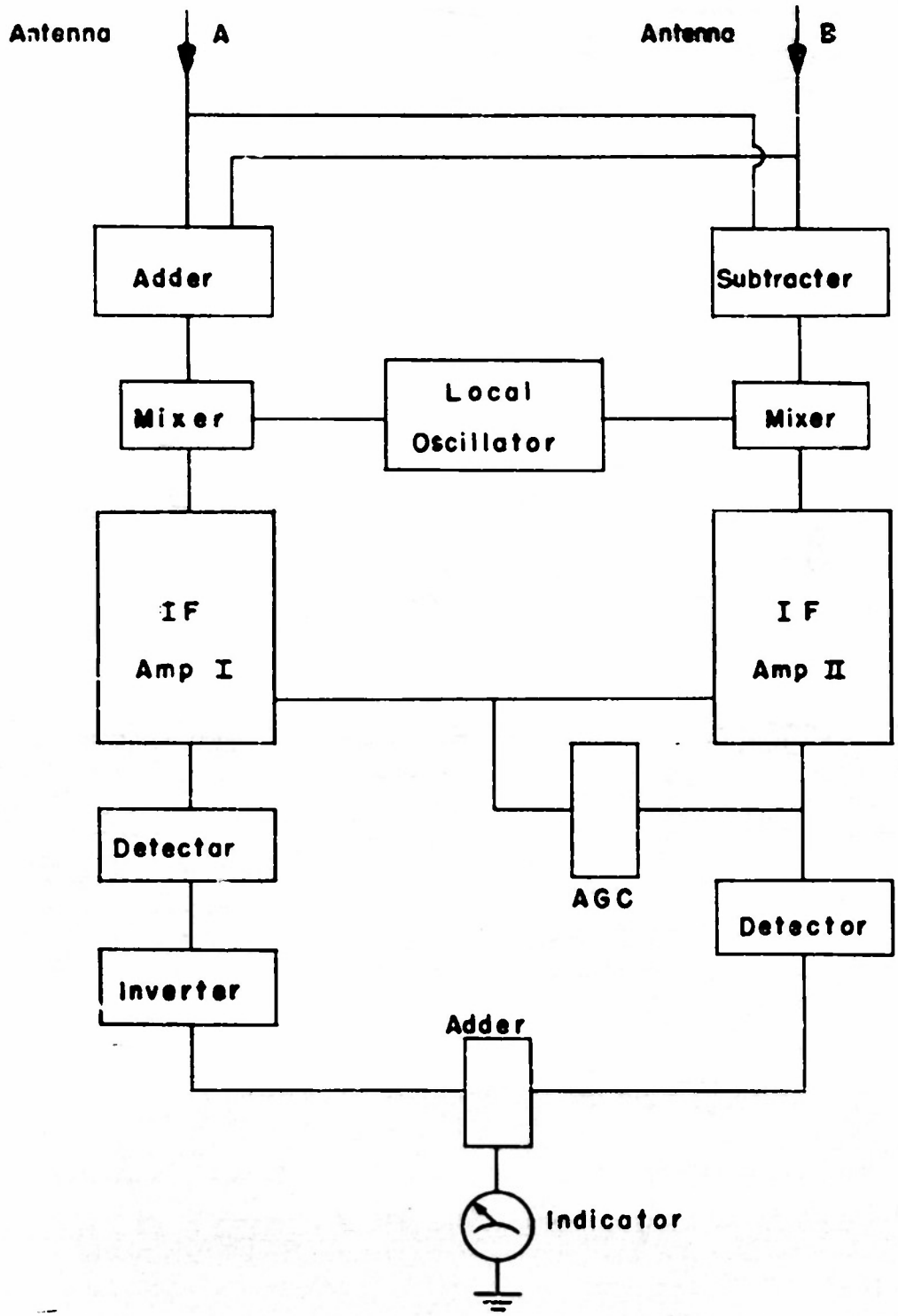

FIGURE 27 HOMING SYSTEM BLOCK DIAGRAM

APPENDIX V

Impedance Calculations for the Tuned Wing-Edge Antenna

The radiation impedance of the tuned wing-edge antenna may be estimated by considering it to be a short slot wrapped around the leading edge of the wing. By using Babinet's principle the impedance of the slot may be obtained from the impedance of the equivalent flat-strip dipole. In addition the radiation conductance is increased by a factor, which has been assumed for this case to be approximately 8 times, due to the bending of the slot antenna about on edge.*

At 63.3 mc, L = λ/10, W = λ/5 and s = λ/100, and the complimentary dipole for the transverse slot has the configuration shown below.

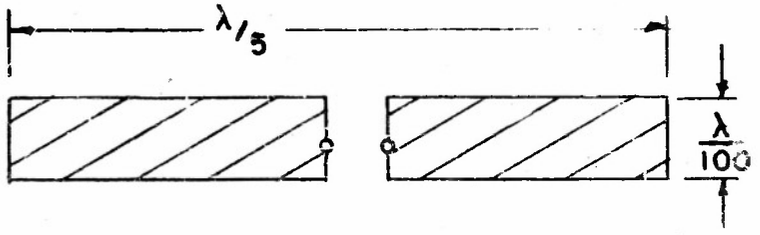

$s = \lambda/100 = 2\pi r_o$

$r_o/\lambda \cong 0.0016$

For short antennas the radiation resistance R_r is approximately

$$R_r \cong 20\pi^2 \left(\frac{l}{\lambda}\right)^2 = 8 \text{ ohms.}$$

The reactance is available from impedance curves.**

$$X_r = -j400.$$

Therefore the dipole impedance is

$$Z_d = 8 - j400.$$

By Babinet's principle the impedance of the slot is $Z_s = \frac{\eta^2}{4Z_d}$ and η is the impedance of free space.

$$Y_s = \frac{4Z_d}{\eta^2} = g_s - jb_s = 1.15 \times 10^{-4} - j5.63 \times 10^{-3}$$

Increasing the radiation conductance by a factor of 8 due to the bent configuration changes Y_s to

$$Y_s = 9.2 \times 10^{-4} - j5.63 \times 10^{-3}$$

For the short-circuit, strip transmission line, the input impedance is

$$Z_{T.L.} = jZ_o \tan BL$$

where Z_o is the characteristic impedance in terms of

$$Z_o = \eta \frac{4}{\pi}.$$

* Wong, James Y., "Radiation of Slots in Elliptic Cylinders", Ph. D. Thesis, University of Illinois, June 1952.

** Jordan, E.C., *Electromagnetic Waves and Radiating Systems*, Prentice-Hall, p. 364.

Hence

$$Y_{T.L.} = b_{T.L.} = \frac{-j}{Z_o} \cos Bl = -j7.3 \times 10^{-2}$$

The equivalent circuit for the antenna input is

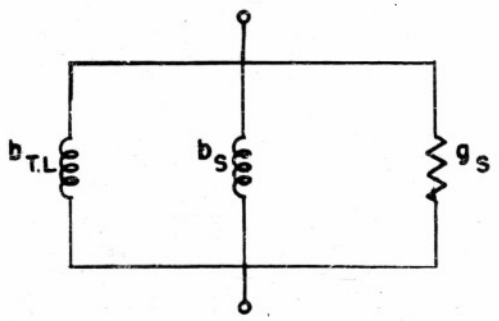

so that the antenna input admittance Y_a is

$$Y_a = 9.2 \times 10^{-4} - j7.9 \times 10^{-2}$$

By tuning out the susceptance

$$Z_a = \frac{1}{9.2 \times 10^{-4}} = 1087 \text{ ohms.}$$

Similarly at 40 mc

$$Y_a = 3.36 \times 10^{-4} - j1.35 \times 10^{-1}$$

and by tuning out the susceptance

$$Z_a = 2980 \text{ ohms}$$

at 100 mc

$$Y_a = 4.84 \times 10^{-3} - j3.76 \times 10^{-2}$$

and

$$Z_a = 206 \text{ ohms.}$$

These values are the radiation resistances referred to the open end of the antenna. By tapping down at an appropriate point on the inside of the sleeve these resistances can be transformed to center about any desired value, e.g. 50 ohms. The actual measured values can be expected to differ from those calculated by this means because of (a) approximations in the calculations and (b) neglect of loading due to ohmic losses of the circulating currents. The latter effect can be expected to be negligible at 100 mc but quite appreciable at 40 mc. A rough estimate of the tapped down impedance range when centered about 50 ohms would be 120 ohms at 40 mc to 20 ohms at 100 mc.